Aus der
Universitätsklinik für Kinder- und Jugendmedizin Tübingen
Abteilung Kinderheilkunde I mit Poliklinik
(Schwerpunkt: Hämatologie, Onkologie, Gastroenterologie,
Nephrologie, Rheumatologie)

# Uridine-depleted hCFTR mRNA-delivery to restore hCFTR expression and function in vitro and in vivo

**Inaugural-Dissertation**
**zur Erlangung des Doktorgrades**
**der Medizin**

**der Medizinischen Fakultät**
**der Eberhard-Karls-Universität**
**zu Tübingen**

**vorgelegt von**
**Dorhs, Clarissa Charlotte**

**2024**

| | |
|---|---|
| Dekan: | Professor Dr. B. Pichler |
| 1. Berichterstatter: | Professorin Dr. J. Skokowa, Ph.D |
| 2. Berichterstatter: | Professorin Dr. M. Avci-Adali |

Tag der Disputation: 09.03.2022

# Table of Content

## List of Tables

## List of Figures

## List of Abbreviations

Ψ ..... Pseudouridine
5moC ..... 5-Methoxycytidine
AATD ..... Alpha-1-antitrypsin-deficiency
AAV ..... Adeno-associated virus, Adeno-associated virus
ABC-transporter ..... ATP-binding cassette transporter
ac4C ..... N4-acetylcytidine
AMP ..... Adenosine-mono-phosphate
ASL ..... Airway surface liquid
ATP ..... Adenosine triphosphate
AV ..... Adenovirus
cDNA ..... Complementary DNA
CF ..... Cystic Fibrosis
CFBE41o$^{-}$- cells ..... Cystic fibrosis bronchial epithelial cells
CFTR ..... Cystic Fibrosis Transmembrane Conductance Regulator
CLNP ..... Cationic Nanoliposomes
CRISPR/Cas9 ..... Clustered Regularly Interspaced Short Palindromic Repeats/CRISPR associated protein 9
DOPE ..... 1,2-dioleoyl-sn-glycero-3-phosphoethanolamine
DOTAP ..... 1,2-dioleoyl-3-trimethylammonium-propane
DOTMA ..... 1,2-di-O-octadecenyl-3-trimethylammonium-propane
dsRNA ..... double-stranded RNA
ELISA ..... Enzyme-linked immunosorbent assay
ENaC ..... Epithelial Na channel
ER ..... Endoplasmic reticulum
FCS ..... Fetal calf serum
FEV ..... Forced expiratory volume
GL67A ..... cholest-5-en-3-ol(3β)-,3-[(3-aminopropyl)[4-[(3-aminopropyl)amino]butyl]carbamate]
HBE-cells ..... Human bronchial epithelial cells
HPLC ..... High-performance liquid chromatography
HRP ..... Horseradish peroxidase
HSC ..... hematopoietic stem cells

Hsp ..... Heat shock protein
i.t. ..... Intratracheally
i.v. ..... Intravenously
IFIT ..... Interferon-induced tetratricopeptide repeat
IFN ..... Interferon
IL ..... Interleukin
IVT ..... In Vitro Transcription
LB ..... Luria broth
LNP ..... Lipid-based nanoparticles
m1Ψ ..... N1-Methylpseudouridine
m5C ..... 5-Methylcytidine
m6A ..... N6-Methyladenosine
m7G ..... N7-methylguanosine
MAD ..... multiple ascending doses
MDA 5 ..... Melanoma differentiation associated protein 5
MEM ..... Minimum essential media
MSD ..... Membrane spanning domain
MTT ..... 3-(4,5-dimethylthiazol-2-yl)-2,5-diphenyltetrazolium bromide
NBD ..... Nucleotide binding domain
NPFE ..... negative pressure-driven forced expiration
ORF ..... Open reading frame
p[DMAEMA] ..... (Dimethylamino)ethyl methacrylate
PBAE ..... Poly-beta-aminoester
PBS ..... Dubecco's phosphate buffered saline
pDNA ..... Plasmid DNA
PEG ..... Polyethylene glycol
PEI ..... Polyethyleneimine
PKR ..... RNA dependent protein kinase
PLGA ..... Poly(lactic-co-glycolic) acid
PLL ..... Poly-L-lysine
ppFEV$_1$ ..... Percentage predicted forced expiratory volume in 1 second
PRR ..... Pattern recognition receptor

R848 ..... Resiquimod
RIG-I .....Retinoic acid inducible gene I
RT-qPCR .....Real-time quantitative polymerase chain reaction
s2U..... 2-Thiouridine
SAD.....single ascending dose
SD ..... Standard deviation
SeV .....Sendai virus
ssODN ..... single-stranded oligodeoxynucleotides
ssRNA..... single-stranded RNA
TALEN ..... Transfection activator like effector nucleases
TLR .....Toll-like-receptor
TNF ..... Tumor-necrosis-factor
UD..... Uridine-depletion
V-ATPase..... Vacuolar-type $H^+$ ATPase
ZFN ..... Zink-finger nucleases

# 1 Introduction

## 1.1 Cystic Fibrosis

### 1.1.1 Epidemiology

Cystic Fibrosis (CF) is considered the most common lethal monogenic disease among Caucasians with a carrier rate about 1:25 and a prevalence of 1:2,500 (1). Worldwide there are approximately 70,000 – 100,000 people suffering from CF (1), with an incidence accounting for 1:3,300 newborns in Germany.

Since 1962 median life expectancy of CF patients has increased from 10 to approximately 40 years (2). Therefore, nowadays CF is no longer solely considered as a pediatric disease. Adult patients make around 50 % of CF patients in industrial nations. The increase in life expectancy also leads to an increase in the number of patients suffering from CF and in complications during disease progression. (3)

### 1.1.2 CFTR-channel

The Cystic Fibrosis Transmembrane Conductance Regulator (CFTR) or ABCC7 -protein is a cyclic Adenosine-mono-phosphate (AMP)-activated anion channel at the apical membrane of epithelial cells. It consists of 1480 amino acids (1). The channel is part of the ATP-binding cassette transporter (ABC-transporter) superfamily. In this context it is further classified into the ABCC-subfamily (4). It is built up of five domains: two membrane spanning domains (MSD 1 and MSD 2), two cytoplasmic nucleotide binding domains (NBD 1 and NBD 2) and a cytoplasmic regulatory domain that allows phosphorylation dependent gating (5). Upon activation of the channel through phosphorylation, binding and hydrolysis of adenosine triphosphate (ATP), the NBDs dimerize and the two transmembrane domains form the channel's anion pore, allowing transit of anions from intra- to extracellular (6). The CFTR-channel directly conducts chloride ($Cl^-$) and bicarbonate ions ($HCO_3^-$) (1, 7). Moreover, it inhibits major sodium-absorbing channels (ENaCs) (1). All these functions make this channel important for the regulation of ion and fluid homeostasis (1).

CFTR is expressed in excretory cells in lungs, kidneys, intestine and pancreas making CF a multiorgan disease. In the lung, the recently discovered pulmonary

Ionocytes are assumed to be the major CFTR expressing cells (8, 9). These pulmonary Ionocytes specifically express the transcription factor FOXI1, the vacuolar-type $H^+$ - ATPase (V-ATPase) and CFTR (8, 9). In mice, Ionocytes only comprise around 0.42 % of the airway epithelium but express 54.4 % of all CFTR transcripts (8). They are mainly found in murine submucosal glands, nasal and olfactory epithelia and probably originate from basal cells (8, 9). These Ionocytes were also found in human bronchi, where they comprise 0.5 – 1.5 % of the epithelial cells in the conducting airways and are highly enriched in CFTR (8). Moreover, Plasschaert et al. found Ionocytes in airway-liquid cultures of human bronchial epithelial cells (HBE-cells), again being the major source of CFTR activity (9). Further investigation of this newly discovered rare cell type is needed, but these current findings implicate that pulmonary Ionocytes and their progenitors constitute a relevant target for treatment of CF lung disease.

To explain the pathogenesis of CF lung disease the so called “low volume hypothesis” is the most common approach.

In healthy individuals, the airway epithelium is covered by a thin layer of airway surface liquid (ASL). The ASL consists of a periciliary layer and a mucus gel on the top and plays an important role for the lung’s innate defense. Within the periciliary layer, the ciliary beating transports mucus towards the mouth (mucociliary clearance), cleaning the airways from inhaled pathogens. Moreover, the ASL contains antimicrobial substances as lactoferrin or lysozyme, which induce bacterial killing. (7, 10)

Mutations in the CFTR-gene, leading to an impaired function of the CFTR channel, affect ASL production. The secretion of chloride and bicarbonate decreases, while ENaC activity increases, as the CFTR channel no longer inhibits ENaC activity (11). The decrease in chloride secretion and the hyperabsorption of sodium through ENaCs built up an osmotic gradient which leads to an increase in water absorption (11). These changes severely affect the ASL composition, inducing a depletion of the periciliary layer and increase viscosity of the mucus gel by dehydration (10, 11). This consequently results in disruption of the mucociliary clearance and retention of mucus in the airways, which facilitates airway infections (10). Additionally, as the $HCO_3^-$ secretion also reduces, the ASL

pH decreases. The reduction of the airway surface pH inhibits the activity of antimicrobial substances (e.g. lysozyme and lactoferrin) in the ASL, which promotes airway infections as well (7). Other factors, such as impairment of the adaptive immune response, due to mutations in the CFTR gene or environmental factors, might also contribute to the development of CF lung disease (11).

Generally Cystic Fibrosis affects several organs such as the airways, pancreas, intestine or sweat ducts. The main cause of CF patient's morbidity and mortality however is the respiratory disease (11). In consequence of the defective mucus clearance and acidic surface pH, pathogen colonization increases, leading to repetitive inflammatory responses and disruption of the epithelial cell lining (12-14). Typical pathogens are *Burkholderia cepacia*, *Staphylococcus aureus* and *Pseudomonas aeruginosa* (15). Chronic inflammation of the airways and augmented release of proteases and oxidants, induce remodeling of the lung tissue and result in irreparable lung damage, leading to mucus obstruction and respiratory failure (16). Patients suffering from CF present with recurrent airway infection, sinusitis, and bronchiectasis. The increasing pulmonary fibrosis promotes occurrence of portal hypertension, which might lead to cardiac arrest. (12).

Apart from the pulmonary disease patients suffer from exocrine pancreas insufficiency, pancreatitis and eventually from diabetes mellitus. Bile duct obstruction may lead to cholestasis, cholecystolithiasis and even liver cirrhosis. Males may present with obstructive azoospermia, causing sterility. Women suffer from decreased fertility as well, due to increased viscosity of cervical mucus, which decreases spermatozoa's mobility. Caused by the chloride-channel's defect, NaCl-concentration in sweat increases which is used as a diagnostic tool. (15)

### 1.1.3 Genetics

The disease of Cystic Fibrosis is due to an autosomal-recessive mutation in the CFTR-gene, which was first fully identified in 1989 (1). This gene is located on the long arm of chromosome 7 at position 7q21 - 24 (1). At present there are more than 1,800 mutations identified, from which about 200 cause the CF phenotype. These mutations are further classified into six classes (5).

Class I mutations, like G543X or R1162X are mostly nonsense - or frameshift mutations, which lead to defective protein translation through premature stop codons (1).

Class II mutations cause incorrect protein processing and retention of the protein in the endoplasmic reticulum (ER), which induces early degradation of the protein (17, 18). The most common and prominent mutation F508del is a class II mutation. The F508del mutation is described in detail later in this chapter.

Mutations that result in defective protein regulation are considered class III mutations (1). Class III mutations affect the CFTR channel's gating and conductivity, such as the G551D mutation which leads to reduced binding of ATP (1).

While class III mutations mainly influence activation of the CFTR channel, e.g. by binding of ATP (3), class IV mutations, like R117H and D115H, are associated with decreased channel conductivity for chloride ions (1).

Class V mutations, like A455E, cause promotor defects or changes in splicing reactions which reduce protein synthesis (1).

Finally, class VI mutations, as C.120del23, lead to reduced protein surface retention, due to impaired biosynthesis or decreased stability of CFTR (1) .

In general class I - III mutations are considered more severe, as they tend to completely abolish CFTR expression or function. Whereas class IV to VI mutations cause milder forms of CF, since they only reduce expression or function of CFTR (11)

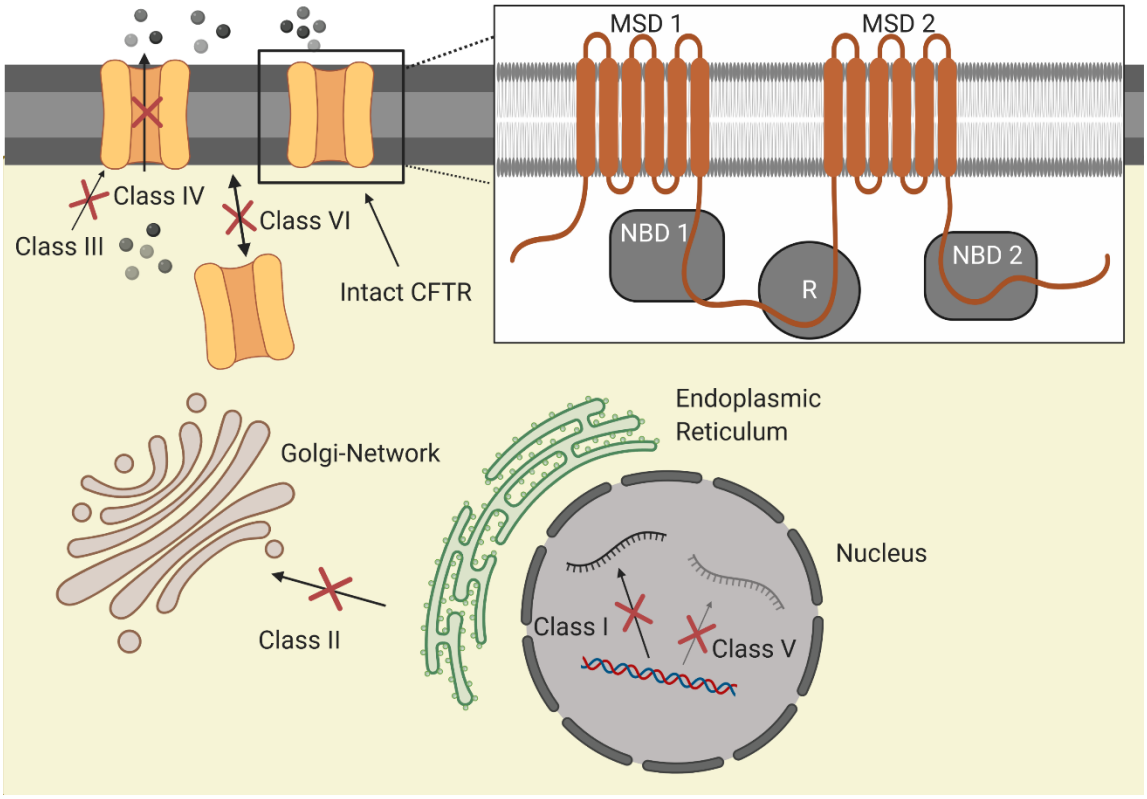


**Figure 1.1** CFTR protein structure and mutation classes**.** The CFTR protein is built of two membrane spanning domains, two nucleotide binding domains and one regulatory domain. There are six different mutation classes. While mutation classes I – III abolish CFTR protein expression, classes IV – VI reduce expression or function of CFTR.

As mentioned before, the most common CFTR-mutation is the F508del class II-mutation, affecting about 70 – 80 % of CF patients (1). This mutation is located on exon 10 and leads to a removal of phenylalanine 508 from the first nucleotide binding domain due to a deletion of three basepairs (19). The F508del-mutation within the NBD 1 impairs domain-domain interactions that are crucial for correct protein folding and thus leads to a misfolded CFTR protein (18).

To explain the underlying cause why the F508del-mutation results in unfunctional CFTR-protein, it is important to first understand the processing of CFTR in healthy individuals. As all proteins targeted to the plasma membrane CFTR passes the secretory pathway within the cell. It is co-translationally inserted into the endoplasmic reticulum (ER), where two N-linked glycosyl groups are added to

the CFTR-polypeptide and it undergoes quality control, mainly concerning correct folding (17, 18). This core-glycosylated protein is then transferred to the Golgi-network, where its glycosylation is further modified and the CFTR-protein eventually receives complex-glycosylation (17, 18). This mature form of the CFTR-protein reaches the plasma membrane. At the plasma membrane, the CFTR levels are regulated through anterograde CFTR delivery, endocytosis, and recycling (18).

The misfolded F508del-CFTR is recognized at different checkpoints throughout the secretory pathway. However, the majority of the protein does not even reach the Golgi-network but is trapped in the ER mainly through binding of chaperones (e.g. heat shock proteins (Hsp) 70/90 and 40), which induce degradation of the protein through the ubiquitin-proteasome pathway (17, 18). Since most F508del-CFTR is retained in the ER and does not reach the Golgi-apparatus, the CFTR-protein is only present in its core-glycosylated but not in the mature complex-glycosylated form (17). Taken together, the underlying cause for the CF phenotype in patients carrying the F508del mutation is misfolding of the CFTR-protein, retention in the ER and early degradation through the ubiquitin-proteasome pathway.

## 1.2 Current therapies for CF

### 1.2.1 Channel modulators

Until 2012 there was no causal therapy for cystic fibrosis available. The symptom-based therapy mainly consists of supplementation of pancreatic enzymes and fat-soluble vitamins as well as secretolysis and mucolysis via administration of β-sympathomimetics, dornase alfa or hypertonic saline. Further options to treat CF lung disease are physiotherapy, antibiotic therapy and lung transplantation as ultima ratio. (20)

In 2012 the first so-called channel modulator was authorized, targeting the cause underlying CF for the first time. Channel modulators can be divided into potentiators and correctors. The first channel modulator authorized in Germany in 2012 was Ivacaftor (VX-770, Kalydeco®). Ivacaftor, a potentiator, increases the open probability of CFTR and consequently the chloride and bicarbonate

transport through the CFTR channel (21, 22). Nowadays Ivacaftor is available for patients with G551D and other class III and IV gating and conducting mutations (22, 23). Nonetheless, the mutations targeted by Ivacaftor only account for about 1 % of the CF patients (1).

Correctors as Lumacaftor (VX-809) or Tezacaftor (VX-661) facilitate processing and trafficking of the CFTR-protein and reduce intracellular degradation to increase the amount of CFTR-protein at the cell surface (24, 25). Therapeutically targeting CFTR-processing, correctors should benefit patients with class II mutations, such as the F508del mutation, affecting approximately 70 - 80 % of CF patients, as mentioned before (1). Yet, administration of Lumacaftor alone failed to improve lung function in CF patients carrying the F508del mutation (26). It is assumed that the F508del mutation does not only cause a trafficking defect, but also impairs the CFTR-protein's opening (27). In 2017 and 2018 dual therapies combining correctors and potentiators have been approved in Germany. The dual therapies first combined Lumacaftor and Ivacaftor (Orkambi®), which was later followed by a combination of Tezacaftor and Ivacaftor (Symdeko®). Both therapies are now available for patients from the age of six, who are homozygous for the F508del mutation.

Moreover, in October 2019 triple therapy combing Elexacaftor (VX-445), Tezacaftor (VX-661) and Ivacaftor (VX-770) (Trikafta®) has been approved in the USA (24, 28). This decision was followed by approval of triple therapy in the EU as well in August 2020 (Kaftrio®) (29). The triple therapy is now available in the USA and the EU for the treatment of CF patients ≥ 12 years, carrying ≥ 1 F508del mutation.

Currently, channel modulators are the best treatment option available for CF patients with F508del, G551D and certain other class III and IV mutations. They have shown significant improvement of lung function in numerous clinical trials (22, 23, 27, 30-32). However, the overall improvement of lung function, that can be achieved through the channel modulators is still rather modest. Dual therapy only increased the percentage predicted $FEV_1$ ($ppFEV_1$) by 2 – 4 % (27, 32, 33) and even triple-therapy (Trikafta®) only achieved a maximum of 14 % improvement of the $ppFEV_1$ (30, 31). Moreover, channel modulators might induce

rare but serious adverse effects, which were most prominently found for dual therapy with Lumacaftor and Ivacaftor (Orkambi®). As some observational studies pointed out, for Orkambi® there is a relatively high rate of drug intolerance and it might even lead to a decrease in $FEV_1$, which is opposite to the therapeutic intention (34, 35). Drug intolerance might even lead to discontinuation of the therapy. Furthermore, dual therapy only benefits patients who are homozygous for the F508del mutation. They comprise around 45 % of CF patients. The new triple therapy (Trikafta®/ Kaftrio®) will also be addressing heterozygous patients, leaving around 10 % of CF patients who are not eligible for channel modulator therapy (36). Generally, one great issue concerning the channel modulators is that they act mutation-specific. This means there must be different channel modulators developed targeting the different underlying causes of the CF phenotype, to make this therapy available for all CF patients. Taking all this together, although the development of channel modulators means a great step forward in treating CF, there is still a need for looking into alternative, more effective therapeutic approaches, that work mutation-independently, can be applied to all CF patients and might even offer a cure for CF lung disease.

## 1.3 Gene supplementation therapy

### 1.3.1 Introduction to gene therapy

Gene therapy constitutes a promising approach to cure Cystic Fibrosis and has been extensively investigated since the first cloning of the CFTR gene in 1989.
The American Society of Gene & Cell Therapy defines gene therapy as *“introduction, removal or change in genetic material – specifically DNA or RNA - into the cells of a patient to treat a specific disease”* (37).
Generally, gene therapy for CF includes two different approaches. The first one is gene correction, which aims to repair the defective CFTR-gene (38). This repair can be mediated by engineered nucleases, such as Zink-finger nucleases (ZFN), transcription activator-like effector nucleases (TALEN) or CRISPR/Cas9 (Clustered Regularly Interspaced Short Palindromic Repeats/CRISPR associated protein 9) , which induce double strand breaks into the DNA and enable introduction of the correct CFTR gene by homology directed repair. The

other approach is gene supplementation. The underlying idea of gene supplementation can be found in the central dogma of life, describing the flow of genetic information: DNA is transcribed into mRNA, which is then translated into protein. Basically, gene supplementation can target all three levels of genetic information. It is possible to administer a functional gene, as plasmid DNA (pDNA) which is transferred to the nucleus and transcribed into stable mRNA, which is translated into functional protein in the cytoplasm. Alternatively, mRNA can be used as a vehicle for gene supplementation, which can be immediately translated into functional protein. Finally, it is also possible to administer the functional protein itself, requiring neither transcription nor translation.

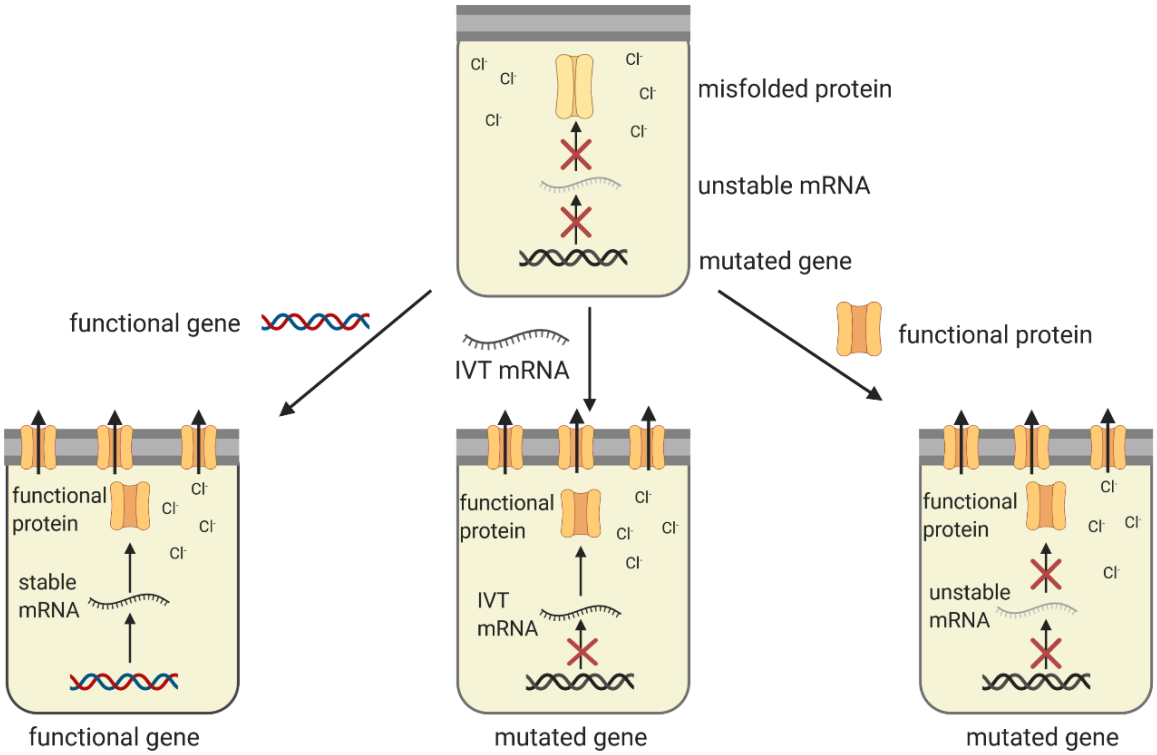


**Figure 1.2** Strategies of protein supplementation therapy. For expression of functional hCFTR protein all three levels of genetic information can be targeted. It is possible to deliver either the functional hCFTR gene, mRNA or the hCFTR protein itself.

The great potential of gene therapy lies in the ability to provide functional CFTR protein independently from the mutation class underlying the CF phenotype. Therefore, gene therapy could be available for all CF patients, in contrast to channel modulators. Gene therapy targets the molecular cause of CF, might provide a cure and help to prevent development of lung disease if administered early. (11)

As the lung disease is considered the main cause for CF patient's morbidity and mortality, the conducting airways are seen as primary target for gene therapy (39).

Recently gene therapy using an adeno-associated viral (AAV) vector carrying the RPE65-gene (Luxturna®) was proven successful in treating congenital blindness (40). Other AAV-based gene therapies which already received marked approval are for example Glybera®, an AAV-vector carrying the lipoprotein lipase gene for patients with severe lipoprotein lipase deficiency and Zolgensma®, which is an AAV-based gene therapy for infants suffering from spinal muscular atrophy (41). These examples of successful gene therapy further encourage investigation of gene therapy approaches for treatment of monogenic diseases such as Cystic Fibrosis.

### 1.3.2 Direct protein supplementation and DNA-therapy

For direct protein delivery as a therapy for CF there have been attempts of *in vivo* transfer via phospholipid liposomes. Although only limited membrane incorporation took place, an improvement in nasal potential difference measurement was found (42).

Moreover, protein supplementation therapy via DNA-based vectors has been investigated thoroughly since the 1990s. Vectors for delivery of complementary DNA (cDNA) are mainly of viral origin, based on cationic lipids or based on DNA nanoparticles or polymers (43).

In the 1990s delivery of CFTR cDNA using viral vectors has been broadly explored (44-48). Adenoviral (AV) vectors and adeno-associated viral (AAV) vectors were the main vectors utilized. They show natural tropism to the lung and do transduce non-proliferating cells, which constitute the majority of respiratory cells (44). Initial encouraging results demonstrated restoration of functional CFTR

*in vitro* and showed the general feasibility of CFTR cDNA delivery via adenoviral vectors *in vivo* (44, 47). However, all in all cDNA delivery mediated by AV- or by AAV-vectors has shown to be mainly inefficient, achieving only little or no restoration of the ion transport defect (43, 46, 48, 49). These somewhat disillusioning findings had several reasons. First, AV- and AAV-mediated CFTR gene transfer only results in transient gene expression, requiring repeated administration for gene therapy to be efficient (46, 48, 50). Second, repeated administration of AV- and AAV-vectors induces immune responses and might even lead to development of neutralizing antibodies, further decreasing gene transfer efficiency (43, 46, 48, 50, 51). Interestingly, endosomal processing and ubiquitination of AAV-based vectors has shown to be another limiting step in AAV-mediated CFTR transfer (52). Furthermore, the coxsackie-adenovirus receptor, that mediates binding and cellular internalization of the AV- and AAV vectors, is located on the basolateral side of the airway epithelium, which accounts for the inefficient CFTR gene transfer as well (43, 53). To increase gene transfer efficiency, mechanical injury of the airway epithelium would be necessary, for example through use of tight junction openers. Taking the heavy bacterial colonization of CF airways into consideration and the potential risk of systemic invasion, this hardly seems appropriate (54). Taken together, it seems unlikely that AV- or AAV-based vectors are appropriate vehicles for CFTR gene transfer.

Currently, the use of pseudotyped lentiviral vectors is discussed as a possible alternative to AV- and AAV vectors (55-57). Lentiviral vectors pseudotyped with hemagglutinin and fusion protein of the Sendai virus (SeV) are able to efficiently transduce airway epithelial cells from the apical surface and have high tropism towards the respiratory tract (55). In the last years, efficient transduction and restoration of CFTR expression has been demonstrated *in vitro* (55, 56). Moreover, repeated administration of lentiviral vectors has shown to be feasible in mice (55-57). However, it must be noted that, although they are generally considered to have an acceptable safety profile (56), lentiviruses are integrating vectors. Therefore, they always hold a possible risk of genotoxicity, as has been observed for the use of $\gamma$-retroviruses, which induced leukemia in patients

suffering from severe combined immunodeficiency syndrome (58). Moreover, although they achieved partial correction of the ion conductance defect in intestinal organoids, their efficiency in other experimental animals is still unclear (57). Safety and efficiency of lentiviral-mediated CFTR gene transfer in men remains to be assessed as well (57). Taken together further extensive toxicology studies and clinical trials, evaluating lentiviral-mediated CFTR gene transfer to CF patients, must be conducted before coming to a definite conclusion whether lentiviral vectors are suitable vehicles for CFTR gene transfer.

As an alternative to the use of viral vectors delivery of h*CFTR* cDNA using cationic liposomes has also been closely investigated. In contrast to viral vectors, they do not contain protein, which decreases the risk of inducing immune responses (59). In 1993 Hyde, Gill et al. successfully transfected HeLa cells and murine airway epithelial cells with h*CFTR* plasmid DNA complexed with cationic liposomes, correcting the ion conductance defect (60). Further promising results in the following years (61-63) encouraged the first phase 2b trial delivering GL67A/pGM169 h*CFTR* pDNA to CF patients in 2015. However, this trial showed only modest success (64). There was a stabilization of lung function observed, but no improvement of the patient's quality of life could be achieved (64). Consequently, immediate progression to a phase III trial was not initiated (59). These somewhat disappointing results emphasize the need to investigate new alternatives of gene delivery.

Taken together the use of h*CFTR* DNA to replace the missing CFTR-protein in CF patients, despite promising pre-clinical results, has not yet shown to be suitable for clinical use and to efficiently restore lung function in CF patients. These current findings additionally highlight the need to investigate alternative approaches for therapeutic protein delivery. A further promising alternative is mRNA-mediated CFTR delivery.

### 1.3.3 mRNA-therapy

RNA is a ribonucleic acid, which is transcribed from DNA in the nucleus. Unlike DNA, RNA is single-stranded and contains ribose instead of deoxyribose and uridine instead of thymidine. There are numerous different RNA forms, which can be divided into coding RNAs, as mRNA, and non-coding RNAs, e.g., tRNA, rRNA,

and siRNA. mRNA comprises 2 – 5 % of the cellular RNA and constitutes a template for protein synthesis in the cytosol. In eukaryotic cells mRNA is co- and post-transcriptionally processed, which includes capping, polyadenylation and splicing. Mature mRNA is built of five elements: a 5'-cap, a 3' poly(A)-tail, a 3'- and a 5'-untranslated region and an open reading frame (ORF). (65). The 5'-cap consists of a N7-methylguanosine (m7G), which is connected to the 5'-end of the mRNA through a 5'-5'-triphosphate bridge (Cap 0). Additionally, the first and second nucleotide downstream of the m7G can be 2'-O-methylated, forming Cap 1 or Cap 2 structures. (66). The 5'-cap is important for stabilization of the mRNA and increasing its translational efficiency (67). Moreover, its presence enables innate immune receptors to differentiate between "self" and "foreign" mRNA (66, 67). The poly(A) tail is built of 100 – 250 adenine residues and improves translational efficiency as well (68). Additionally, it protects the mRNA from degradation (66, 68). Finally, the untranslated regions are essential for post-transcriptional regulation of gene expression (69) and the ORF is the protein encoding region.

In the early 90's the therapeutic potential of mRNA-delivery for protein supplementation *in vivo* was already demonstrated (70, 71). However, until 2010, the use of and research on clinical application of mRNA has been limited to the use of mRNA as a potential cancer and antiviral vaccine, inducing specific cytotoxic T-cell responses (72-74). The use of mRNA for therapeutic protein delivery was not possible mainly due to mRNA's immunogenicity and instability *in vivo*. These obstacles are based on various endosomal and cytoplasmic pattern recognition receptors (PRRs), which particularly recognize RNA-structures. As these PRRs are involved in the host's antiviral defense, they induce inflammatory responses upon activation. (75) The major source for immune activation by mRNA, are endosomal toll-like-receptors (TLRs). TLR 3 recognizes double-stranded RNA (dsRNA) (76), while TLR 7 and 8 are activated through single-stranded RNA (ssRNA) structures, especially those containing uridine-stretches (77-79). Throughout the last years, more PRRs, activated by exogenous mRNA, were identified, such as retinoic acid-inducible gene I (RIG-I), melanoma differentiation-associated protein 5 (MDA 5), interferon-induced

tetratricopeptide repeat (IFIT), the 2'-5'-oligoadenylate synthetase/RNase L system and RNA-dependent protein kinase (PKR) (67, 75, 76, 80-83). Upon activation these PRRs induce secretion of proinflammatory cytokines, as type I interferons (IFN), tumor-necrosis-factor (TNF) and interleukins (IL-6, -12). Through downstream signaling pathways, these cytokines lead to inflammation, translational inhibition and mRNA-degradation. (12). Consequently, activation of these PRRs must be avoided for successful mRNA-mediated protein delivery (75).

#### 1.3.3.1 Overcoming immunogenicity

##### Chemically modified nucleosides and HPLC purification

Incorporation of chemically modified nucleosides, which naturally occur in mammalian cells, is one powerful tool for avoiding recognition by cytoplasmic and endosomal PRRs, as TLR 3, 7 and 8, RIG-I, PKR or the 2'-5'-oligoadenylate-synthetase-RNase L system. Chemical modifications, as methylation or isomerization, are abundant in mammalian RNA, not only in mRNA but also in rRNA, tRNA and other RNA structures (84). Their post-transcriptional introduction is considered part of the RNA maturation process. Interestingly, in mammalian RNA methylation and other modifications of nucleosides occur significantly more often than in bacterial RNA (84). This comprises an important difference which most probably serves as a molecular means of discrimination between "self" and "foreign" for the innate immune system (84). Incorporation of chemically modified nucleosides, such as inosine, 5-methylcytidine (m5C), N6-methyladenosine (m6A), 2-thiouridine (s2U), 5-methoxycytidine (5moC), pseudouridine ($\Psi$) and N1-methylpseudouridine (m1$\Psi$), significantly inhibits mRNA-mediated activation of the innate immune system, increasing mRNA's biological stability and translational capacity *in vitro* and *in vivo* (75, 81, 82, 84-90). Another tool for decreasing immune activation is purification of synthetic mRNA by high-performance liquid chromatography (HPLC). HPLC purification purifies the mRNA from contaminants, especially dsRNA, which is a major source of immune activation (91). In 2011 Karikó, Muramatsu et al. demonstrated a 10 - to 1000 - fold increase of translational levels in primary cells, following HPLC purification

(91). Additionally, they successfully administered HPLC-purified Ψ-modified *erythropoietin* mRNA to mice, observing high levels of translation and no induction of proinflammatory cytokines (88). Their findings indicated that HPLC purification of synthetic mRNA might be a promising augmentation to introduction of chemical modifications. However, recent investigations on different approaches to improve *Cas9* mRNA's stability and decrease its immunogenicity indicate that incorporation of certain chemical modifications in combination with uridine-depletion, which will be discussed later, might outperform HPLC purification regarding translational efficiency and immunogenicity of synthetic mRNA (75). The authors suggested that, in their experimental context, the remaining dsRNA after performing HPLC purification, still might have been sufficient to induce immune responses (75). These findings are somewhat questioning the usefulness of HPLC purification of synthetic mRNA to decrease immune responses.

### Sequence-Engineering

Sequence-engineering of a gene or mRNA means altering the nucleotide sequence by substitution of specific nucleotides or whole codons, without altering the amino acid composition of the encoded protein (75). This comprises a further means for improving mRNA's stability, processing and translational efficiency to increase the protein yield.

The idea of sequence-engineering is based on numerous observations that the codon-composition of a gene influences gene expression (92-97). Within the genetic code, one can differentiate between "optimal" and "suboptimal" codons (95, 97, 98). These are partially interchangeable, due to the degeneracy of the genetic code. mRNAs with a high content of "optimal" codons, show increased steady-state levels and translational efficiencies, compared to mRNA's that mainly contain "suboptimal" codons (93, 94, 97, 98). Consequently, it is possible to influence mRNA stability and protein expression by exchanging "suboptimal" codons associated with low protein expression to "optimal" codons for an increase in protein yield. On the other hand, it is also possible to decrease mRNA stability and protein expression by exchanging "optimal" codons with "suboptimal" codons. (93, 95, 97). In the human genome all "optimal" codons end with G or C

in the third degenerative position, so consequently GC-rich genes are usually expressed a several-fold higher than GC-poor genes (93, 95). That is why a common approach of sequence-engineering means to increase a gene's or mRNA's GC-content. However, it is important to note that the codon-composition of a gene may impact protein folding and function as well, and that "suboptimal" codons may have essential functions for final maturation of the protein (98, 99).
Another effective means of sequence-engineering is reducing the uridine content of mRNA (75). Uridine residues in mRNA are crucial for activation of different PRRs, as TLR 7 and RIG-I, which recognize poly(U) stretches (83). Karikó et al. showed that replacement of uridine with Ψ, induces a 10 – 1000 - fold increase in protein expression, which might be due to decreased binding to PKR, decreased activation of the 2'-5'-oligoadenylate-synthetase-RNase L pathway and resistance to RNase L mediated cleavage (79-82, 84, 85, 88). These findings highlight the importance of uridine for immune activation and implicate that reduction of an mRNA's uridine content, might increase its stability and translational efficiency, while decreasing its immunogenicity.
Sequence-engineered mRNA has shown to be competitive to chemically modified mRNA, and might even outperform the latter, depending on the individual mRNA sequence and route of administration (75, 100, 101). Furthermore, as mentioned before, Vaidyanathan et al. also showed that a combination of uridine-depletion and incorporation of 5-methoxy-cytidine into a *Cas9* mRNA, substantially increases its translational efficiency, while eliciting only minimal immune responses (75). All in all, sequence-engineering comprises an additional powerful tool, to improve mRNA's translational efficiency and reduce its immunogenicity *in vivo* (75, 88, 100).

#### 1.3.3.2 Efficient mRNA-delivery

For delivering mRNA *in vivo* there are certain obstacles to overcome. In general mRNA's fragility and the ubiquitous existence of RNases and PRRs constitute the need for an appropriate vehicle system (12). Its highly negative charge makes it difficult for mRNA to cross cellular membranes (2). Moreover, there is a need to implement delivery systems that are able to target specific cell populations or tissues. In case of CF the primary target for CF gene therapy would be the lung's

epithelia (8, 12). In addition to that, targeting lung cell populations, as in CF treatment, leads to certain lung specific challenges to be overcome. These respiratory barriers include respiratory mucus, which is pathologically increased in CF patients and contains mucins, glycoproteins and free DNA, which might interact with therapeutics delivered or cause sterical obstruction. Moreover, mucociliary clearance and alveolar fluid, containing negatively charged surfactant, must be considered. (12, 102-105). Taken together, vehicle systems for mRNA-delivery, should enable targeting a specific tissue, cellular internalization and release of the mRNA into the cytosol, so that it can be translated into protein (106).

A suitable approach to overcome those obstacles for mRNA delivery may be the use of nanocarriers as mRNA-delivery systems (2, 12, 107, 108). Nanocarriers can be roughly divided into lipid-based nanoparticles and polymer-based nanoparticles.

Lipid-based nanoparticles (LNP) are built of an ionizable lipid, which facilitates mRNA's packaging, membrane fusion and endosomal escape (2, 108). In addition to that, they are built of cholesterol and a helper lipid, which increase the stability of the lipid bilayer and promote membrane fusion. The outer layer of the LNP contains a lipid-anchored polyethylene-glycol- (PEG)-lipid which protects the nanoparticles from the respiratory fluid and surfactant, prevents mucosal trapping and increases the mRNA-LNP's physiological stability. (2, 12, 105, 106, 109). Commonly used ionizable lipids for mRNA delivery are 1,2-di-O-octadecenyl-3-trimethylammonium-propane (DOTMA), 1,2-dioleoyl-3-trimethylammonium-propane (DOTAP) and 1,2-dioleoyl-sn-glycero-3-phosphoethanolamine (DOPE), a zwitterionic phospholipid (12). The most prominent lipid-based nanoparticle used is cholest-5-en-3-ol(3β)-3-[(3-aminopropyl)[4-[(3-aminopropyl)amino]butyl]carbamate] (GL67A), which was used by Alton et al. in the first clinical trial administering h*CFTR* pDNA to CF patients (64), due to its well-defined safety-parameters and gene transfer potency (12, 110, 111). Furthermore, h*CFTR* mRNA-LNPs were successfully delivered to murine nasal airways by Robinson et al. in 2018, providing proof-of-concept for the general feasibility of delivering h*CFTR* mRNA via lipid-based nanoparticles (2).

Polymer-based nanocarriers contain cationic polymers, which can complex the negatively charged mRNA, building compact polyplexes and facilitate membrane crossing and cellular uptake via endocytosis (12, 106, 112). Cationic lipids include polyethyleneimine (PEI), poly-L-lysine (PLL), poly(lactic-co-glycolic) acid (PLGA) and poly(2-(dimethylamino)ethyl methacrylate (p[DMAEMA]) (12, 106, 112). As with lipid-based nanoparticles, coating with PEG further increases stability, by protection from degradation and helps in passing respiratory mucus and sputum (12, 105, 113, 114). Furthermore, Chitosan coating of polymer-nanoparticles might improve serum stability as well and even enable deeper lung delivery in CF treatment (115). Encouragingly, chitosan-coated PLGA nanoparticles have been shown to penetrate CF mucus and sputum and h*CFTR* mRNA complexed to chitosan-coated PLGA nanoparticles has already been successfully administered to murine airways by Haque et al. in 2018 (115).

Apart from coating with PEG or Chitosan, administration of nanocarriers with mucolytic agents as human DNase 1 or N-Acetylcysteine, is another way of facilitating mRNA delivery to the lung (12, 116-119).

Important factors for *in vivo* use of nanocarriers are their biodegradability and biocompatibility. Biodegradability means, the degradation of molecules through *in vivo* biological actions, while biocompatibility means that materials, which are administered *in vivo*, do not elicit any toxic, injurious or immunogenic response (120). While LNPs are generally biocompatible, some polymers, as PEI can have toxic effects *in vivo*, due to their non-degradability and formation of aggregates with negatively charged serum proteins (12, 121). Material, which is not biodegradable and biocompatible is therefore unsuitable for nucleic acid delivery.

Other nanocarriers include hybrid polymer-lipid nanoparticles, for example containing poly-β-aminoesters (PBAEs) and PEG-lipid (107) and receptor-based technologies, which can be used for mRNA-based therapy of α1-antitrypsin deficiency (AATD), for example (12).

To target lung diseases as CF, mRNA-based therapeutics can be administered either intravenously (i.v.) or intratracheally (i.t). Intravenous application has the advantage of circumventing certain lung-specific barriers, as respiratory mucus, and surfactant. However, by leading to a systemic distribution of the drug

administered, i.v. application also requires higher doses to achieve an effective dose in the lung (12, 115, 122). Furthermore, it might be difficult to reach lung regions which are farther away from the capillaries, as these are not suitable for larger molecules to pass (12, 123). On the other hand, intratracheal administration leads to a local distribution of the mRNA, and the large alveolar surface area is most suitable for drug absorption, which might ease mRNA-delivery to the lung (12, 124). Moreover, i.t. application might be more successful in targeting specific lung cells (12, 102).

#### 1.3.3.3 RNA-based therapy: possible applications

Encouraging findings of mRNA-mediated protein expression *in vitro* were followed by investigation of its applicability *in vivo*. In 2010, Warren et al. first demonstrated the feasibility of modified mRNA-mediated therapeutic protein delivery *in vivo*, administering modified mRNA encoding different transcription factors for induction of pluripotent stem cells (87). Their findings were followed by numerous trials, investigating *in vivo* use of mRNA for therapeutic protein delivery, which constitute important milestones in the development of mRNA-based gene supplementation therapy (88-90, 100). Throughout the last years therapeutic potential of mRNA-treatment for numerous diseases has been demonstrated. Some examples are listed in the table below.

Table 1.1: mRNA-based therapy – possible applications

| Disease | Gene/Protein | Administration route | Organism | Reference |
|---|---|---|---|---|
| SP-B deficiency | SP-B | intratracheal | mice | Kormann, Hasenpusch et al. 2011 (90) |
| Allergic asthma | FOXP3 | intratracheal | mice | Mays, Ammon-Treiber et al. 2013 (125) |
| Myocardial infarction | VEGF-A | intramyocardial | mice | Zangi, Lui et al. 2013 (89) |
| Allergic asthma | TLR 1/2; TLR 2/6 | intratracheal | mice | Zeyer, Mothes et al. 2016 (126) |
| $\alpha_1$-Antitrypsin deficiency | SERPINA1 | intravenous | mice | Connolly, Isaacs et al. 2018 (127) |
| Vascular Disease | VEGF-A | intradermal | human | Gan, Lagerstrom-Fermer et al. 2019 (128) |
| SP-B deficiency | ZFN + AAV6 donor | intratracheal | mice | Mahiny, Dewerth et al. 2015 (129) |
| β-Thalassemia | Cas9 + ssODN* donor | electroporation | K562, $CD34^+$ HSC** | Antony, Latifi et al. 2018 (130) |

* ssODN (single-stranded oligodeoxynucleotides)

** HSC (hematopoietic stem cells)

#### 1.3.3.4 mRNA-based CF gene therapy

Kormann's findings from 2011, presented a proof-of-concept for delivery of chemically modified mRNA to murine lungs *in vivo*. By successfully targeting SP-B deficiency in mice, they demonstrated the general feasibility of mRNA-based therapy to target lung diseases (90).

Indeed, in the following years the concept of protein supplementation via mRNA delivery was applied to therapy of CF lung disease in several studies, presenting encouraging results *in vitro* as well as *in vivo* (2, 115, 131).

h*CFTR* mRNA delivery via lipid-based as well as via PLGA nanocarriers has shown to efficiently deliver h*CFTR* mRNA to murine airway epithelia, restoring hCFTR expression and function (2, 115). In order to increase the h*CFTR* mRNA's stability and translational efficiency and to reduce its immunogenicity introduction of chemical modifications was necessary and significantly improved h*CFTR* mRNA's efficiency, finally resulting in a restoration of lung function in a CF mouse model (115). Moreover, chemically modified h*CFTR* mRNA could be administered both topically as well as systemically (115).

Encouragingly in 2018 Translate Bio initiated a phase I/II first-in-human clinical trial, investigating safety and tolerability of LNP-mediated h*CFTR* mRNA (MRT5005) delivery by nebulization to adult CF patients (132). The trial aims to evaluate single (SAD) and multiple ascending doses (MAD) of MRT5005 in adult CF patients. In October 2019, interim results of the SAD portion of the trial were presented. 12 adult CF patients received either a single dose of MRT5005 or placebo. MRT5005 was administered in three different doses: 8, 16 and 24 mg. There were no treatment-emergent serious adverse effects observed, all treatment-emergent adverse effects were considered mild to moderate. To evaluate the lung function of the patients, $ppFEV_1$ was measured at pre-defined timepoints. While there was no marked improvement found in the pooled placebo group and the group receiving 8 mg of MRT5005, there was a mean maximum change from baseline $ppFEV_1$ throughout day 8 of 15.7 % in the 16 mg group and of 9.7 % in the 24 mg group. (133). These highly encouraging findings comprise an additional step forward towards realization of mRNA-based gene

therapy for CF. Presentation of the next interim results, including the MAD portion of the trial, in 2021 is highly anticipated.

### 1.4 My question

Taken together, there is no doubt that mRNA-based protein supplementation holds several advantages over pDNA-based protein delivery: lower risk of severe immune reactions and insertional mutagenesis, cytosolic delivery, efficiency in non-dividing cells and biodegradability, thereby avoiding permanent adverse effects (12, 90, 108, 131, 134). Overcoming mRNA's immunogenicity by introduction of modified nucleosides, HPLC purification and sequence-engineering has finally brought mRNA-based protein supplementation therapy into clinical trials.

Being a monogenic disease, based on missing or unfunctional CFTR protein, renders CF a suitable and promising application field for protein supplementation therapy. As channel modulators only provide modest improvement of lung function and pDNA-based h*CFTR* delivery has shown mainly unsuccessful in clinical trials, there is still a strong need for alternative treatment strategies for CF lung disease (27, 32, 33). hCFTR protein delivery via chemically modified mRNA has shown successful in murine airways, reaching increases of the $FEV_{0.1}$ (murine analog to $FEV_1$ in humans) of up to 23 percentage points (2, 115). These encouraging results are further supported by the currently ongoing phase I/II clinical trial, administering h*CFTR* mRNA to adult CF patients (133). Taken together, mRNA-based h*CFTR* delivery has come up as a new, promising alternative to efficiently treat CF lung disease.

Until now only modified h*CFTR* mRNA has been investigated in pre-clinical trials. However, sequence-engineered mRNA has shown to be at least competitive to modified mRNA *in vivo* (100). Recently, uridine-depletion of *Cas9* mRNA has shown to significantly reduce its immunogenicity and increase protein expression *in vitro* and *in vivo* (75). These findings indicate that uridine-depletion of h*CFTR* mRNA might increase its translational efficiency and decrease its immunogenicity as well and constitute a further means of generating efficient h*CFTR* mRNA for protein supplementation.

Finally, this thesis investigates the use of sequence-engineered uridine-depleted (UD) h*CFTR* mRNA for protein-replacement therapy *in vitro and in vivo*. Administration of UD h*CFTR* mRNA is compared to UD h*CFTR* pDNA and non-UD h*CFTR* mRNA. Expression of the hCFTR gene and protein in CFBE41o$^-$ cells and murine airways is investigated. Moreover, the hCFTR protein's functionality is assessed as well as the cytotoxicity of uridine-depleted h*CFTR* mRNA.

# 2 Material and Methods

## 2.1 Material

Table 2.1: Devices

| Device | Manufacturer |
|---|---|
| Agilent 2100 Bioanalyzer | Agilent Biotechnologies |
| Autoklav Systec VX-150 | Lonza |
| BD FACS X-20 Fortessa | Systec |
| Centrifuge 5430R | eppendorf |
| $CO_2$ incubator HERAcell 150i/HERAcell VIOS 160i | Thermo Fisher Scientific |
| Darkhood DH-50 | Biostep |
| EnSight Multi Mode Plate Reader | Perkin Elmer |
| Exposure Cassette-K | Bio-Rad |
| FlexiVent FX1 | Scireq |
| Forceps (sharp, curved) | DUMONT |
| Forceps (blunt, straight, atraumatic) | Asanus |
| Freezer MediLine (-20°C) | Liebherr |
| Freezer Model 905 (-80°C) | Thermo Fisher Scientific |
| Fridge MediLine (4°C) | Liebherr |
| Gelchamber model 40-0911 | peqlab |
| Gel Knife for XCell II Mini-Cell | Thermo Fisher Scientific |
| HERASAFE KS 12 | Thermo Fisher Scientific |
| IKA MS 3 Vortexer | IKA |
| Incubator INFORS HT Ecotron | infors |
| Iris-scissors (sharp; straight, curved) | Carl Roth |
| Kern EW 2200-2NM scale | KERN und SOHN |
| Laminar-flow hood BDK 6.12S | BDK Luft- und Reinraumtechnik GmbH |
| Microscope, Type Wilvert 30 | Hund WETZLARF |
| Medisana IRL | Philips |
| MP-300V power supply | Major science |

| | |
|---|---|
| Nanodrop 2000c | Implen |
| Neubauer improved cell counting chamber | Assistent |
| Perfect Spin P | VWR peqlab |
| Pipettes (0.1 µl – 2.5 µl, 0.5 – 10 µl, 2 – 20 µl, 10 – 100 µl, 20 – 200 µl, 100 – 1000 µl, 1 – 5 ml) | eppendorf |
| Pipetus | Hirschmann Laborgeräte |
| Powerease 500 Powersupply | BioTech Products GmbH |
| Precellys Evolution | Bertin Technologies |
| RS-TR05 horizontal roller | Phoenix instrument |
| Tailveiner restrainer standard 1 ¼ ‘’ id | Braintree Scientific |
| Thermocycler peqSTAR 96 universal | VWR peqlab |
| Thermoshaker | Universal Labortechnik |
| Tissue Ruptor | QIAGEN |
| Viia 7 Real-Time PCR System | Thermo Fisher Scientific |
| Vortex Genie 2 | Scientific Industries |
| Waterbath | neolab |
| XCell II Blot Moule | Thermo Fisher Scientific |
| XCell SureLock | Thermo Fisher Scientific |

Table 2.2: Reagents and Solution

| **Reagent/Solution** | **Manufacturer** |
|---|---|
| 2- Propanol | AnalaR NORMAPUR |
| Agarose LE | Biozym |
| Anti reverse cap analog (ARCA) | Jena Bioscience |
| Adenosine-Triphosphate (ATP) | New England Biolabs |
| Chitosan-PLGA Nanoparticles | - |
| Chloroform | Sigma Aldrich |
| CutSmart Buffer (10x) | New England Biolabs |
| DESCOSEPT AF | Dr. Schumacher |

| | |
|---|---|
| DNA AWAY, 4/ | Molecular BioProducts |
| DNA ladder 1 kb, GeneRuler, 0.5 µg/ml | Thermo Fisher Scientific |
| DNA loading dye (6x) | Thermo Fisher Scientific |
| dNTP mix (10 mM each) | VWR peqlab |
| Dulbeccos's phosphate buffered saline (PBS) | Thermo Fisher Scientific, Sigma Aldrich |
| Dithiothreitol (DTT) | Thermo Fisher Scientific |
| Ethanol absolute | AnalaR NORMAPUR |
| FACSClean solution | BD |
| FACSRinse solution | BD |
| Fentadon (50 µg/ml) | Albrecht |
| Fetal bovine serum (FBS) | Biochrom GmbH |
| GelRed Nucleic Acid Stain, 10,000x in water | Biotium |
| Glycerol | Carl Roth |
| HCl 0.02 N solution | Thermo Fisher Scientific |
| Kanamycin Sulfate | Thermo Fisher Scientific |
| Lipofectamine 2000 | Thermo Fisher Scientific |
| Luria Broth (LB) | Thermo Fisher Scientific |
| LB-agar | Thermo Fisher Scientific |
| Medetomidine | - |
| Methanol | MERCK |
| Midazolam | - |
| Minimum essential medium (MEM) | Thermo Fisher Scientific |
| MTT 3-(4,5-dimethythiazol-2-yl)-2,5-dephenyltetrazolium bromide | Carl Roth |
| NEB-buffer 2 | New England Biolabs |
| Non-fat dry milk | Cell Signaling Technology |
| Novex Sharp Pre-Stained Protein Standard | Thermo Fisher Scientific |

| | |
|---|---|
| NuPAGE MOPS SDS Running buffer (20x) | Thermo Fisher Scientific |
| NuPAGE Transfer Buffer (20x) | Thermo Fisher Scientific |
| NuPAGE LDS Sample Buffer | Thermo Fisher Scientific |
| NuPAGE Sample Reducing Agent (10x) | Thermo Fisher Scientifc |
| Opti-MEM, serum reduced medium | Thermo Fisher Scientific |
| Penicillin-Streptomycin (10,000 U/ml) | Genaxxon bioscience |
| Ponceau S Staining Solution | Cell Signaling Technology |
| Power SYBR Green PCR Master Mix | Thermo Fisher Scientific |
| Protease Inhibitor Cocktail P8340 | Sigma Aldrich |
| RIPA Buffer | Sigma Aldrich |
| RNASE AWAY, 4/ | Molecular BioProducts |
| SDS sodium dodecyl sulfate | Sigma Aldrich |
| SeaKem LE Agarose | Lonza |
| Sheath fluid | BD |
| TWEEN 20 | Sigma Aldrich |
| TAE buffer (Tris-acetate-EDTA) (10x) | Thermo Fisher Scientific |
| Trypan Blue 0.4% | MERCK |
| Trypsin-EDTA 0.25% | Thermo Fisher Scientific |
| TriFast | VWR peqlab |
| Water (DEPC-treated) | ambion |

Table 2.3: Consumables

| **Consumable** | **Manufacturer** |
|---|---|
| Amersham Hyperfilm ECL | GE Healthcare Limited |
| 3M Aura Health Care Respirator (FFP3) | 3M |
| Bolt 4-12% Bis-Tris Plus (1.0 mm x 12 well) | Thermo Fisher Scientific |
| Capillaries (heparinized) | Hirschmann |

| | |
|---|---|
| Cell culture flasks (T-75 -75 $cm^2$, T-25 25 $cm^2$) | Greiner bio-one |
| Cell culture plates (12-well, 96-well) | Corning |
| Dualfilter pipette tips (0.1 – 10 µl, 10 – 200 µl, 100 – 1000 µl) | eppendorf |
| FACS tubes (5ml, PS) | Corning |
| Falcon tubes (15 ml, 50 ml) | Greiner bio-one |
| Gloves Peha-soft nitrile | Hartmann |
| Injekt-F single-use syringes (1 ml, 20 ml) | B. Braun |
| Kimwipes | Kimberly-Clark |
| MicroAmp optical 96-well reaction plate | Thermo Fisher scientific |
| Microlance 3 (20G x 1 ½ ‘’) | BD |
| Micro tube for serum separation | Sarstedt |
| Nitrocellulose Membrane (0.45 µm Pore Size) | Thermo Fisher Scientific |
| Omnican 40 single-use insuline synringe (1 ml) | B. Braun |
| Parafilm M sealing | Parafilm |
| Pasteur Capillary Pipettes (230 mm) | neoLab |
| Polymerase Chain Reaction (PCR) strips (8 tubes, 0.2 ml) | Greiner bio-one |
| Pipetting Reservoir (25 ml) | ARGOS Technologies |
| Petri dishes (96 nm) | Greiner bio-one |
| Pipette tips, 10 µl | Biozym |
| Pipette tips, 200 µl | Sarstedt |
| Pipette tips, 1000 µl | Greiner bio-one |
| qPCR Seal | 4titude |
| Reaction tubes (Safe-lock 0.5 ml, 1.5 ml, 2 ml) | eppendorf |
| Safety-Multifly-Needle | Sarstedt |

| | |
|---|---|
| Serological pipettes (5 ml, 10 ml, 25 ml, 50 ml) | Corning |
| Surgical disposable scalpels | B. Braun |
| Tissue Culture Dish | BD |
| TopSeal-A Plus | PerkinElmer |

Table 2.4: Kits

| **Kit** | **Manufacturer** |
|---|---|
| Agilent RNA 6000 Nano Kit | Agilent Technologies |
| Chloride Assay Kit | Sigma Aldrich |
| HiScribe T7 High Yield RNA Synthesis Kit | New England Biolabs |
| IL-6 human uncoated ELISA Kit | Thermo Fisher Scientific |
| IL-12 human uncoated ELISA Kit | Thermo Fisher Scientific |
| Human CFTR ELISA Kit | Elabscience |
| iScript cDNA synthesis kit | Bio-Rad |
| MEGAclear Transcription Clean-Up Kit | Thermo Fisher Scientific |
| MEGAscript T7 Transcription Kit | Thermo Fisher Scientific |
| Monarch PCR & DNA Cleanup Kit (5 µg) | New England BioLabs |
| Monarch RNA Cleanup Kit | New England BioLabs |
| Novex ECL HRP Chemiluminescent Substrate Reagent Kit | Thermo Fisher Scientific |
| NucleoSpin Tissue | Macherey-Nagel |
| peqGOLD Xchange Plasmid Midi Kit | VWR peqlab |
| Pierce BCA Protein Assay Kit | Thermo Fisher Scientific |
| Precellys Lysing Kit | Bertin Technologies |
| PureLink RNA Mini Kit | Thermo Fisher Scientific |
| RNeasy Mini Kit | QIAGEN |

| | |
|---|---|
| TNF alpha human uncoated ELISA Kit | Thermo Fisher Scientific |

Table 2.5: Enzymes

| **Enzyme** | **Manufacturer** |
|---|---|
| *Not*I-HF | New England BioLabs |
| iScript reverse transcriptase | Bio rad |
| T7 RNA Polymerase Mix | New England BioLabs |
| Turbo DNase | Thermo Fisher Scientific |

Table 2.6: Plasmids

| **Plasmid** | **Insert** | **Manufacturer** |
|---|---|---|
| pVax.A120 | - | Thermo Fisher Scientific |
| pVax.A120 | h*CFTR* UD | cloning |
| pVax.A120 | h*CFTR* non-UD | cloning |

Table 2.7: Primers

| **Primer** | **Sequence (5’ → 3’)** |
|---|---|
| 18S fwd | GTA ACC CGT TGA ACC CCA TT |
| 18S rev | CCA TCC AAT CGG TAG TAG CG |
| | |
| h*CFTR* fwd | GAG ATG CTC CTG TCT CCT GG |
| h*CFTR* rev | CCT CTC CCT GCT CAG AAT CT |
| | |
| h*CFTR* UD fwd | CGC CCA TTA TGA CCA TGA GCA G |
| h*CFTR* UD rev | CGC CCA TTA TGA CCA TGA GCA G |

Table 2.8: Antibodies

| Antibody | Antigen | Source | Conjugate | Manufacturer |
|---|---|---|---|---|
| Anti-β-Actin | β-Actin | rabbit | - | Cell signaling technology |
| Mouse anti-rabbit IgG | rabbit | mouse | HRP | Santa Cruz Biotechnology |
| Goat anti-mouse IgG | mouse | goat | HRP | Santa Cruz Biotechnology |
| Anti-hCFTR clone 596 | CFTR | mouse | - | Provided by CFF |

Table 2.9: Software

| Software | Manufacturer |
|---|---|
| ApE | M. Wayne David (open source) |
| BD FACSDiva | BD |
| BioRender.com | BioRender |
| FlowJo | FlowJo LLC |
| GraphPad PRISM | GraphPad Software, Inc. |
| ImageJ | NIH Image |
| Microsoft Excel | Microsoft |
| ViiA7 | Thermo Fisher Scientific |

## 2.2 Methods

### 2.2.1 Cell culture: HEK-293, HBE- and CFBE41o-cells

All the cells used were kept in 37°C at 5 % $CO_2$ in a 95 % humidified chamber culture.

The CFBE41o$^-$- cells were kept in MEM +10% FCS + 1 % L-Glutamine + 1 % Penicillin/Streptomycin.

When they reached 80 - 90 % confluency, media was removed, cells were washed with 10 ml cold, sterile PBS, then trypsinized with 2 ml of 0.025 % EDTA-Trypsin for 5 min. After adding 8 ml of minimal essential medium (MEM + 10 % FCS + 1 % L-Glutamine + 1 % Penicillin/Streptomycin) they were collected and spun down at 500 x g for 5 min. Afterwards media was removed, and the cells were resuspended in fresh MEM and split 1:3 or 1:2.

### 2.2.2 Amplification and purification of the pVax h*CFTR* plasmid

To produce pVax UD/non-UD h*CFTR* plasmids, a UD/non-UD h*CFTR* template was cloned into a pVax.A120 plasmid and amplified by transformation of the plasmid into chemically competent TOP 10 *E. coli.* After transformation, the bacteria were grown on LB-agar plates with kanamycin at 37°C overnight, to select the bacteria that express the pVax h*CFTR* plasmid, carrying a kanamycin resistance. For further use, single colonies were picked up from the LB-agar plate and were inoculated in 5 ml of LB-Kanamycin medium. The liquid culture was incubated overnight at 37°C and constant shaking (160 rpm). The next day, a glycerol stock was prepared for long term storage of the bacteria. In this context, 500 µl of bacterial suspension were added to 500 ml glycerol, mixed well and stored in - 80°C.

In order to obtain pVax UD/non-UD h*CFTR* plasmids for *in vitro* and *in vivo* experiments, 50 µl of the bacterial glycerol solution were added to 50 ml LB-Kanamycin medium and incubated again overnight at 37°C and constant shaking (160 rpm). The next day, plasmid purification was performed at midi-scale, using the QIAGEN Plasmid Midi Kit as well as the peqGOLD xChange Plasmid Midi Kit,

following the manufacturer's instruction with the exception of spinning at 7,197 g for 1 hour/20 min instead of 15,000 g for 30 min/10 min.

### 2.2.3 *In vitro* transcription (IVT): h*CFTR*-mRNA-synthesis

For generating a template for *in vitro* transcription (IVT) of UD/non-UD h*CFTR* mRNA a UD/non-UD h*CFTR* pVax plasmid was used as a template.

The plasmid was *Not*I-linearized. The setup for the restriction digest is shown in the table below.

For confirmation of linearization an agarose gel electrophoresis (100 V, 50 min) was performed to separate the nucleic acids by size. For performing an agarose gel electrophoresis an electric field is applied, so that the negatively charged nucleic acids migrate to the positive electrode. The smaller the molecule, the faster it migrates through the gel.

The gel electrophoresis was followed by purification of the linearized plasmid using the NEB Monarch PCR & DNA cleanup kit following the manufacturer's instruction.

Table 2.10: Plasmid linearization setup

| **Component** | **Amount [µl]** |
|---|---|
| pVax.A120 UD/non-UD h*CFTR* plasmid | 5 µg |
| *Not*I restriction enzyme | 2.5 |
| 10x CutSmart Buffer | 5 |
| Water | *Ad* 50 |
| **Total** | 50 |

For IVT of the UD h*CFTR* mRNA we utilized a recombinant T7 polymerase. The IVT was performed using the NEB High Yield RNA Synthesis Kit (reaction setup shown in Table 2.11).

The samples were then incubated for 2 hours at 37°C, then the template DNA was digested by 1 µl Turbo DNase/sample for 15 min at 37°C. Subsequently RNA cleanup was performed using the NEB Monarch RNA cleanup kit, following the manufacturer's instruction.

Table 2.11: IVT reaction setup

| Component | Amount [µl] |
|---|---|
| ATP | 3 |
| CTP | 3 |
| UTP | 3 |
| GTP | 1.5 |
| ARCA | 2,4 |
| 10x reaction buffer | 4 |
| pVax.A120 h*CFTR* plasmid | 2000 ng |
| Enzyme mix | 4 |
| DEPC-water | *Ad* 40 |
| **Total** | 40 |

Finally, we determined the RNA's integrity using the Agilent 2100 Bioanalyzer with the RNA 6000 Nano Kit.

### 2.2.4 Transfection of h*CFTR* pDNA/h*CFTR* mRNA into CFBE41o$^-$-cells

To assess therapeutic protein delivery mediated by uridine-depleted h*CFTR* mRNA *in vitro*, a transfection of either UD h*CFTR* pDNA, UD h*CFTR* mRNA or non-UD h*CFTR* mRNA into CFBE41o$^-$ cells was performed. For the transfection Lipofectamine 2000 was used. CFBE41o$^-$ cells are derived from a cystic fibrosis bronchial epithelial cell line, which is homozygous for the F508del-mutation, so they do not naturally express hCFTR.

For transfection 350,000 cells/well were seeded in a 12-well plate and grown overnight in antibiotic-free MEM. In this context, cells were washed with PBS and trypsinized for 5 min. Then trypsin was inactivated by adding 8 ml of antibiotic-free media, cells were centrifuged for 5 min at 500 x g, resuspended in 10 ml of new antibiotic-free media and counted using a NeubauerImproved counting chamber. The 12-well plates were prepared by adding 1 ml of antibiotic-free media to each well, and then the appropriate volume of cell suspension was added dropwise to each well. Cells were incubated overnight to reach 50 – 80 % confluency on the next day.

The next day the transfection was performed, using Lipofectamine 2000. Cells were treated either with UD h*CFTR* pDNA, UD h*CFTR* mRNA or non-UD h*CFTR* mRNA. Moreover, additional duplicates were transfected with *mKate2* mRNA and *mKate2* pDNA respectively, to determine transfection efficiency 24 hours post-transfection. Untransfected CFBE41o$^-$ cells were taken as a negative control.
The day of transfection, two tubes were prepared. The first tube contained plasmid DNA/mRNA and opti-MEM was added to a final volume of 100 µl. The second tube contained Lipofectamine 2000 and opti-MEM at a final volume of 100 µl as well. Both tubes were incubated for 5 min. Then, 100 µl of the second tube were added to the first tube, to obtain 200 µl transfection solution per well. This mixture was incubated again for 7 min. The reaction setup is shown in the tables below.

Table 2.12: Transfection - setup transfection mixture

| **Component** | **Amount [µl]** |
|---|---|
| pDNA/ mRNA | 2000 ng (mRNA)<br>1000 ng (pDNA) |
| Lipofectamine™ 2000 | 3 |
| Opti-MEM | *Ad* 200 µl |
| **Total** | 200 |

Meanwhile media was removed from the wells, cells were washed with PBS and slowly 500 µl of opti-MEM were added. Then 200 µl of transfection mixture were added dropwise to each well.
Cells were incubated for 5 hours at 37°C and tapped every hour, to increase transfection efficiency.
After 5 hours the media was changed to 1 ml normal media (MEM + 10 % FCS+ 10 % Penicillin/Streptomycin).

### 2.2.5 Flow cytometry for assessing transfection efficiency

For Flow Cytometry analysis a BD FACS X-20 Fortessa was used. Cells were first transfected, as described above, with *mKate2* mRNA or *mKate2* pDNA.

mKate2 is a fluorescent protein, emitting fluorescent signals with excitation and emission maxima at 588 and 633 nm respectively. These fluorescent signals can be measured using flow cytometry analysis.

24 hours after transfection, cells were washed with PBS, trypsinized for 5 min and then suspended in FACS buffer (90 % FCS, 10 % PBS). Cells were spun down for 5 min at 500 x g, afterward media was removed, cells were resuspended in PBS and subsequently Flow Cytometry analysis was performed.

Data were analyzed using FlowJo software version 10.

### 2.2.6 RT-qPCR for analysis of hCFTR gene-expression

In order to quantify and assess h*CFTR* expression 24 hours after transfection of UD/non-UD h*CFTR* mRNA or UD h*CFTR* pDNA into CFBE41o$^-$ cells, a Power SYBR®-Green based real-time quantitative PCR (RT-qPCR) was performed using a Viia7 Real-Time PCR System. In a RT-qPCR a sequence of interest is amplified through the binding of primers, that are specific for that sequence and subsequent polymerization by DNA polymerases, as in a PCR reaction. Additionally, in RT-qPCR, a fluorescent dye is added which binds to dsDNA and gives a fluorescent signal, which increases when the amount of dsDNA increases. By measuring in which amplification cycle a particular threshold of fluorescent signal is reached, the RT-qPCR allows conclusions to the extent of gene expression in the cells investigated. When the threshold is reached in an early cycle this is translated into a high gene expression.

#### Total RNA-isolation for RT-qPCR

First total RNA was isolated from CFBE41o$^-$-cells 24 hours post-transfection.

Cells were washed with PBS two times. Then the total RNA-isolation was performed using the QIAGEN RNeasy Mini Kit, following the manufacturer's instruction.

Afterwards the concentration was determined using an Implen® Nanophotometer.

**RT-qPCR: quantification of hCFTR gene expression**

For RT-qPCR the total RNA isolated from the CFBE41o$^-$ cells was used as a template for cDNA synthesis, based on reverse transcription. For cDNA synthesis the iScript cDNA Synthesis Kit was used. The samples were set up in the thermocycler for 30 min. The reaction setup and the thermocycler program are shown the tables below.

Table 2.13: cDNA-synthesis - reaction setup

| **Component** | **Amount [µl]** |
|---|---|
| RNA-sample | 200 ng |
| 5x reaction mix | 4 |
| Reverse transcriptase | 1 |
| Water | *Ad* 20 |
| **Total** | 20 |

Table 2.14: cDNA-synthesis - thermocycler program

| **Step** | **Temperature [°C]** | **Time [min]** |
|---|---|---|
| Heat lid | 110 | |
| Priming | 25 | 5 |
| Reverse Transcription | 46 | 20 |
| Reverse Transcriptase Inactivation | 95 | 1 |

For RT-qPCR the cDNA was diluted 1:20.

To be able to properly assess h*CFTR* expression, a supplementary setup was prepared using 18S-Primers, for amplification of ubiquitously expressed 18S ribosomal RNA. That way, h*CFTR* gene expression could be quantified in relation to 18S gene expression.

The RT-qPCR reaction setup and thermocycler program are shown in the tables below. The MIQE protocols for RealTime experiments were strictly followed.

Table 2.15: RT-qPCR - reaction setup

| **Component** | **Amount [µl]** |
|---|---|
| 2x SYBR Green Master Mix | 7.5 |
| Primer Forward | 0.9 |
| Primer Reverse | 0.9 |
| Template | 5 |
| dd$H_2o$ | 0.8 |
| **Total** | 15 |

The following primers were used in a 1:10 dilution:

h*CFTR* fwd: 5'- GAG ATG CTC CTG TCT CCT GG -3'

h*CFTR* rev: 5'-CCT CTC CCT GCT CAG AAT CT-3'

UD h*CFTR* fwd: 5'-CGC CCA TTA TGA CCA TGA GCA G- 3'

UD h*CFTR* rev: 5'- CGC CCA TTA TGA CCA TGA GCA G- 3'

18S fwd: 5'- GTA ACC CGT TGA ACC CCA TT -3'

18S rev: 5'- CCA TCC AAT CGG TAG TAG CG -3'

Table 2.16: RT-qPCR - Thermocycler program

| **Step** | **Temperature** | **Time [min]** |
|---|---|---|
| Incubation | 95 | 10 |
| Annealing | 95 | 15 s |
| Extension | 60 | 1 |
| | Standard melting curve analysis | |

Analysis of relative gene expression 24 hours after transfection was done based on the ΔΔCt values, calculated using the Viia7 real-time PCR and Microsoft Excel software.

### 2.2.7 Analysis of hCFTR protein-expression using Western Blot

**Protein-isolation for Western Blot**

For Western Blot analysis 24 hours post-transfection of CFBE41o$^-$-cells with either UD h*CFTR* pDNA or UD/non-UD h*CFTR* mRNA, protein was isolated from the CFBE41o$^-$ cells.

For protein-isolation a 1:100 dilution of protease inhibitor cocktail in RIPA-buffer, was prepared.

Cells were washed two times with PBS and centrifuged for 5 min at 500 x g. Afterwards the supernatant was removed and 50 µl of the RIPA-PIC cocktail were added. To promote homogenization of the cells, the samples were mixed thoroughly with a 20 G syringe. Samples were then incubated on ice for 20 min and centrifuged at 20,000 x g for 20 min at 4°C. The supernatant was stored at -20°C for further use.

**BCA-Assay: Determination of protein concentration**

After protein-isolation the protein-concentrations had to be determined. Therefore, a BCA-Assay was performed. For the BCA Assay the Pierce BCA Protein Assay Kit was used, following the manufacturer's instructions for the microplate procedure.

The Assay was performed using two replicates for each sample/standard.

The absorption was then measured using an Ensight Multimode plate reader and the Kalaido® software and concentrations were calculated using the WorkOut Plus® software.

**Western Blot: Assessment of hCFTR-protein expression**

To assess hCFTR-protein expression a western blot was performed. First a sodium dodecyl sulfate polyacrylamide gel electrophoresis (SDS-PAGE) was run to separate the proteins by molecular weight. For SDS-PAGE a NuPAGE® Bis-Tris Gel and a Bolt Mini Gel Tank was used. Electrophoresis buffer, transfer buffer and protein samples were prepared as shown in the tables below.

The gel was loaded with a total of 40 µl per well, for the protein ladder 10 µl were used.

The Gel was run for 1 hour on 200 V and 120 mA.

Table 2.17: Western Blot - setup for electrophoresis buffer

| **Component** | **Amount [ml]** |
|---|---|
| NuPAGE® SDS Running buffer (20 x, MOPS) | 25 |
| NuPAGE® Antioxidant | 0.5 |
| $ddH_2O$ | 475 |
| **Total** | 500.5 |

Table 2.18: Western Blot - setup for transfer buffer

| **Component** | **Amount [ml]** |
|---|---|
| Methanol | 100 |
| NuPAGE® Buffer (20 x) | 25 |
| NuPAGE® Antioxidant | 0.5 |
| $ddH_2O$ | 375 |
| **Total** | 500.5 |

Table 2.19: Western Blot - setup for protein samples

| **Component** | **Amount [µl]** |
|---|---|
| Sample | 20 µg |
| LDS Sample Buffer (4 x) | 10 |
| Sample Reducing Agent (10 x) | 4 |
| $ddH_2O$ | *Ad* 40 |
| **Total** | 40 |

After SDS-PAGE was run, immunoblotting was performed, using a XCell II Mini-Cell and blot modules. Blotting pads, filter paper and nitrocellulose transfer membranes (pore size = 0.45 µm) were pre-soaked and assembled together with the gel.

The assembly was done starting with two blotting pads, filter paper, gel, transfer membrane, filter paper and finishing again with two blotting pads.

The transfer was then run for 1 hour at 30 V and 170 mA. Through application of an electric field, the proteins were transferred onto the nitrocellulose membrane. Subsequently the transfer membranes were transferred into 20 ml blocking buffer (95 % PBS-T 0.05 %, 5 % nonfat dry milk) and incubated on a horizontal roller for 1 hour at room temperature.

For the primary staining two different antibodies were used. For detection of hCFTR a mouse anti-hCFTR 596 monoclonal antibody was used in a 1:500 dilution (kindly provided by the cystic fibrosis foundation therapeutics Inc.), for detection of β-Actin, as a housekeeping protein to normalize band intensities, a rabbit anti-β-Actin monoclonal antibody was used in a 1:1000 dilution. Both antibodies were diluted in a total of 2.5 ml blocking buffer and incubated on a horizontal roller overnight at 4°C.

After washing the transfer membranes 6 times for 5 min in 20 ml PBS-T 0.05% secondary staining was performed using a goat-anti-mouse antibody diluted 1:5000 for hCFTR staining and a goat-anti-rabbit antibody diluted 1:1000 for β-Actin staining. Both antibodies were horseradish peroxidase-conjugated and diluted in a total of 2.5 ml blocking buffer. The transfer membranes were incubated for 1 hour on a horizontal roller in dark. After incubation, the transfer membranes were washed again 6 times for 5 min in 20 ml of PBS-T 0.05 %.

Finally, the detection was performed. First both membranes were incubated in 2 ml detection solution, which was prepared using the Novex® ECL HRP chemiluminescent substrate reagent kit. After 1 min incubation the transfer membrane was turned and incubated for another 30 s.

Afterwards the detection was continued in a dark room. Exposure was done for 5 min, 1 hour and 2 hours and then the film was incubated for 1 min in development solution, then 1 min in fixation solution and finally incubated for 1 min in water.

Semi-quantitative analysis was conducted using the ImageJ software.

### 2.2.8 MTT-Assay: assessment of cell viability following transfection

In order to quantify cell death following transfection of CFBE41o$^-$ cells with either UD h*CFTR* mRNA, non-UD h*CFTR* mRNA or UD h*CFTR* pDNA an MTT (3-(4,5-dimethylthiazol-2-yl)-2,5-diphenyltetrazolium bromide) - Assay was carried out.

CFBE41o$^-$ cells were seeded in a 96-well plate (40,000/well) in 100 µl antibiotic-free MEM and grown overnight in 37°C at 5 % $CO_2$ and 95 % humidity to reach a 90-100 % confluency. The next day, cells were washed with cold sterile PBS and then transfected with either UD/non-UD h*CFTR* pDNA, UD/non-UD h*CFTR* mRNA, *mKate2* mRNA or *mKate2* pDNA. The setup is shown in the table below. All transfections were done in triplicates. Untransfected CFBE41o$^-$ cells were taken as a positive control. Moreover, we included a triplicate receiving Lipofectamine 2000 only.

Table 2.20: MTT-Assay - transfection setup

| **Component** | **Amount [µl]** |
|---|---|
| mRNA/pDNA | mRNA: 250 ng<br>pDNA: 125 ng |
| Lipofectamine 2000 | 0.4 |
| OPTI-MEM | *Ad* 25 |
| **Total** | 25 |

The transfection was performed, as described before. After five hours the media was changed to 100 µl normal MEM and cells were grown overnight in 37°C at 5 % $CO_2$ in 95 % humidity. Subsequently, the media was changed again to 100 µl of fresh MEM and 10 µl of MTT were added to the cells, which were then incubated for four hours in 37°C at 5 % $CO_2$ in 95 % humidity. During these four hours MTT is reduced to insoluble purple formazan crystals. Subsequently, 100 µl of 10 % sodium dodecyl sulfate (SDS) in 0.02 N HCl solution were added to the cells and pipetted up and down to mix it well. That way the formazan crystals were dissolved. The cells were then again incubated overnight in 37°C at 5 % $CO_2$ and 95 % humidity.
Finally, the absorbance was measured at 570 nm using an Ensight multimode plate reader.

### 2.2.9 Animal Experiments

For further investigation of the therapeutic potential of sequence-engineered h*CFTR* mRNA *in vivo* experiments were carried out. For these experiments $Cftr^{-/-}$ mice were used, as a murine model of Cystic Fibrosis lung disease. As a positive control healthy $Cftr^{+/+}$ mice were used.

All animal experiments were approved by the Regierungspräsidium Tübingen, Baden-Württemberg and performed while strictly following the guidelines of the German law for the protection of animals (file number: K3/16). For the experiments $Cftr^{-/-}$ mice, aged 6 to 8 weeks, were used. These mice were purchased from Jackson laboratory. The mice were kept in standardized, pathogen-free conditions under a 12-hour light-dark cycle. Food, water, and nesting material were fully provided.

At day 1 and 4 40 µg of UD h*CFTR* mRNA (n = 4), non-UD h*CFTR* mRNA (n = 3) and UD h*CFTR* pDNA (n = 4) respectively, complexed with chitosan-coated PLGA nanoparticles [Chitosan (83% deacetylated (Protasan UP CL 113) coated PLGA (poly-D,L-lactide-co-glycolide 75:25 (Resomer RG 752 H)) nanoparticles] were administered intravenously (i.v.) via tailvain injection. The four $Cftr^{-/-}$ mice comprising the control group did not receive any treatment. The total volume administered per injection was 200 µl.

After seven days all mice were sacrificed, and the lungs were isolated for endpoint analysis.

### 2.2.10 Assessment of lung functionality using Flexivent®

The respiratory system presents the main target of therapeutic protein delivery via h*CFTR* mRNA or pDNA. To evaluate the impact of the treatment with UD h*CFTR* mRNA, non-UD h*CFTR* mRNA or UD h*CFTR* pDNA on the murine lung function, lung functionality was assessed using Flexi Vent ®, equipped with FX1 module and negative pressure-driven forced expiration (NPFE) extension and operated by the flexiWare v7.2 software.

Before tracheostomy mice were intraperitoneally anesthetized with a combination of medetomidine (0.5 mg/kg), midazolam (5 mg/kg) and fentanyl (50 µg/kg). Subsequently tracheostomy was performed, starting with a 0.5 cm incision from

rostral to caudal and retraction from a flap of skin. To expose the trachea the connective tissue was dissected and between the second and third cartilage ring a blunt-end stub adapter was installed for connection of the murine respiratory system to the Flexi Vent® system. Ventilation was performed quasi sinusoidally with a tidal volume of 10 ml/kg, a breathing frequency of 150 breaths/min and an inspiratory to expiratory ratio of 2:3.

For determination of the airway resistance (Rn) a coefficient of determination ≥ 0.9 was required. To calculate the static compliance (Cst), a ramp style pressure-driven maneuver (PVr-P) was performed and then the static compliance was calculated from the deflating arm of the pressure-volume (PV) loop. For determination of the $FEV_{0.1}$, an NPFE maneuver was carried out, which is rapidly exposing the murine airways to negative pressure to generate a forced expiratory flow signal. The murine lung was inflated by a pressure of + 30 $cmH_2O$ over 1.2 s and then rapidly deflated to a negative pressure of - 55 $cmH_2O$. That way, FV loops and FE-related parameters were generated, from which the $FEV_{0.1}$ could be calculated.

### 2.2.11 Salivary assay

For augmentation of the Flexi Vent® analysis of lung functionality, saliva chloride concentrations from the mice were measured.

After tracheostomy and Flexi Vent® analysis, 50 µl of 1 mM acetylcholine were injected in the mice's cheek to stimulate saliva production. The fluid was then collected via glass capillaries.

To determine the salivary chloride concentrations, a chloride assay was performed, using the Chloride Assay Kit, following the manufacturer's instruction, using a 1:100 dilution of the saliva samples. Finally, the absorption was measured at 620 nm using an Ensight Multimode plate reader and the Kalaido® software. To calculate the chloride concentration the WorkOut Plus® software was used.

### 2.2.12 RNA extraction from murine lungs

In order to analyze hCFTR gene expression following injection of either UD h*CFTR* mRNA, non-UD h*CFTR* mRNA or UD h*CFTR* pDNA, total RNA had to be isolated from the murine lungs.

Therefore, after isolation of the lungs, half of the organ was taken for total RNA extraction. The other half was used for protein extraction. For total RNA isolation the lungs were cut into small pieces, 500 µl of TRIzol® reagent was added and the organs were homogenized using a QIAGEN Tissue Ruptor. Subsequently total RNA was isolated using the PureLink RNA Mini Kit, following the manufacturer`s instruction. Finally, total RNA was eluted in 32 µl of RNase-free water and concentrations were determined, using an Implen® Nanophotometer. For assessment of hCFTR gene expression, cDNA was synthesized, and a RT-qPCR was performed, as described above.

### 2.2.13 Protein extraction from murine lungs

For analysis of hCFTR protein-expression in the murine lungs following injection of UD or non-UD h*CFTR* mRNA or UD h*CFTR* pDNA respectively, protein was isolated from the second half of the murine lungs.

To isolate protein from the lungs, the organ was cut into small pieces and homogenized in 600 µl of RIPA buffer and 6 µl of protease-inhibitor cocktail, using a QIAGEN Tissue Ruptor. For further homogenization the samples were put through a 20 G syringe ten times and incubated on ice for 20 min. Finally, the samples were centrifuged at 13,000 x g for 20 min at 4°C. The supernatant was collected and stored in - 20°C.

### 2.2.14 Enzyme-linked immunosorbent assay (ELISA)

To determine the hCFTR-protein content of the murine lungs, protein was extracted from the tissue as described above and subsequently an enzyme-linked immunosorbent assay was performed, using the human CFTR ELISA Kit following the manufacturer’s instruction.

First, the protein concentration of the samples was determined by carrying out a BCA Assay, as described above, using the Pierce BCA Protein Assay Kit. Then, the ELISA was performed for hCFTR detection. Optical density was determined at a wavelength of 450 nm using an Ensight Multimode plate reader and the Kalaido® software. hCFTR concentrations were then calculated using the WorkOut Plus® software.

### 2.2.15 Immune responses *in vivo*

For evaluation of immunogenic reactions that might be induced by i.v. administration of UD h*CFTR* mRNA complexed to cationic nanoliposomes (CLNP), further ELISA experiments were carried out, targeting IL-6, IL-12 and TNF-α in murine sera.

Animal experiments were carried out as described above, with injections taking place at day 1 and day 4. Each group consisted of 3 - 4 $Cftr^{-/-}$ mice. To obtain a positive control group, mice were treated with Resiquimod (R848) intravenously for two times. The negative control group did not receive any treatment. The other groups were treated with either UD h*CFTR* mRNA or UD h*CFTR* mRNA $s2U_{0.25}$ $m5C_{0.25}$ ($s2U_{0.25}$ = 25 % 2-Thio-UTP, $m5C_{0.25}$ = 25 % 5-Methyl-CTP) via i.v. administration for two times. Moreover, four groups were treated with cationic nanoliposomes only. The groups received different total amounts of either h*CFTR* mRNA or cationic nanoliposomes (20, 40, 80 or 160 µg).

6 hours after the second injection blood was collected for cytokine measurement. Finally, the mice were sacrificed, and serum was obtained from the murine whole blood using a serum separator. Finally, an IL-6, IL-12 and TNF-α ELISA was carried out, using an IL-6/IL-12/TNF-α uncoated ELISA Kit following the manufacturer's instructions. ELISA analysis of IL-12 and TNF-α levels was done in duplicates.

### 2.2.16 Statistics

All statistical analyses were carried out with GraphPad Prism Version 8 using the Kruskal-Wallis-Test. $P \leq 0.05$ was considered statistically significant.

### 2.2.17 Graphical illustrations

All graphical illustrations were created with BioRender.com.

# 3 Results

## 3.1 *In vitro* experiments

To investigate uridine-depleted h*CFTR* mRNA as a potential vehicle for therapeutic protein delivery to CF patients, we first conducted *in vitro* experiments. All *in vitro* experiments were carried out with CFBE41o$^-$ cells. CFBE41o$^-$ cells are a human cystic fibrosis bronchial epithelial cell line and are homozygous for the F508del mutation, so that they do not naturally express hCFTR. These cells were transfected with uridine-depleted (UD) h*CFTR* mRNA, non-uridine-depleted (non-UD) h*CFTR* mRNA and UD h*CFTR* pDNA using Lipofectamine 2000. 24 hours post-transfection protein and total RNA was isolated from the cells and a RT-qPCR and Western Blot Analysis were conducted to assess hCFTR gene - and protein expression following transfection with h*CFTR* mRNA or pDNA.

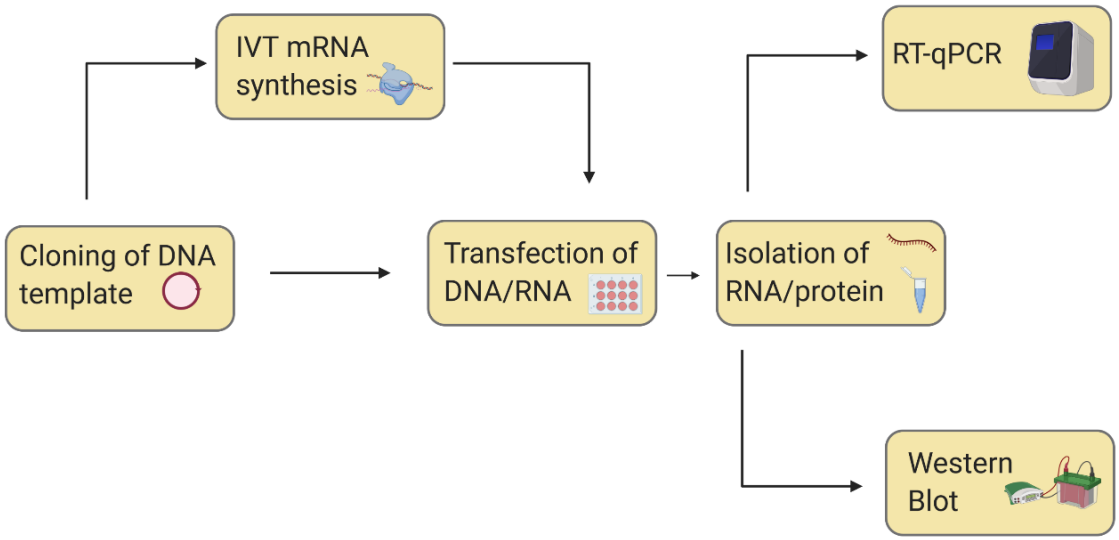


**Figure 3.1** Workflow for the *in vitro* experiments.

### 3.1.1 IVT h*CFTR* mRNA synthesis

Before the transfection of CFBE41o$^-$ cells could be performed, UD and non-UD h*CFTR* mRNA had to be made. The h*CFTR* mRNA that was used for the *in vitro* experiments was produced by *in vitro* transcription from a pVax.A120 plasmid, carrying the h*CFTR* template which was either uridine-depleted or unmodified. These plasmids were obtained by cloning, amplification, isolation, and subsequent linearization, via *Not*I-mediated restriction digest, as described in methods.

Before performing the IVT, linearization of the pVax.A120 h*CFTR* plasmid is essential. Through the restriction digest mediated by *Not*I the plasmid is cut right after the h*CFTR* encoding sequence. That way the T7 polymerase can bind to the promotor prior to the h*CFTR* encoding sequence, transcribe the h*CFTR* template and is then stopped, since the plasmid ends after that sequence. If the plasmid was not linearized, the T7 polymerase would not be stopped after finishing transcription of the h*CFTR* template but it would transcribe the whole plasmid into mRNA.

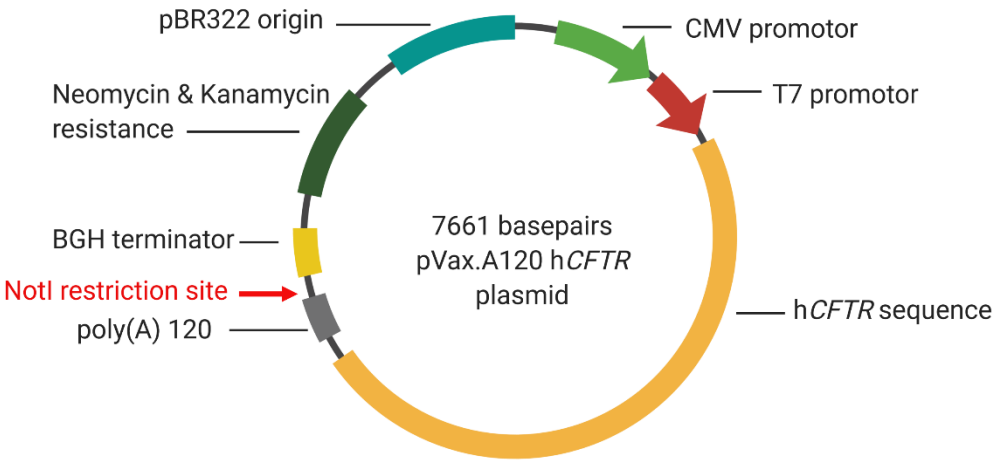


**Figure 3.2** pVax.A120 h*CFTR* plasmid. The pVax.A120 h*CFTR* plasmid was linearized by *Not*I mediated restriction digest and subsequently used as a template for IVT.

Linearization success was confirmed by running an agarose gel electrophoresis, which is separating nucleic acids by size.

The expected band size for the h*CFTR* plasmid is around 7 kB. As a control sample an unlinearized pVax UD h*CFTR* plasmid was run. An intact plasmid can take three different conformations: coiled, supercoiled, or uncoiled. Most of the intact plasmids are usually taking in the supercoiled conformation. Since the supercoiled structure is more compact than the linearized plasmid it migrates faster on the agarose gel. This difference enables distinction between a linearized and an unlinearized plasmid. The gel picture (figure 3.3) shows one broad band (left) between 6.5 and 8 kB formed by the intact plasmid, representing the three different conformations it can take, and two sharp bands (center, right) at 7 kB, representing the linearized plasmid and confirming the linearization success.

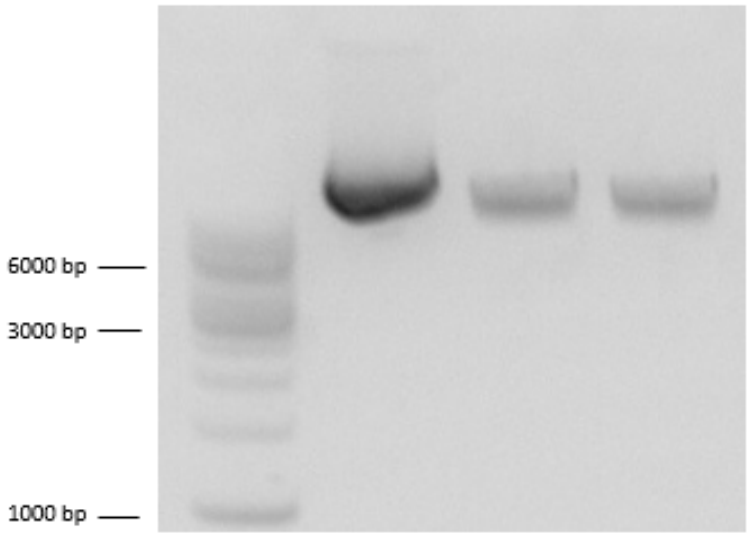


**Figure 3.3** Agarose gel electrophoresis of unlinearized (left) and linearized (center, right) pVax.A120 UD h*CFTR* plasmid. Samples were run along with a 1 kB ladder.

The linearized plasmids were used for performing the IVT and subsequently the mRNA's integrity was determined using an Agilent bioanalyzer 2100. The bioanalyzer is separating the RNA fragments in the sample by size via electrophoresis. By adding a fluorescent dye to the samples to be investigated,

they can be detected by their fluorescence. For both mRNAs, uridine-depleted as well as non-uridine-depleted, the electropherogram shows a characteristic peak after 40 seconds around 4000 nucleotides, which represents the size of the h*CFTR* mRNA produced (4591 nucleotides). This confirms that indeed there is an intact h*CFTR* mRNA present. Moreover, there is a smaller peak around 25 nucleotides, which represents the so called “lower marker”, a part of the method, which is needed for alignment of all samples with the RNA ladder. Additionally, in the electropherogram of the non-UD h*CFTR* mRNA there is a small peak around 500 nucleotides, probably caused by minor contaminations.

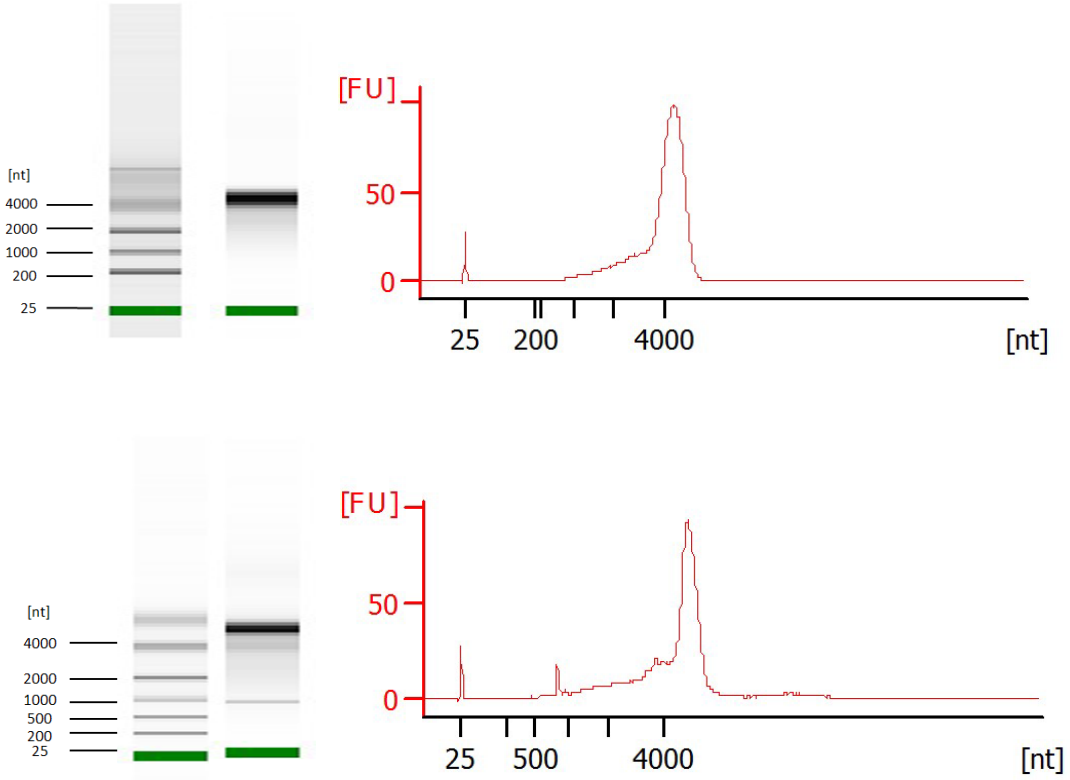


**Figure 3.4** Electropherogram and gel equivalent of bioanalyzer analysis of UD h*CFTR* mRNA (top) and non-UD h*CFTR* mRNA (bottom): sharp peak around 4000 nucleotides, representing h*CFTR* mRNA sized 4500 nucleotides. Gel equivalent: ladder (left), UD/non-UD h*CFTR* mRNA (right).

These results show that the mRNA used for the *in vitro* experiments is intact. However, this analysis is not suitable for drawing conclusions on the mRNA's functionality.

### 3.1.2 Flow Cytometry: assessment of transfection efficiency

After obtaining the UD/non-UD h*CFTR* mRNA via IVT and confirming their integrity with the Agilent bioanalyzer 2100, we could move on to transfection of CFBE41o$^-$ cells with either these mRNAs or UD h*CFTR* pDNA. The transfection was done in four biological replicates. The major objective was to investigate therapeutic protein expression after delivery of uridine-depleted h*CFTR* mRNA and compare this protein expression to protein expression induced by transfection of non-UD h*CFTR* mRNA or UD h*CFTR* pDNA. The transfection was performed using Lipofectamine 2000. 24 hours after transfection of CFBE41o$^-$ cells, follow up experiments were planned. However, before these experiments could be initiated, transfection success had to be confirmed. To assess the transfection efficiency two additional transfections into CFBE41o$^-$ cells were carried out, transfecting *mKate2* mRNA and *mKate2* pDNA following the same protocol as for transfection of UD/non-UD h*CFTR* mRNA and UD h*CFTR* pDNA. Determination of the number of cells that express mKate2 via flow cytometry allows conclusions on transfection efficiency. Flow cytometry of mKate2 expression was performed 24 hours after transfection.

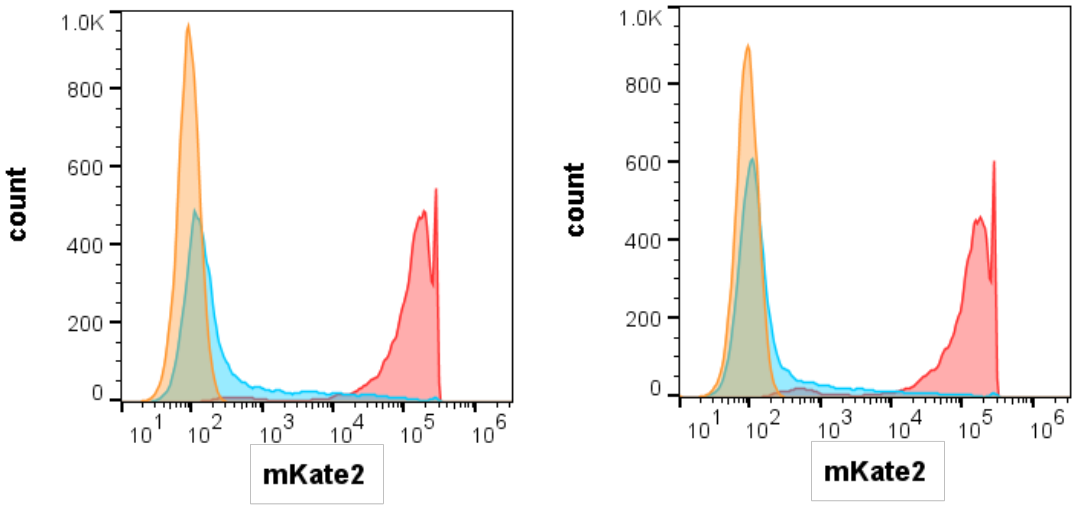


**Figure 3.5** Flow cytometry analysis of mKate2 expression 24 hours after transfection of CFBE41o$^-$ cells with *mKate2* mRNA and *mKate2* pDNA respectively (N = 4). Orange: untransfected controls, blue: transfection with *mKate2* pDNA, red: transfection with *mKate2* mRNA.

Both, transfection with *mKate2* mRNA as well as transfection with *mKate2* pDNA resulted in mKate2 positive cells 24 hours after transfection. Transfection with *mKate2* pDNA resulted in a mean of 26.5 % mKate2 positive cells, which is a satisfactory result when assessing transfection with pDNA. Due to different expression kinetics, pDNA reaches its expression maximum after approximately 72 hours. On the other side 24 hours after transfection with *mKate2* mRNA 99.3 % of CFBE41o$^-$ cells were mKate2 positive. This high number of mKate2 positive cells, is due to faster translation of transfected mRNA into protein, as mRNA does not need to be transferred into the nucleus and can be translated immediately. These findings can be translated into a transfection efficiency of 26.5 % following pDNA transfection and of 99.3 % following mRNA transfection after 24 hours (figure 3.5).

Since transfection of CFBE41o$^-$ cells with h*CFTR* mRNA and h*CFTR* pDNA was successful we could move on to further analysis of h*CFTR* expression.

### 3.1.3 Real-time quantitative PCR: evaluation of hCFTR gene expression

After the transfection success was confirmed, the next step was to analyze whether hCFTR gene- and protein expression was induced by transfection of UD/non-UD h*CFTR* mRNA and UD h*CFTR* pDNA into CFBE41o$^-$ cells. To evaluate the h*CFTR*-expression on a genetic level 24 hours after transfection of CFBE41o$^-$ cells, total RNA was isolated from the cells and used as a template for reverse transcription into cDNA. Subsequently a RT-qPCR was performed, using 1:20 dilutions of cDNA.

The RT-qPCR allows assessment of the relative expression of the hCFTR gene. The use of primers, that are specific for a sequence of interest allows amplification of that sequence. In this case the primers that were used were specific for either UD h*CFTR*, non-UD h*CFTR* or 18S. In RT-qPCR a fluorescent signal is measured during the amplification cycles, which increases, when the amount of dsDNA rises. When a particular threshold of fluorescent signal is reached in an early cycle this is translated into a high gene expression. h*CFTR* expression was normalized to 18S gene expression since 18S is considered a housekeeping gene, which is ubiquitously expressed in eukaryotic cells.

As can be seen in figure 3.6, all three treatments led to hCFTR gene expression in CFBE41o$^-$ cells. Indeed, relative hCFTR gene expression after transfection with UD h*CFTR* mRNA was significantly higher as compared to the untransfected control group ($p < 0.05$, $N = 4$). The difference between the three treatments was not significant, however there is an apparent trend, with uridine-depleted mRNA resulting in highest relative h*CFTR* expression whereas UD h*CFTR* pDNA - transfected cells showed the lowest relative h*CFTR* expression after 24 hours.

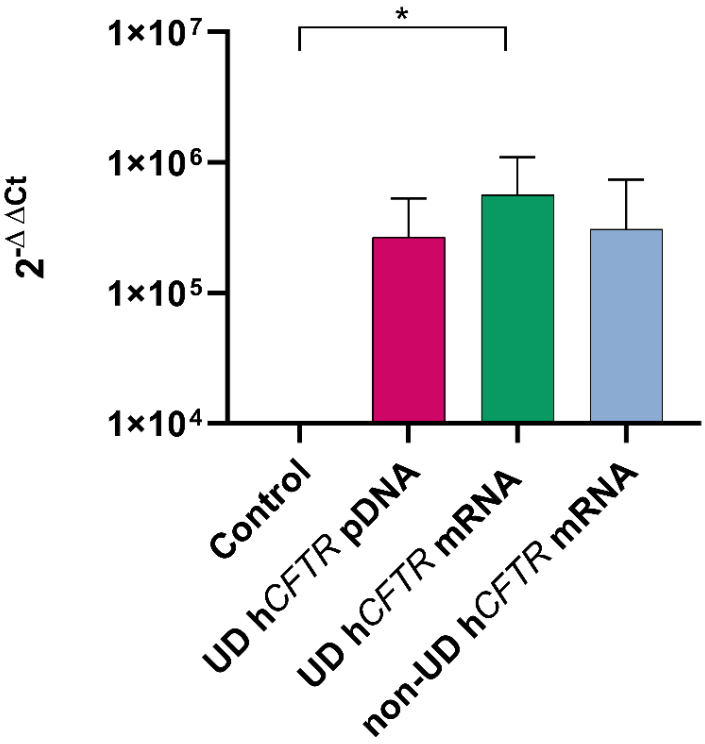


**Figure 3.6** Real-time quantitative PCR analysis: CFBE41o$^-$ cells 24 hours post-transfection with UD/non-UD h*CFTR* mRNA or UD h*CFTR* pDNA (N = 4). hCFTR gene expression was normalized to 18S gene expression. The bar graphs are showing the mean values + / - standard deviation (SD).

These findings indicate that UD h*CFTR* mRNA might be a suitable means for inducing hCFTR gene expression, resulting in highest hCFTR gene expression after 24 hours compared to treatment with UD h*CFTR* pDNA and non-UD h*CFTR* mRNA.

### 3.1.4 Western Blot: Assessment of hCFTR protein-expression

The general objective of gene therapy is to induce therapeutic protein expression. That is why, in addition to performing a RT-qPCR, a Western Blot analysis was done to determine whether this objective was achieved 24 hours after transfection of CFBE41o$^-$ cells with UD/non-UD h*CFTR* mRNA or UD h*CFTR* pDNA.

In this context, protein lysates were taken from the cells, protein concentration was determined by performing a BCA-Assay and a Western Blot was carried out.

β-Actin protein levels were used to normalize band intensities. The western blot enables qualitative and semi-quantitative analysis of hCFTR-protein expression. During Western Blot, proteins isolated from the cells are separated by molecular weight and are then transferred onto a membrane. Finally, hCFTR and β-Actin on that membrane were stained with specific antibodies. That way, hCFTR protein expression induced by either of the three treatments could be detected.

Within the cell the CFTR protein is present in three different forms: non-glycosylated, core-glycosylated, and complex-glycosylated. After translation, the unglycosylated protein becomes core-glycosylated in the ER, by addition of two N-linked glycosyl groups. During transit of the Golgi-network, the CFTR protein receives further complex-glycosylation. The complex-glycosylated protein represents the mature CFTR-protein. These three different forms are reflected in western blot by the A -, B - and C - Band. The unglycosylated protein has the lowest molecular weight (approximately 130 kDa) and migrates fastest on the gel, forming the A - Band. The core-glycosylated, immature protein migrates a little slower, and forms the B - Band (approximately 150 kDa), while the complex-glycosylated form is represented by the C - Band, associated with the highest molecular weight (approximately 170 kDa). However, presence of the C - Band does not necessarily mean, that the CFTR protein reached the plasma membrane.

CFBE41o$^-$ cells were transfected with UD h*CFTR* pDNA, UD h*CFTR* mRNA and non-UD h*CFTR* mRNA, respectively. Untransfected CFBE41o$^-$ cells were taken as negative controls. In the Western Blot analysis 24 hours after transfection, in control cells and cells transfected with non-UD h*CFTR* mRNA no or only very little hCFTR protein expression was observed. Yet, transfection with UD h*CFTR* pDNA resulted in robust hCFTR protein expression, showing complex-glycosylated (C - Band at approximately 170 kDa) as well as core-glycosylated hCFTR protein (B - Band at approximately 150 kDa). Transfection with UD h*CFTR* mRNA resulted in hCFTR protein expression, as well, as indicated by a protein band around 160 kDa, for this group clear distinction between A -, B - and C - Band was not possible (Figure 3.7).

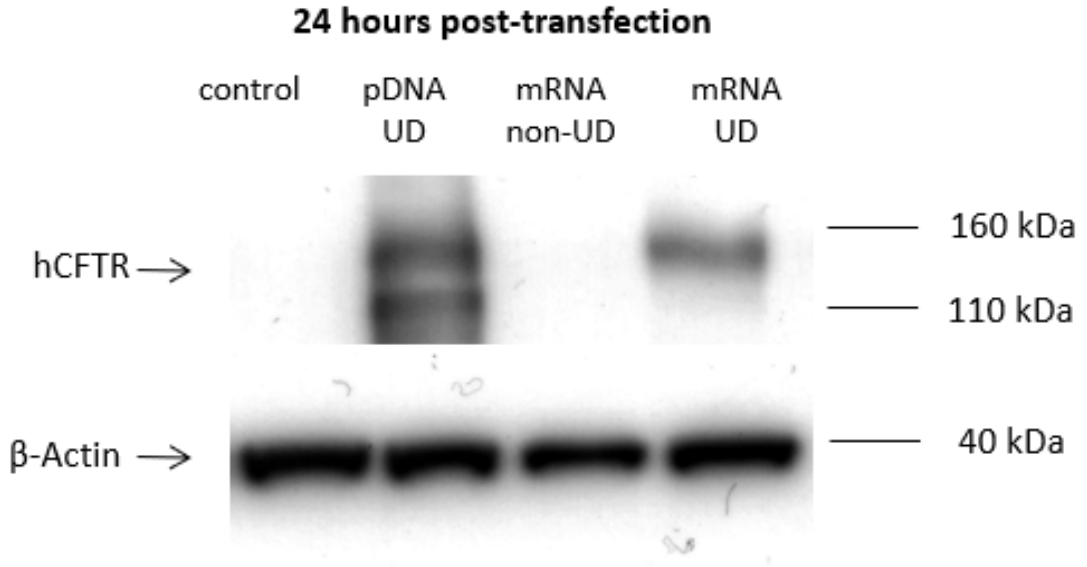


**Figure 3.7** Qualitative western blot analysis 24 hours post-transfection of CFBE41o$^-$ cells with UD/non-UD h*CFTR* mRNA or UD h*CFTR* pDNA. hCFTR levels are normalized to β-Actin protein levels.

In a semi-quantitative analysis, using the ImageJ software, hCFTR protein levels were normalized to β-Actin protein levels. Finally, protein expression was put relative to hCFTR levels, following UD h*CFTR* pDNA transfection. CFBE41o$^-$ cells transfected with UD h*CFTR* pDNA were taken as a positive control, since transfection with h*CFTR* pDNA is a well-established model for therapeutic hCFTR protein delivery *in vitro*, showing solid transfection efficiencies and robust protein expression. Transfection with UD h*CFTR* mRNA resulted in a mean hCFTR protein expression of 49.1 % of protein expression after UD h*CFTR* pDNA transfection.

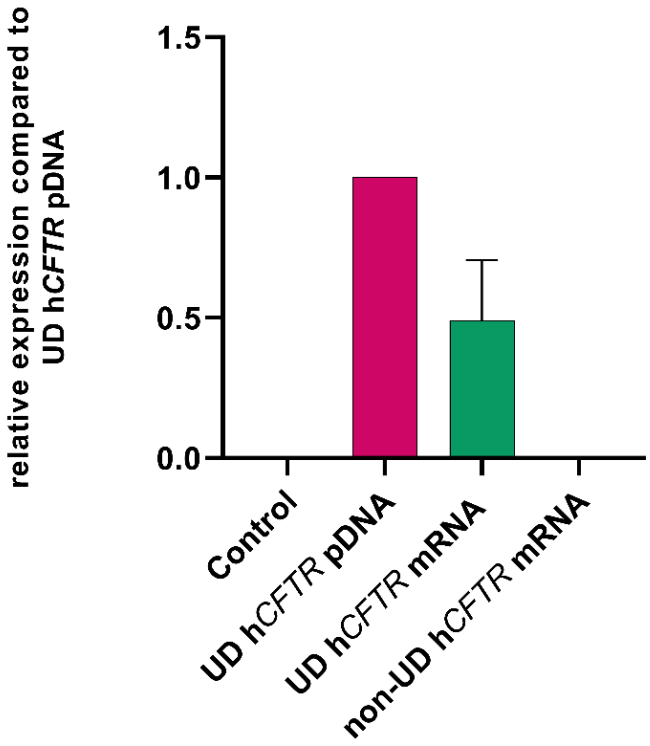


**Figure 3.8** Semi-quantitative western blot analysis 24 hours post transfection of CFBE41o$^-$ cells with UD/non-UD h*CFTR* mRNA or UD h*CFTR* pDNA (N = 4). Untransfected CFBE41o$^-$ cells were taken as a negative control. hCFTR protein expression levels were put relative to hCFTR protein levels induced by UD h*CFTR* pDNA transfection. The bar graphs are showing the mean values + / - SD.

Taken together these results show, that pDNA as well as UD h*CFTR* mRNA transfection can restore hCFTR protein expression *in vitro*, while non-uridine depleted mRNA did not induce hCFTR-protein expression.

### 3.1.5 MTT-Assay: evaluation of cell viability following transfection

When performing the transfection of UD h*CFTR* pDNA or UD/non-UD h*CFTR* mRNA into CFBE41o$^-$ cells with Lipofectamine 2000, we observed that 24 hours after transfection a lot of cells had died. This increase in cell death was apparent especially for CFBE41o$^-$ cells that were receiving transfection with non-UD h*CFTR* mRNA.

To further quantify cell viability following transfection of CFBE41o$^-$ cells with either h*CFTR* pDNA or mRNA we conducted an MTT-Assay. This colorimetric assay is using MTT, which is taken up into cells via endocytosis and is then reduced in the cell's mitochondria by NAD(P)H - dependent oxidoreductase enzymes. MTT is reduced to insoluble purple formazan crystals. Subsequently these crystals are dissolved. Finally, the absorbance of the samples is measured. The amount of purple formazan crystals in the solution reflects the metabolic activity of the cells and is therefore seen as an indicator for cell viability, proliferation and cytotoxicity. CFBE41o$^-$ cells were transfected with UD h*CFTR* pDNA, non-UD h*CFTR* pDNA, UD h*CFTR* mRNA, non-UD h*CFTR* mRNA, *mKate2* mRNA and *mKate2* pDNA, respectively. All transfections were performed in triplicates. CFBE41o$^-$ cells that did not receive any transfection were taken as a positive control. Moreover, an additional triplicate of cells was treated with Lipofectamine 2000 only. 24 hours after transfection the MTT-assay was performed, and the absorbance of the samples was measured at 570 nm.

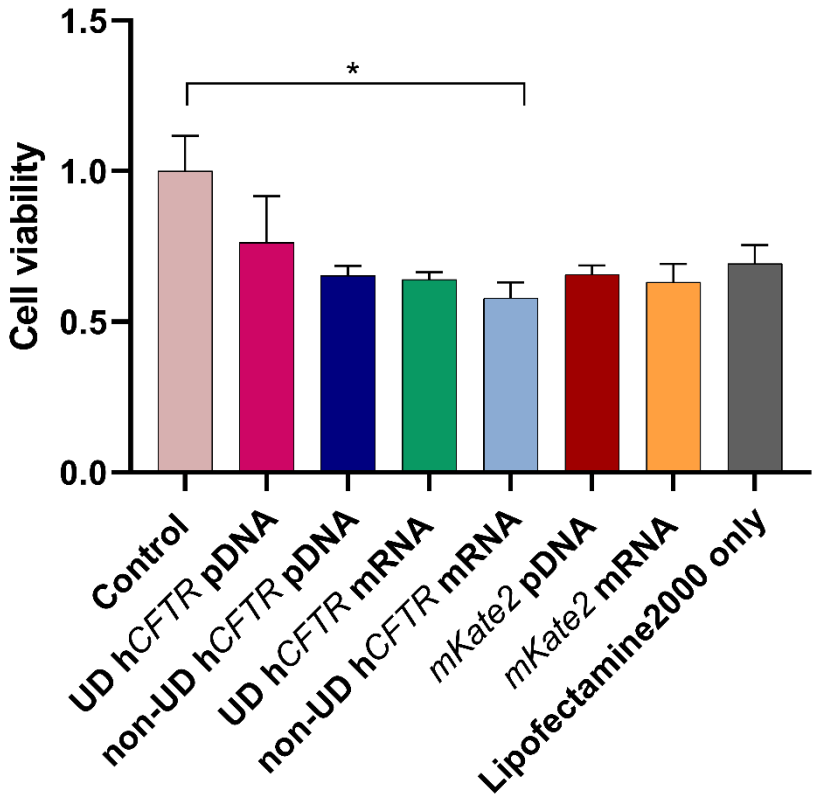


**Figure 3.9** MTT-Assay: 24 hours post-transfection of CFBE41o$^-$ cells with UD/non-UD h*CFTR* pDNA, UD/non-UD h*CFTR* mRNA, *mKate2* mRNA, *mKate2* pDNA or treatment with Lipofectamine 2000 only. Untreated CFBE41o$^-$ cells were taken as a positive control. All analyses were done in triplicates. The bar graphs are showing the mean values + / - SD.

As expected, the highest cell viability was observed in untreated control cells (mean = 1.00, SD = 0.10). Generally, all transfections induced an increase in cell death.

Interestingly, treatment with Lipofectamine 2000 only, already induced cell death of 30.7 % as compared to untreated cells. Lipofectamine 2000 is a cationic lipid, that disrupts the cellular membrane, and that way enables transfer of nucleic acids in the cells. However, destabilizing the cellular membrane might also induce cell death, as reflected in our findings. Yet, apart from transfection with UD h*CFTR* pDNA, all other treatments induced higher cell death than Lipofectamine;

this increase compared to treatment with Lipofectamine only, can then be attributed to effect of the nucleic acid itself.

The highest rate of cell death was found for cells transfected with non-UD h*CFTR* mRNA (42.2 %), as we already observed during our previous experiments qualitatively. Cell viability 24 hours after transfection of non-UD h*CFTR* mRNA was significantly decreased, as compared to the untreated control cells ($p \leq 0.05$, N = 3). Encouragingly, Uridine-depletion of h*CFTR* mRNA decreased the onset of cell death by 6.2 percentage points, compared to non-UD h*CFTR* mRNA to 36.0 % cell death. Generally, transfection with pDNA resulted in higher cell viability as compared to transfection with mRNA. Transfection of UD h*CFTR* pDNA, non-UD h*CFTR* pDNA and *mKate2* pDNA only induced 23.7 %, 34.7 % and 34.3 % cell death, respectively.

These results show that indeed, non-UD h*CFTR* mRNA induces high rates of cell death. Uridine-depletion of h*CFTR* mRNA reduces cytotoxicity, resulting in lower rates of cell death. However, it must be noted that the transfection reagent Lipofectamine 2000 itself, contributes to cell death induced by transfection of nucleic acids, as well.

### 3.1.6 *In vitro* experiments: concluding remarks

To sum up our *in vitro* experiments, we can say, that indeed, transfection of uridine-depleted h*CFTR* mRNA induces hCFTR gene - and protein expression and was found to be superior to non-UD h*CFTR* mRNA. Moreover, uridine-depletion of h*CFTR* mRNA was found to decrease cytotoxicity as compared to non-UD h*CFTR* mRNA. However, these findings do not allow any conclusions on the CFTR protein's functionality. As a next step mouse experiments were conducted, to testify whether our results are transferrable to *in vivo* use and whether UD h*CFTR* mRNA leads to a restoration of hCFTR expression and function in Cftr $^{-/-}$ mice.

### 3.2 *In vivo* experiments

For further analysis of sequence-engineered h*CFTR* mRNA as a potential therapeutic for Cystic Fibrosis, we wanted to test, whether the findings from the *in vitro* experiments are transferrable to *in vivo* conditions. In this context, 11 $Cftr^{-/-}$ mice were receiving i.v. treatment with 80 µg of either UD h*CFTR* pDNA, UD h*CFTR* mRNA or non-UD h*CFTR* mRNA complexed to chitosan-coated PLGA nanoparticles (N = 3 - 4). The mice in the positive ($Cftr^{+/+}$) and negative ($Cftr^{-/-}$) control groups (N = 4 - 5) did not receive any treatment. The mice received two injections (40 µg per injection) on day one and day four. Six days after the first injection Flexi Vent® analysis was carried out and saliva was collected for performance of a saliva chloride assay. The mice were sacrificed, and lungs were isolated for extraction of total RNA and protein to assess hCFTR gene- and protein expression.

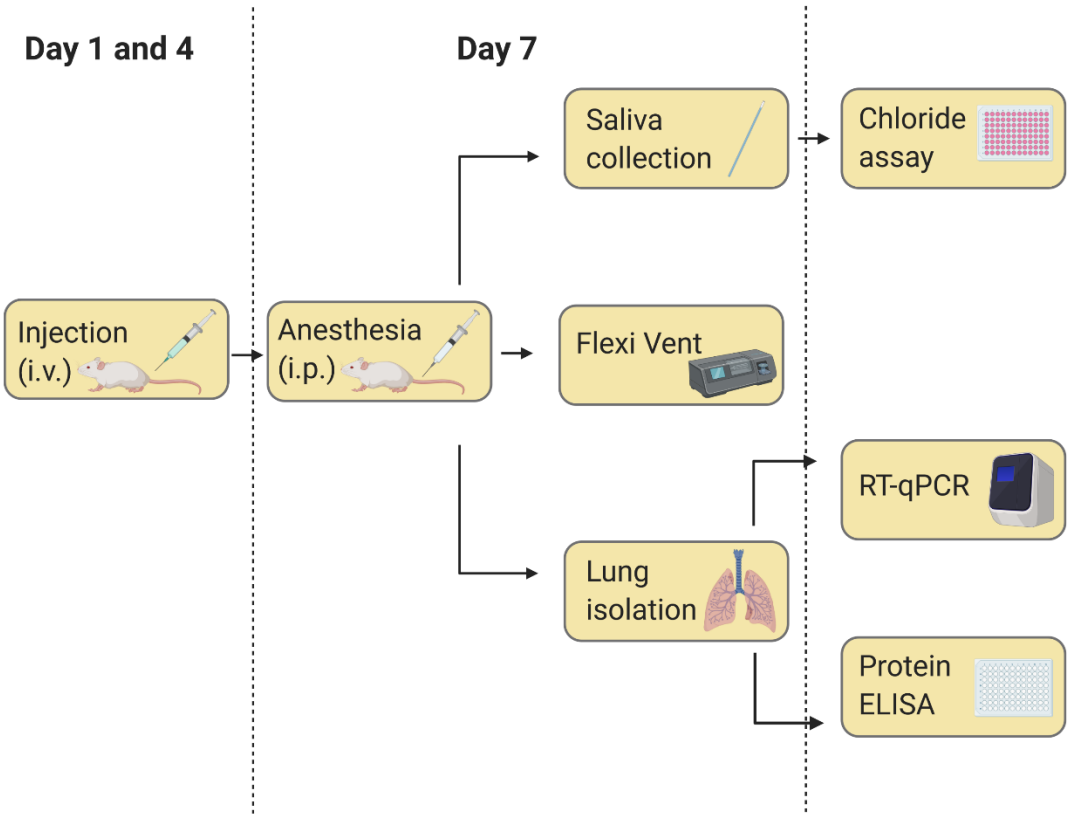


**Figure 3.10** Workflow oft the *in vivo* experiments.

### 3.2.1 Lung function: Flexi Vent®-analysis

As the respiratory system is the major target of gene therapy, assessment of the murine lung functionality six days after the first injection was of great interest. In this regard an important parameter is the $FEV_{0.1}$ (forced expiratory volume), which constitutes the maximal volume that can be exhaled in 0.1 seconds and allows conclusions on the lung's functionality. Therefore, the $FEV_{0.1}$ was determined using the Flexi® Vent system. Mice were anesthetized before tracheostomy was carried out and subsequently, they were connected to the Flexi® Vent system, as described in methods. The Flexi Vent® is measuring the $FEV_{0.1}$ by rapidly exposing the murine airways to negative pressure (negative pressure-driven forced expiration; NFPE-maneuver). That way a forced expiratory flow signal is generated. It must be noted that this method differs from human spirometry measurements, where maximal expiration is driven by an increase of intrapulmonary pressure.

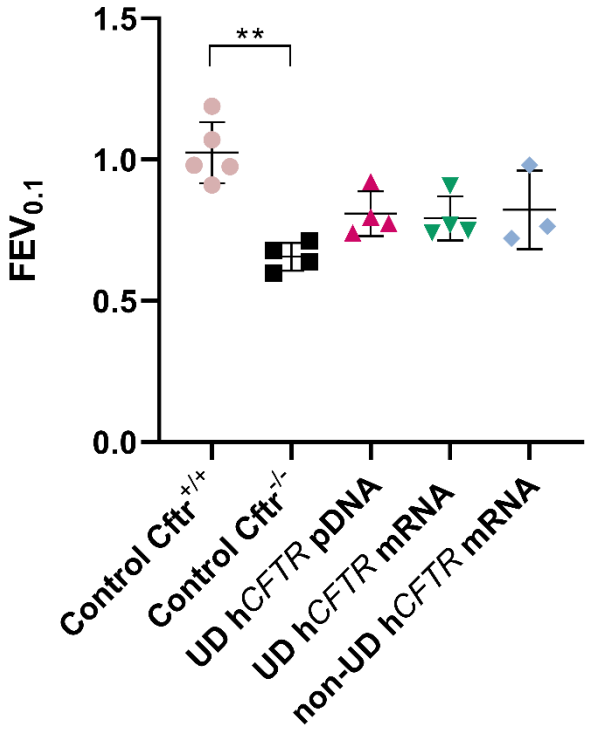


**Figure 3.11** *In vivo* $FEV_{0.1}$ values determined six days after the first i.v. treatment of $Cftr^{-/-}$ mice with either UD/non-UD h*CFTR* mRNA or UD h*CFTR* pDNA; N = 3

- 5 per group. The figure is showing the mean values + / - SD and individual values depicted with different symbols.

There were two groups investigated, that did not receive any treatment. As a positive control $FEV_{0.1}$ values of $Cftr^{+/+}$ mice, expressing functional CFTR protein, were taken. The second control group consisted of $Cftr^{-/-}$ mice only, expressing no functional CFTR protein and was taken as a negative control. The $FEV_{0.1}$ of the untreated $Cftr^{-/-}$ mice was significantly lower compared to the $FEV_{0.1}$ obtained for the untreated $Cftr^{+/+}$ mice ($p \leq 0.01$, N = 4 - 5 per group). The mean $FEV_{0.1}$ of the $Cftr^{-/-}$ mice (mean = 0.66 ml/s, SD = 0.05 ml/s) only reached 64 % of the $FEV_{0,1}$ of the $Cftr^{+/+}$ mice (mean = 1.03 ml/s, SD = 0.11 ml/s).
Treatment with either UD/non-UD h*CFTR* mRNA or UD h*CFTR* pDNA resulted in an increase of the $FEV_{0.1}$ as compared to the untreated $Cftr^{-/-}$ mice. The strongest effect was found for the group treated with non-UD h*CFTR* mRNA (mean = 0.82 ml/s, SD = 0.14 ml/s). Their $FEV_{0.1}$ was increased by 16.1 percentage points, as compared to untreated $Cftr^{-/-}$ mice, reaching 80.2 % of the $FEV_{0.1}$ observed for healthy $Cftr^{+/+}$ mice. Treatment with UD h*CFTR* pDNA led to an increase of 14.5 percentage points, compared to $Cftr^{-/-}$ mice, reaching 78.9 % of the $FEV_{0.1}$ observed for healthy $Cftr^{+/+}$ mice. The lowest increase in $FEV_{0.1}$ however was found for mice treated with UD h*CFTR* mRNA. Compared to the untreated $Cftr^{-/-}$ mice, their $FEV_{0.1}$ values increased by 13.2 percentage points, to 77.3 % of $FEV_{0.1}$ values of the healthy $Cftr^{+/+}$ mice.
However, none of these increases were statistically significant as compared to both control groups. Also, differences between the treatments were not significant.
Considering these results, we can say that, although not statistically significant, the groups that received i.v. treatment showed a modest improvement of lung function compared to untreated $Cftr^{-/-}$ mice, with non-UD h*CFTR* mRNA resulting in the strongest effect.

### 3.2.2 Saliva Chloride Assay: evaluation of chloride transport

For augmentation of the functional Flexi® Vent results, a saliva chloride assay was performed, which is another possibility of drawing conclusions on the hCFTR channel's functionality. Saliva of the mice was collected via glass capillaries after the Flexi® Vent analysis was finished and subsequently chloride concentrations were determined, as described in methods.

In healthy $Cftr^{+/+}$ mice, the saliva chloride concentration is approximately 748.8 ng/µl, as shown by Haque et al. in 2018 (115). Due to the mutation of the CFTR-channel in $Cftr^{-/-}$ mice the transport of sodium and chloride ions from extra- to intracellular in saliva- and sweat-glands is impaired. Consequently, chloride accumulates extracellularly and the saliva chloride concentration increases. Successful treatment with h*CFTR* mRNA or pDNA should lower the chloride concentrations, by inducing expression of functional hCFTR protein. The saliva chloride assay acts analog to the sweat test, which is gold standard for diagnosis of CF in humans.

Yet, the treatments did not result in a reduction of the saliva chloride concentrations (figure 3.12). Clearly, all values observed were significantly higher than in healthy $Cftr^{+/+}$ mice, indicating that there is still no functional hCFTR expressed in the murine saliva glands. The lowest saliva chloride concentration was measured for the untreated control group (mean = 2984 ng/µl, SD = 589.5 ng/µl), the highest chloride concentration was found for the group treated with UD h*CFTR* mRNA (mean = 4187 ng/µl, SD = 591.9 ng/µl). However, the differences between the different groups were not significant.

All in all, considering the saliva chloride concentration there was no effect of treatment with UD/non-UD h*CFTR* mRNA or UD h*CFTR* pDNA apparent.

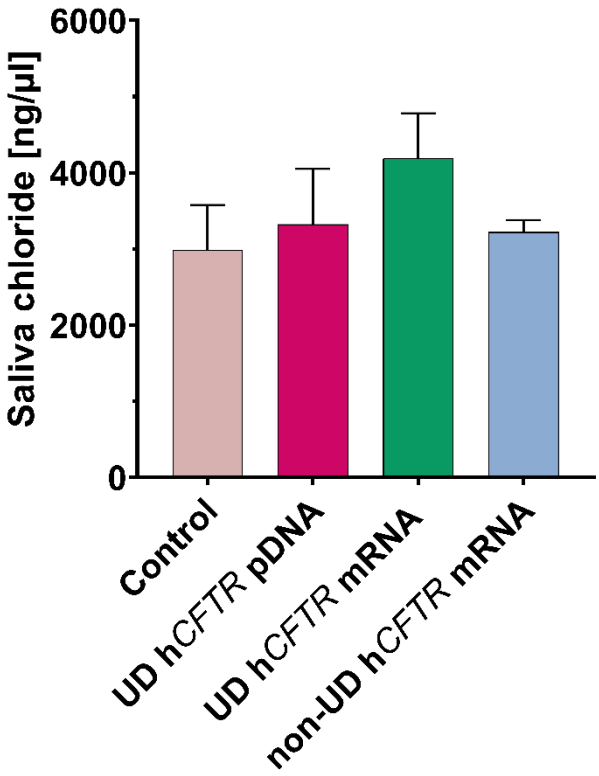


**Figure 3.12** Saliva chloride assay six days after the first i.v. treatment of Cftr$^{-/-}$ mice with either UD/non-UD h*CFTR* mRNA oder UD h*CFTR* pDNA; N = 3 - 4 per group. The bar graphs are showing the mean values + / - SD.

### 3.2.3 RT-qPCR: hCFTR gene expression in the murine lung

A further important objective was to evaluate hCFTR gene expression following i.v. treatment of the mice with either UD/non-UD h*CFTR* mRNA or UD h*CFTR* pDNA complexed with chitosan-coated PLGA nanoparticles (N = 3 - 4 per group). Therefore, the mice were sacrificed after Flexi Vent® analysis was finished and saliva was collected. Subsequently the murine lungs were isolated for protein- and total RNA extraction. To isolate total RNA half of the murine lung was homogenized in TRIzol® reagent and total RNA was extracted, as described in methods. The total RNA obtained from RNA extraction was used as a template for synthesis of cDNA, which was then used for RT-qPCR in a 1:20 dilution.

In order to properly quantify hCFTR gene expression, the data was put relative to 18S gene expression, a housekeeping gene, which is ubiquitously expressed in eukaryotic cells.

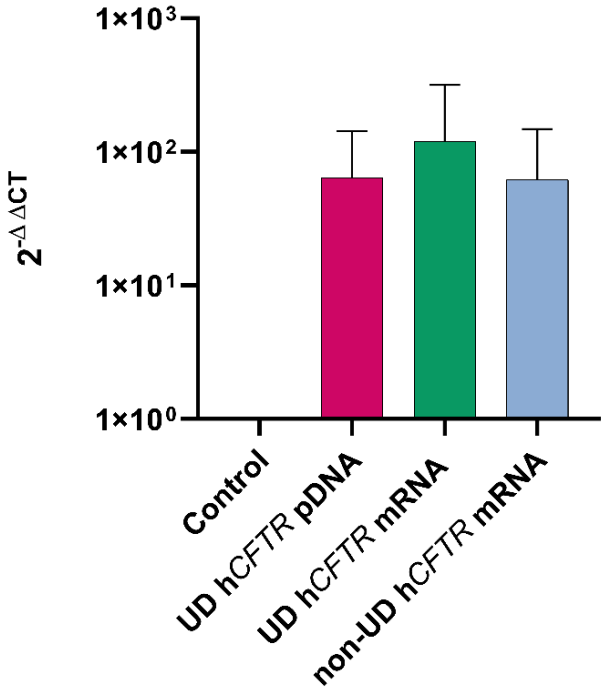


**Figure 3.13 :** RT-qPCR six days after the first i.v. treatment of Cftr$^{-/-}$ mice with either UD/non-UD h*CFTR* mRNA or UD h*CFTR* pDNA; N = 3 - 4 per group. The bar graphs are showing the mean values + / - SD. hCFTR gene expression was normalized to 18S gene expression.

RT-qPCR confirmed, that indeed the hCFTR gene was expressed in the murine lungs, following i.v. treatment with UD/non-UD h*CFTR* mRNA and UD h*CFTR* pDNA, respectively. The relative hCFTR gene expression in the lungs was highest in the group treated with UD h*CFTR* mRNA (mean = 120.7, SD = 195.9). Treatment with UD h*CFTR* pDNA (mean = 64.3, SD = 78.96) and non-UD h*CFTR* mRNA (mean = 62.1, SD = 86.3) resulted in similar extends of hCFTR gene expression. Nonetheless, the individual values were highly scattered, especially for treatment with UD h*CFTR* mRNA, resulting in high standard deviations.

Furthermore, no significant difference between the three treatments and no significant difference to the untreated control group could be observed (figure 3.13).

Taken together, there was expression of the hCFTR gene in the murine lungs apparent, six days after the first i.v. treatment with either UD/non-UD h*CFTR* mRNA or UD h*CFTR* pDNA. However, due to high scattering of the individual results, the findings are rather inconclusive, and no significant difference could be found between the different groups.

### 3.2.4 hCFTR ELISA: hCFTR protein expression in the murine airways

As mentioned before, restoring hCFTR expression and function in the respiratory system is the major objective of gene therapy. To evaluate whether i.v. treatment with UD/non-UD h*CFTR* mRNA and UD h*CFTR* pDNA respectively induced hCFTR protein expression in the murine airways, lungs were isolated after the mice were sacrificed. Half of the lung tissue was used for total RNA extraction; the second half was homogenized in RIPA-buffer and protease-inhibitor cocktail for subsequent protein extraction. To determine the protein concentration of the samples a BCA-Assay was performed. The protein samples were then used for conducting an enzyme-linked immunosorbent assay (ELISA), quantifying hCFTR-protein expression in the respiratory tissue, as described in methods. The micro plate that was used for the ELISA was pre-coated with an antibody specific for hCFTR. That way any hCFTR present in the sample was bound to this antibody. Subsequently a second biotinylated antibody targeting hCFTR and avidin-horseradish peroxidase (HRP) conjugate binds. HRP conjugate and substrate reagent are added and induce a colorimetric reaction. That way the hCFTR content can be determined by measurement of the optical density, which increases the more hCFTR is present in the sample.

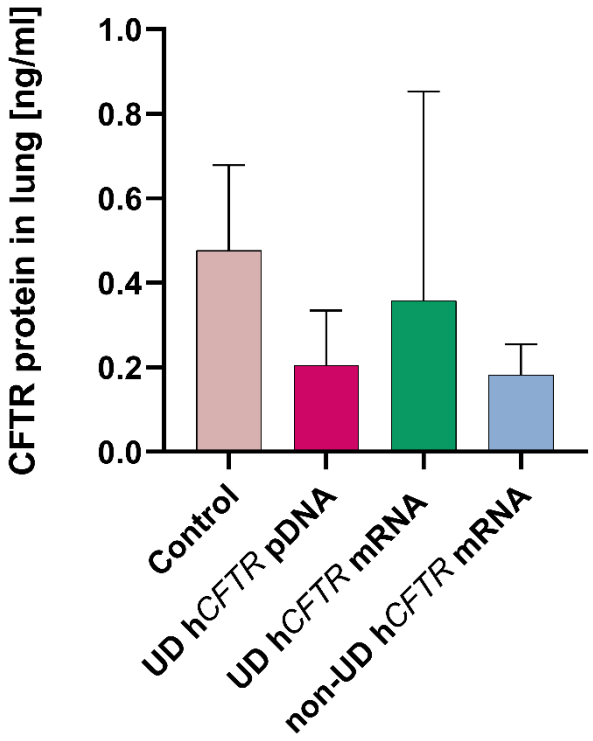


**Figure 3.14** hCFTR ELISA six days after the first i.v. treatment of Cftr$^{-/-}$ mice with either UD/non-UD h*CFTR* mRNA oder UD h*CFTR* pDNA; N = 3 - 4 per group. The bar graphs are showing the mean values + / - SD.

Yet, i.v. treatment with UD/non-UD h*CFTR* mRNA or UD h*CFTR* pDNA did not result in hCFTR protein expression in the murine lungs. Startlingly, the highest protein content was found in the control group (mean = 0.48 ng/ml, SD = 0.2 ng/ml), which did not receive any treatment. Moreover, for the group receiving treatment with UD h*CFTR* mRNA the values obtained, were highly scattered (mean = 0.24 ng/ml, SD = 0.41 ng/ml), leading to high standard deviation, which is mirrored in high error bars in the bar graph. The lowest hCFTR protein concentration was found for the group receiving non-UD h*CFTR* mRNA (mean = 0.12 ng/ml, SD = 0.12 ng/ml).
Taken together there could be no increase in hCFTR protein expression observed and there was no significant difference found between the groups.

### 3.2.5 Cytokine ELISA: *in vivo* immune responses

Since i.v. treatment of Cftr$^{-/-}$ mice with UD h*CFTR* mRNA did not show the expected therapeutic effect, considering lung function and saliva chloride concentration as well as hCFTR protein and gene expression in the murine lungs, we hypothesized that the inefficiency of uridine-depleted h*CFTR* mRNA might be due to unwanted immune reactions induced by h*CFTR* mRNA with uridine-depletion only. In order to evaluate immune reactions induced by i.v. administration of UD h*CFTR* mRNA, an ELISA analysis targeting IL-6, IL-12 and TNF-α in murine sera was performed. This experiment was carried out parallelly to my experiments in our laboratory.

IL-6, IL-12 and TNF-α are cytokines, which are released upon activation of TLR 7 and 8 by IVT mRNA after lysosomal uptake. These cytokines induce inflammatory responses, which might cause degradation of the administered mRNA. Degradation of UD h*CFTR* mRNA might be a reason why i.v. administration to Cftr$^{-/-}$ mice did not show the expected effect. That is why, investigation of the cytokine level induced by administration of UD h*CFTR* mRNA was of great interest.

The mice were receiving two i.v. injections of either UD h*CFTR* mRNA or UD h*CFTR* mRNA $s2U_{0.25}$ $m5C_{0.25}$ ($s2U_{0.25}$ = 25 % 2-Thio-UTP, $m5C_{0.25}$ = 25 % 5-Methyl-CTP) complexed to cationic nanoliposomes. That way, mRNA which was uridine-depleted only was compared to uridine-depleted mRNA carrying additional chemical modifications. Both mRNAs were administered at four different total doses (20, 40, 80 and 160 µg). Negative controls were murine serum only or murine serum treated with cationic nanoliposomes only. Positive controls were treated with R848, which is an immune modulator activating TLR 7 / 8 pathways and that way inducing secretion of IL-6, IL-12 and TNF-α. ELISA analysis was done 6 hours after the second injection.

## IL-6

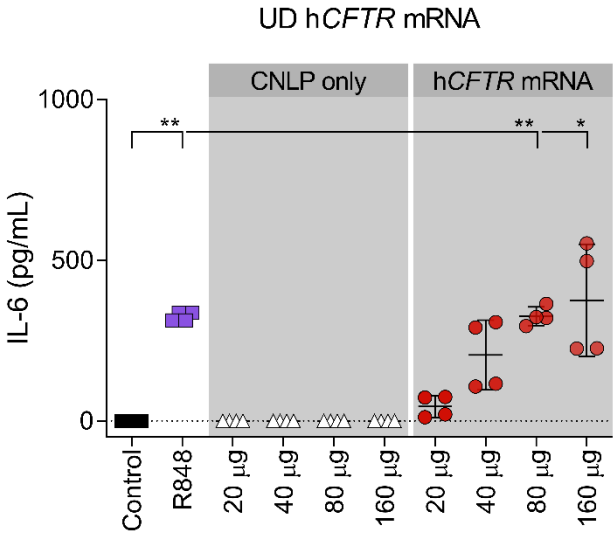
UD h*CFTR* mRNA
CNLP only
h*CFTR* mRNA
IL-6 (pg/mL)
1000
500
0
**
**
*
Control
R848
20 µg
40 µg
80 µg
160 µg
20 µg
40 µg
80 µg
160 µg

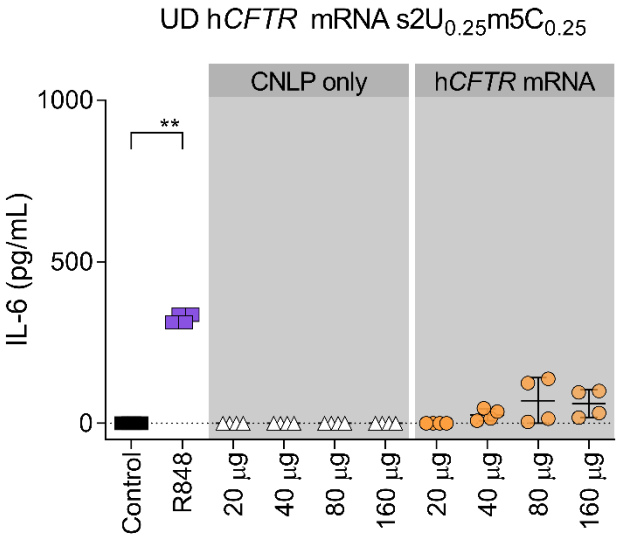
UD h*CFTR* mRNA s2U$_{0.25}$m5C$_{0.25}$
CNLP only
h*CFTR* mRNA
IL-6 (pg/mL)
1000
500
0
**
Control
R848
20 µg
40 µg
80 µg
160 µg
20 µg
40 µg
80 µg
160 µg

## IL-12

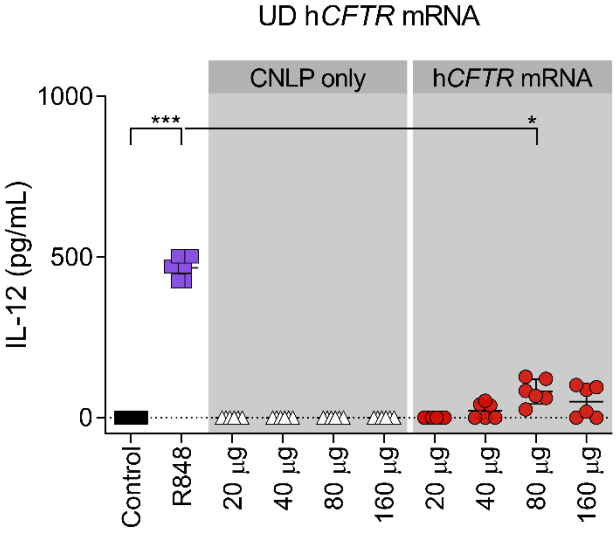
UD h*CFTR* mRNA
CNLP only
h*CFTR* mRNA
IL-12 (pg/mL)
1000
500
0
***
*
Control
R848
20 µg
40 µg
80 µg
160 µg
20 µg
40 µg
80 µg
160 µg

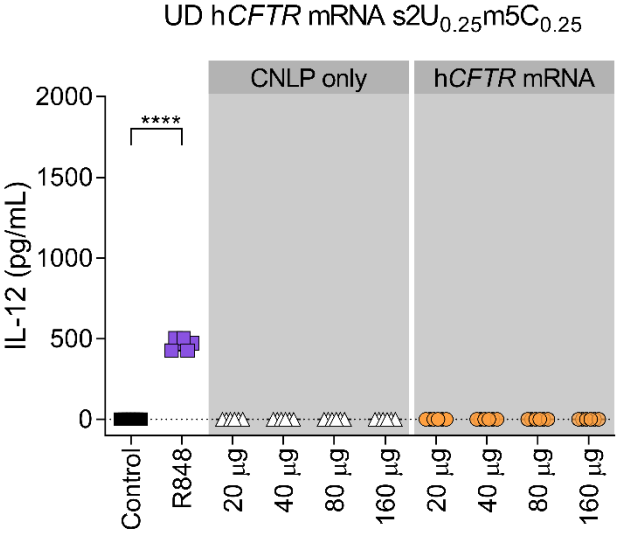
UD h*CFTR* mRNA s2U$_{0.25}$m5C$_{0.25}$
CNLP only
h*CFTR* mRNA
IL-12 (pg/mL)
2000
1500
1000
500
0
****
Control
R848
20 µg
40 µg
80 µg
160 µg
20 µg
40 µg
80 µg
160 µg

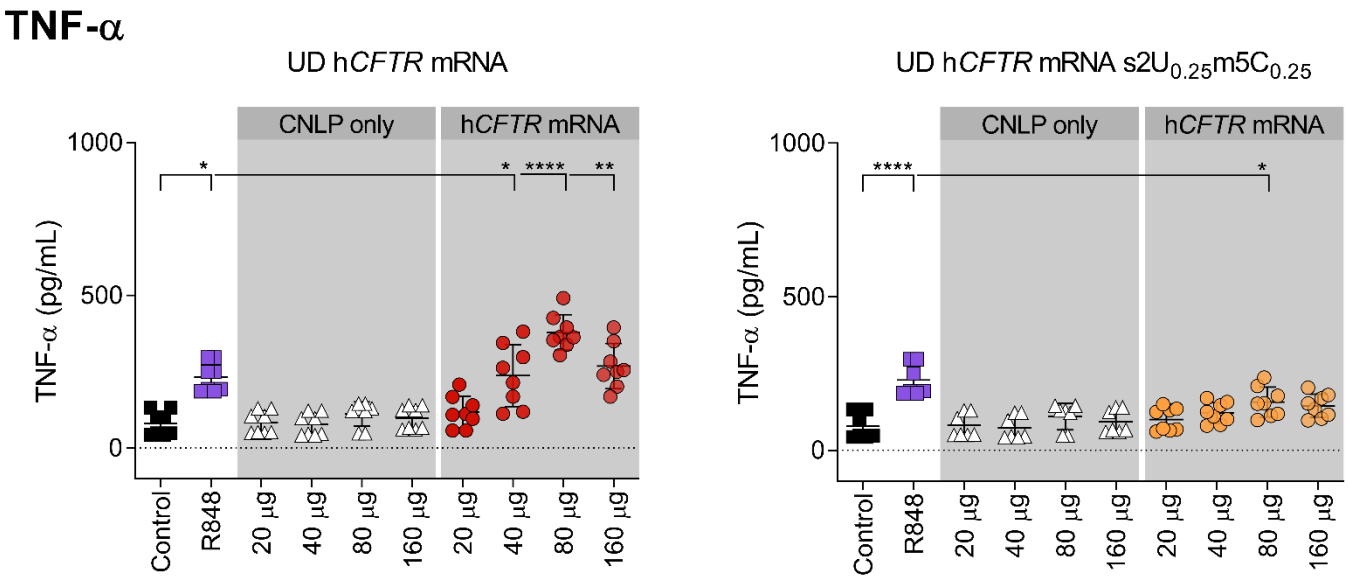


**Figure 3.15, Figure 3.16, Figure 3.17** *In vivo* immune responses determined with ELISA targeting IL-6, IL-12 and TNF-α in murine sera. Responses to i.v. treatment with UD h*CFTR* mRNA (red) and UD h*CFTR* mRNA s2U$_{0.25}$ m5C$_{0.25}$ (orange) (20, 40, 80 or 160 µg) were measured (N ≥ 4). Negative controls were murine serum (black) only or serum treated with cationic lipid nanoparticles (white). Positive controls were treated with R848 (purple). Measurements were performed 6 hours after the second injection. The dotted line represents the ELISA detection limit, box plots are depicted as means + / - SD.

The negative controls did not show any increase in IL-6 and IL-12 levels. However, there were slightly increased TNF-α levels observed in the untreated control as well as for sera treated with nanoparticles only. Treatment with R848 induced significant IL-6, IL-12 and TNF-α responses after six hours.

UD h*CFTR* mRNA raised significant IL-6 and TNF-α responses after six hours compared to the untreated control. IL-6 responses were highest following treatment with 80 and 160 µg of UD h*CFTR* mRNA (80 µg UD h*CFTR* mRNA: mean = 325.8 pg/ml, SD = 28.78 pg/ml, $p \leq 0.01$, N = 4; 160 µg UD h*CFTR* mRNA: mean = 375.4 pg/ml, SD = 174.4 pg/ml, $p \leq 0.05$, N = 4). Similarly, TNF-α levels were highest after treatment with 80 and 160 µg of UD h*CFTR* mRNA (80 µg UD h*CFTR* mRNA: mean = 379.0 pg/ml, SD = 57.78 pg/ml, $p \leq 0.0001$, N

= 8; 160 µg UD h*CFTR* mRNA: mean = 267.7 pg/ml, SD = 74.18 pg/ml, p ≤ 0.01, N = 8)

Overall, IL-12 levels were only mildly increased after six hours. There was a significant increase of IL-12 levels observed after administration of 80 µg UD h*CFTR* mRNA, compared to the untreated control group (mean = 81.03 pg/ml, SD = 38.32 pg/ml, p ≤ 0.05, N = 6).

Interestingly, UD h*CFTR* mRNA $s2U_{0.25}$ $m5C_{0.25}$ did not induce immune reactions as bold as those induced by UD h*CFTR* mRNA. There could be an increase in IL-6 and TNF-α levels observed six hours after the second injection, but this increase was clearly smaller as compared to responses following UD h*CFTR* mRNA treatment. Like the UD h*CFTR* mRNA, IL-6 and TNF-α responses were highest for UD h*CFTR* mRNA $s2U_{0.25}$ $m5C_{0.25}$ with doses of 80 and 160 µg respectively (IL-6: mean = 70.43 pg/ml, SD= 70.40 pg/ml and mean = 61.52 pg/ml, SD = 42.65 pg/ml; TNF-α: mean = 157.2 pg/ml, SD = 48.54 pg/ml and mean = 144.7 pg/ml, SD = 38.36 pg/ml).

These findings show that, h*CFTR* mRNA which was only uridine-depleted but did not undergo any further modification, did induce clear immune responses after six hours in a dose dependent-manner. On the other hand, IL-6 and TNF-α responses induced by UD h*CFTR* mRNA $s2U_{0.25}$ $m5C_{0.25}$ were remarkably weaker.

### 3.2.6 Concluding remarks

To conclude, the *in vivo* experiments, administering uridine-depleted h*CFTR* mRNA to $Cftr^{-/-}$ mice, have shown mainly unsuccessful. Although a modest improvement of lung function and some hCFTR gene expression induced by UD h*CFTR* mRNA was observed, our findings did not indicate towards a superiority of uridine-depleted mRNA over unmodified mRNA or pDNA. Moreover, the high saliva chloride concentrations found in the treated mice und the low concentrations of hCFTR protein in the murine lungs, imply that i.v. administration of either of the three treatments did not result in any effect at all.

Measurement of *in vivo* immune responses following i.v. treatment with uridine-depleted h*CFTR* mRNA via ELISA analysis indicates that chemical modifications augmenting uridine-depletion might be important for inhibiting immune reactions

following treatment with mRNA, which induce the mRNA's degradation and translational inhibition.

# 4 Discussion

CF is the most common lethal monogenic disease among Caucasians (1). It is an autosomal-recessive disorder leading to missing or unfunctional CFTR protein. CF is a multiorgan disease, however the main cause for CF patient's morbidity and mortality is the respiratory disease, which is consequently considered the main target of CF therapy (11, 16). Currently, mono -, dual - and triple therapies with channel modulators, as Ivacaftor, Lumacaftor, Tezacaftor and Elexacaftor, are the best therapeutic option for CF patients available. However, channel modulators are mutation-dependent and do not benefit all CF patients (23, 27, 33). Moreover, they only provide modest improvement of lung function by up to a maximum of 14 % (27, 30, 31, 34). So there still is an urgent need to explore alternative therapy options for CF, one of which is gene therapy. Gene therapy, aiming to replace the missing CFTR protein, constitutes a promising approach to provide a cure for CF, which is mutation-independent and therefore suitable for all CF patients. As clinical trials, investigating CFTR-delivery via DNA-based vectors have shown mainly unsuccessful, mRNA-based h*CFTR*-delivery has come into focus (64). Several pre-clinical studies investigating mRNA-mediated CFTR supplementation *in vitro* and *in vivo* have provided promising findings (2, 115, 131). Most recently Translate Bio initiated a first-in-man clinical trial, administering h*CFTR* mRNA to CF patients (132). In 2019 promising interim results were presented (133).

Previous studies on mRNA-mediated h*CFTR* delivery mainly focused on delivery of modified mRNA to overcome innate immune responses, which might cause degradation and translational inhibition of the mRNA (81, 82, 84, 85). Another promising tool to enhance h*CFTR* mRNA's stability and translational efficiency is uridine-depletion. Previous findings indicated that reducing the uridine-content of h*CFTR* mRNA, might decrease its immunogenicity and enhance its translational efficiency (75, 79, 81-83, 88).

The objective of this thesis was to investigate whether uridine-depleted h*CFTR* mRNA restores functional hCFTR gene and protein expression *in vitro* and *in vivo*.

To assess hCFTR expression mediated by uridine-depleted h*CFTR* mRNA *in vitro,* CFBE41o$^-$ cells were transfected with either UD/non-UD h*CFTR* mRNA or UD h*CFTR* pDNA. 24 hours after transfection we performed a RT-qPCR, a Western Blot, and an MTT-Assay.

By performing a RT-qPCR h*CFTR* gene expression can be assessed, which allows conclusions on h*CFTR* mRNA levels in the cells. RT-qPCR analysis revealed that indeed all three treatments induced hCFTR gene expression. Remarkably, 24 hours after transfection, h*CFTR* mRNA levels were higher after treatment with uridine-depleted mRNA, relative to treatment with non-UD mRNA. hCFTR gene expression induced by UD h*CFTR* mRNA was even significantly higher than in the untreated control cells. This indicates that uridine-depletion might increase h*CFTR* mRNA levels, e.g. through enhancing the mRNA's stability.

The presence of the complex-glycosylated, post-Golgi form of hCFTR in our Western Blot analysis demonstrated that there was fully-processed hCFTR protein expressed after transfection with uridine-depleted mRNA and pDNA, respectively. Moreover, while transfection with UD h*CFTR* mRNA resulted in considerable hCFTR protein expression, non-UD mRNA induced no or only very little hCFTR expression. Taking earlier results and our findings from RT-qPCR, indicating that all three treatments induced hCFTR gene expression, into account (115), it seems unlikely, that unmodified h*CFTR* mRNA induces no hCFTR protein expression at all. To come to a definite conclusion on this question, the experiment needs to be further optimized and repeated. Nonetheless, our observations are in line with previous findings and support our hypothesis, that the nucleotide-composition of h*CFTR* mRNA influences hCFTR expression. Reducing the uridine-content of h*CFTR* mRNA led to a clear increase in hCFTR protein expression, as compared to non-UD h*CFTR* mRNA. Previously, it has been shown that the GC-content of a gene or mRNA influences protein expression (93, 95, 100). In addition to that, Vaidyanathan et al. noted that uridine-depletion of *Cas9* mRNA highly impacts the protein's activity (75). Our findings are now extending Vaidyanathan's approach of *Cas9* mRNA optimization through uridine-depletion to optimization of h*CFTR* mRNA. The increase in

protein expression following optimization of the nucleotide composition through uridine-depletion of the h*CFTR* mRNA, could be mediated by enhanced mRNA properties, as increased stability, and reduced immunogenicity (93, 95). This notion is in line with our findings from RT-qPCR, that indicate an increase in mRNA stability *in vitro* through uridine-depletion. One important mechanism might be evading activation of PRRs. Many PRRs, which are involved in the host's antiviral defense, recognize RNA structures. Since uridine is a characteristic feature of RNA, uridine-stretches are essential for activation of certain innate immune receptors, as RIG - I, TLR 7 and 8 and PKR (79, 81-83). Avoiding activation of these receptors might prevent mRNA degradation and consequently increase mRNA's stability. Moreover, optimizing the nucleotide composition might promote translational efficiencies (98). Taken together we found an increase in protein expression, following uridine-depletion of h*CFTR* mRNA, which might result from improved mRNA properties, enhanced translation, or both.

Encouragingly, transfection with uridine-depleted h*CFTR* mRNA led to expression of 49.1 % of hCFTR protein levels induced by pDNA, which we considered a reliable reference value (44, 60, 115). Since CF is an autosomal-recessive disease 50 % of wild-type CFTR expression are sufficient to prevent development of the CF phenotype (135). Earlier investigations even indicated that only 10 % of wild-type hCFTR expression, might be enough to prevent development of respiratory disease (11, 135). Taking these findings into consideration, our results indicate that indeed, uridine-depleted h*CFTR* mRNA might sufficiently restore hCFTR levels to alleviate CF lung disease. However, as Griesenbach et al. pointed out, there are still lots of open questions to be answered, concerning the number of CTFR expressing cells, that is required and additional factors promoting development of lung disease (11). Recent investigations identified pulmonary ionocytes as major CFTR-expressing cells in murine and human airways (8, 9). Further research on this rare cell type and on targeting strategies is needed to further evaluate UD h*CFTR* mRNA's ability to sufficiently restore hCFTR protein expression.

Performance of an MTT-Assay revealed that all transfections of CFBE41o$^-$ cells induce cell death, which is not surprising as the process of liposome complexes entering the cell either by membrane fusion or endocytosis and the subsequent release of the nucleic acids, expose the cells to high stress. Moreover, nucleic acid delivery, especially delivery of IVT mRNA, might elicit immune reactions, e.g. by activation of Toll-like-receptors, that promote cell death as well. Encouragingly, overall, we observed low cell death rates following nucleic acid transfection. Generally, this shows that nucleic acid delivery is an efficient means to restore hCFTR expression *in vitro*. Furthermore, we found that uridine-depletion of h*CFTR* mRNA decreased its cytotoxicity as compared to non-UD h*CFTR* mRNA. Again, this is most probably due to decreased recognition through PRRs, reducing downstream signaling and cytokine secretion, which results in decreased cytotoxicity.

It is important to note that we performed downstream experiments only at a 24 hours timepoint, due to mRNA expression kinetics, expressing most efficiently 24 hours after transfection. However, it is likely that hCFTR expression induced by pDNA would have further increased at a 72 hours timepoint, due to different expression kinetics: pDNA must be transferred into the nucleus to be transcribed into mRNA which is transferred back into the cytosol where it is translated into protein. Additionally, Haque et al. pointed out, that kinetics of protein expression mediated by modified h*CFTR* mRNAs 24 and 72 hours after transfection, were dependent on the modifications that were used (115). Thorough investigations on expression kinetics of uridine-depleted h*CFTR* mRNA, will be an important and interesting objective for future research.

Furthermore, while western blot analysis confirmed that there is mature hCFTR protein present in the cells, it does not allow definite conclusions on whether the protein reached the plasma membrane and on the protein's functionality. Yet, previous studies already provided evidence, that indeed h*CFTR* mRNA transfection leads to expression of functional hCFTR at the plasma membrane, e.g. by measurement of CFTR-mediated $I^-$ influx through a YFP-based assay (2, 115, 131). Extending these findings on hCFTR localization and function to uridine-depleted h*CFTR* mRNA, should be aimed at in future investigations.

Nonetheless, the expression of mature hCFTR protein in the cells, as found in our experiments, already strongly indicated, that functional hCFTR was expressed at the plasma membrane, following transfection with UD h*CFTR* mRNA.

Taken together RT-qPCR and western blot analysis confirmed the potential of uridine-depleted h*CFTR* mRNA to restore hCFTR expression and demonstrated that its properties are superior to non-uridine-depleted h*CFTR* mRNA *in vitro*. Taking previous investigations into account our results indicate that uridine-depletion is a promising approach to increase gene and protein expression and decrease cytotoxicity *in vitro*, by enhancing mRNA properties and/or increasing translational efficiencies. Finally, our findings extend the spectrum of mRNAs investigated for h*CFTR* delivery *in vitro* to uridine-depleted mRNA and give rise to the question whether these promising findings are transferrable to *in vivo* use. Based on these encouraging findings, we initiated *in vivo* experiments to investigate whether UD h*CFTR* mRNA induces expression of functional hCFTR protein in $Cftr^{-/-}$ mice. In this context, $Cftr^{-/-}$ mice were i.v. treated with either UD h*CFTR* mRNA, non-UD h*CFTR* mRNA or UD h*CFTR* pDNA complexed to chitosan-coated PLGA nanoparticles. After seven days endpoint experiments were conducted.

It has previously been shown that mRNA therapeutics targeted at the respiratory tract can be administered both locally (i.t.) or systemically (i.v.) (90, 115). Systemic delivery of h*CFTR* mRNA circumvents lung specific barriers, as respiratory mucus and mucociliary clearance (12). In CF airways the mucus is pathologically increased and highly viscous, which might further inhibit local delivery of therapeutics (102, 116, 136). For these reasons we considered i.v. delivery of UD h*CFTR* mRNA to be more effective and focused on this application route.

For functional analysis $FEV_{0.1}$ and saliva chloride concentrations were determined. Both values are important parameters for assessment of CFTR function and disease progression. Measurement of the saliva chloride concentration is an analog procedure to the sweat test, which is gold standard in CF diagnostic (1). A decrease in saliva chloride concentration indicates

expression of functional CFTR. In addition to that, determination of the forced expiratory volume in one second ($FEV_1$) is essential for monitoring the progression of CF lung disease and predicting the patient's morbidity and mortality (137, 138). A $FEV_1$ < 30 % of the predicted value is associated with a two-year mortality rate above 50 % (138). In smaller animals as mice the $FEV_{0.1}$ is measured as an analog to the human $FEV_1$. As expected in $Cftr^{-/-}$ mice the $FEV_{0.1}$ was decreased to 64 % of $Cftr^{+/+}$ mice. However, while i.v. delivery of either UD/non-UD h*CFTR* mRNA or UD h*CFTR* pDNA complexed to chitosan-coated PLGA nanoparticles resulted in a modest improvement of lung function, we could neither find a significant increase relative to the negative control nor a significant difference between the three treatments. Additionally, the saliva chloride assay did not show any decrease in chloride concentrations, indicating that there was no functional hCFTR expressed in the saliva gland ducts. These findings indicate that while at least some mRNA or pDNA might have reached the murine airways, the treatment did not achieve restoration of hCFTR expression in the saliva glands. Additionally, in RT-qPCR and hCFTR ELISA we could not find a definite increase in hCFTR gene and protein expression in the murine lung. These observations contradict previous findings, observing a restoration of functional hCFTR expression, resulting in a significant increase of $FEV_{0.1}$ values between 14 and 23 % following i.v. injection of modified h*CFTR* mRNA complexed to chitosan-coated PLGA nanoparticles. Moreover, modified mRNA as well as pDNA were found to decrease saliva chloride concentrations by up to 52 %. (115). Furthermore, Robinson et al. reported a restoration of CFTR-mediated chloride efflux following treatment of the nasal epithelium of $Cftr^{-/-}$ mice with modified mRNA delivered via LNPs (2).

There are different possible reasons for these rather disappointing findings. First, the mouse cohort that was receiving the treatment was quite heterogenous in size and weight and we were not able to completely equalize the male:female ratio. Therefore, it is possible, that in some mice the dosage was not appropriate, resulting in ineffective treatment. Moreover, the delivery mode chosen could have been unsuitable for treatment of $Cftr^{-/-}$ mice. We decided to administer mRNA and pDNA systemically complexed to chitosan-coated PLGA nanoparticles. Since

previous investigations provided evidence that systemic delivery of h*CFTR* mRNA to murine lungs is superior to local delivery, it is unlikely that the intravenous application in our experiments was unsuccessful (115). Alternatively, to the use of polymer-based nanoparticles, mRNA can be delivered to the airways via lipid-based nanoparticles. Kormann and coworkers reported successful delivery of *SP-B* mRNA via TransIT to the murine airways and Robinson et al. demonstrated successful LNP delivery of h*CFTR* mRNA to the murine nasal epithelium (2, 90). Yet, the successful use of polymer-based nanoparticles to deliver nucleic acids to the lung has been demonstrated several times in the past (107, 115, 129). Kaczmarek et al. reported that intravenous delivery of mRNA to murine lungs via polymer-based nanoparticles in feasible (107). Moreover, Mahiny et al. successfully delivered ZFN-encoding mRNA via chitosan-coated PLGA nanoparticles to airways of transgenic SP-B mice (129). Consequently, it is highly probable that delivery of uridine-depleted h*CFTR* mRNA via chitosan-coated PLGA-nanoparticles was successful in our experiments. Thus, the reason for the absence of functional hCFTR expression following treatment with uridine-depleted mRNA might be found in the mRNA itself.

We hypothesized that uridine-depleted h*CFTR* mRNA might still raise considerable immune responses *in vivo*. Cytokine secretion induced by activation of innate immune receptors might have caused degradation and translational inhibition of the mRNA administered. This could be a possible reason underlying the absence of therapeutic effects after administration of uridine-depleted h*CFTR* mRNA. Thus, we took a cytokine ELISA, which was performed parallelly to my experiments in our laboratory into consideration. This ELISA was measuring IL-6, -12 and TNF-α secretion following systemic administration of uridine-depleted h*CFTR* mRNA and uridine-depleted, modified h*CFTR* mRNA to $Cftr^{-/-}$ mice. For this ELISA analysis cationic nanoliposomes were used as vehicles for the mRNA instead of PLGA nanoparticles. Therefore, its significance to my previous results is limited. However, it offers a first indication towards possible reasons underlying the outcome of my *in vivo* experiments. As we assumed h*CFTR* mRNA that was only uridine-depleted induced considerable cytokine secretion 6 hours after injection. These immune responses were greatly reduced by further introduction

of chemically modified nucleosides. Similarly, Vaidyanathan et al. found that while uridine-depletion most impacted indel activity of *Cas9* mRNA, chemical modifications played a crucial role for decreasing immune reactions elicited by *Cas9* mRNA (75). They reported significant immune responses induced by wild-type UD mRNA in an IFN reporter cell line and a whole blood assay, while the majority of UD mRNAs carrying further modifications did not induce significant cytokine secretion (75). However, in contrast to our findings, Vaidyanathan's group did not observe significant cytokine secretion following i.v. injection of uridine-depleted *Cas9* mRNA complexed to chitosan-coated PLGA nanoparticles (75). Nonetheless, we come to the same notion as Vaidyanathan, that further chemical modification of uridine-depleted mRNA is necessary to decrease unwanted immune responses. Further cytokine ELISA measurements using chitosan-coated PLGA nanoparticles as a vehicle for h*CFTR* mRNA are needed to come to a definite conclusion on UD h*CFTR* mRNAs immunogenicity in murine sera. Additionally, a further project was running in our laboratory investigating the effect of uridine-depleted h*CFTR* mRNA, which was modified with 100 % m1Ψ and 100 % N4-acetylcytidine (ac4C). In line with our hypothesis, a significant increase of the $FEV_{0.1}$ induced by the UD h*CFTR* mRNA $m1\Psi_{1.0}$ $ac4C_{1.0}$ to 85 % of the wild-type $FEV_{0.1}$ was observed (data not published). Taking these findings together with our results obtained from FlexiVent®, there is a clear trend apparent: although administration of uridine-depleted h*CFTR* mRNA resulted in a modest improvement of lung function, overall, it did not achieve a restoration of functional hCFTR expression *in vivo*. However, when additional chemical modifications were introduced, there was a significant improvement of lung function apparent. Finally, this notion is supported by the cytokine ELISA, that was conducted, indicating that additional chemical modifications of uridine-depleted h*CFTR* mRNA are needed to diminish its immunogenicity.

Our overall findings and reports from previous investigations, lead me to the conclusion that while uridine-depleted h*CFTR* mRNA outperforms non-UD h*CFTR* mRNA and efficiently restores hCFTR gene and protein expression *in vitro*, uridine-depletion alone is not sufficient to induce therapeutic hCFTR protein expression mediated by h*CFTR* mRNA *in vivo*. I assume, that the absence of

functional hCFTR expression *in vivo* is due to activation of innate immune receptors, which induce cytokine secretion and eventually lead to degradation and translational inhibition of UD h*CFTR* mRNA. Incorporation of additional chemical modifications into the uridine-depleted h*CFTR* mRNA might be necessary to efficiently reduce immunogenicity and enable restoration of functional hCFTR expression *in vivo*.

Further investigations on chemically modified, uridine-depleted h*CFTR* mRNA are needed to evaluate its applicability *in vivo* and eventually in humans. It remains to be assessed whether modified, uridine-depleted h*CFTR* mRNA is competitive or even superior to modified mRNA, which is not sequence-optimized. A comparison between these two treatment options *in vivo* would be an important first step. Remarkably, $FEV_{0.1}$ increases, that were induced by modified h*CFTR* mRNA in Haque's study and by uridine-depleted, modified h*CFTR* mRNA (unpublished data), exceeded $FEV_1$ improvements observed for dual/triple therapy with channel modulators (Orkambi®, Symdeko®, Trikafta®). Moreover, the interim results of the phase I/II clinical study initiated by Translate Bio, indicated that h*CFTR* mRNA is a safe and efficient therapeutic option for treatment of CF lung disease (133). Easy manufacturing, fast and transient expression, the possibility of repeated administration, potent delivery options and decreased immunogenicity due to introduction of modified nucleosides and sequence-engineering, render h*CFTR* mRNA highly suitable for hCFTR protein supplementation (12, 90). Systemic delivery of h*CFTR* mRNA might already be feasible for newborns and infants in the future and consequently prevent development of CF lung disease when administered in this early stage of life. Future investigations on further optimization of the h*CFTR* mRNA and on safety and efficiency in humans will be required. Robinson et al. suggested that combining h*CFTR* mRNA therapy with dietary flavonoids or CFTR potentiators as Lumacaftor or Tezacaftor, might further increase hCFTR's half-life and function (2). Investigations on whether combining h*CFTR* mRNA with channel modulators is beneficial for CF patients are advisable. Finally, h*CFTR* mRNA therapy might provide a safe, mutation-independent and efficient therapy for CF lung disease.

# 5 Summary

Cystic Fibrosis is the most common lethal monogenic disease among Caucasians. It is considered a multiorgan disease, leading to missing, reduced or unfunctional CFTR protein, which plays an important role for the ion and fluid homeostasis. In the respiratory system the lack of CFTR protein results in dry and rigid mucus, recurrent infection and increasing lung damage. The lung disease is the main cause for Cystic Fibrosis patient's morbidity and mortality and is consequently considered the main target of Cystic Fibrosis therapy.

Therapeutic protein delivery, aiming to replace the missing or unfunctional CFTR protein constitutes a potential cure for Cystic Fibrosis. CFTR protein delivery can be mediated either by plasmid DNA (pDNA), mRNA or the CFTR protein itself. As *CFTR* pDNA delivery has shown mainly unsuccessful in clinical trials, mRNA-based *CFTR* delivery has come into focus as a promising alternative. Therapeutic mRNA delivery is facing two major obstacles: immunogenicity and instability *in vivo*. One approach to circumvent these obstacles is sequence-engineering, e.g. uridine-depletion (UD), of the mRNA delivered. Reducing the mRNA's uridine content might decrease its immunogenicity and increase the mRNA's translational efficiency.

This thesis investigates the expression of functional human CFTR (hCFTR) protein following UD h*CFTR* mRNA administration *in vitro* and *in vivo*.

RT-qPCR and Western Blot analysis revealed that UD h*CFTR* mRNA induces hCFTR gene and protein expression in CFBE41o$^-$ cells outperforming unmodified h*CFTR* mRNA. Moreover, uridine-depletion decreased h*CFTR* mRNA's cytotoxicity as compared to unmodified h*CFTR* mRNA, which was demonstrated with an MTT-Assay. However, in murine airways intravenous treatment with UD h*CFTR* mRNA only resulted in modest improvement of lung function and no reduction of the saliva chloride concentration could be observed. Furthermore, RT-qPCR and hCFTR ELISA analysis of the murine lung tissue indicated that treatment with UD h*CFTR* mRNA did not induce considerable hCFTR expression. At last, measurement of cytokine levels in murine sera after application of h*CFTR* mRNA showed that while treatment with UD h*CFTR* mRNA still induces immune

responses *in vivo*, introduction of further base modifications into UD h*CFTR* mRNA decreases immune responses *in vivo* considerably.

All in all, I conclude that while UD h*CFTR* mRNA efficiently restores h*CFTR* gene and protein expression *in vitro*, uridine-depletion alone does not decrease immune reactions sufficiently to result in efficient translation and protein expression *in vivo*. However, introduction of further chemical modifications augmenting uridine-depletion might efficiently reduce immunogenicity and result in therapeutic h*CFTR* protein expression *in vivo*. Therefore, combining uridine-depletion with additional base modifications might constitute a possible way to go for therapeutic hCFTR delivery *in vivo*. Further investigation on uridine-depleted, chemically modified h*CFTR* mRNA and its applicability *in vivo* will be an important objective for future research. Finally, h*CFTR* mRNA therapy might provide a mutation-independent and efficient therapy for Cystic Fibrosis lung disease.

# 6 German summary

Zystische Fibrose ist die häufigste monogene, lebensverkürzende Erkrankung unter Kaukasiern. Bei der Zystischen Fibrose fehlt der CFTR-Ionenkanal bzw. ist dieser in seiner Funktion eingeschränkt. Im respiratorischen System führt das Fehlen von CFTR zur Produktion von zähflüssigem, viskösem Mukus, zum wiederkehrendenden Auftreten von Infektionen und zu zunehmenden Lungenschäden. Der Hauptgrund für Morbidität und Mortalität der Patient:innen mit Zystischer Fibrose ist die Lungenerkrankung, weshalb diese als primäres Ziel möglicher Therapien angesehen wird.

Als eine kausale Therapieoption für die Zystische Fibrose wird die Proteinersatztherapie diskutiert. Ziel dieser Behandlung ist es, das fehlende CFTR Protein zu ersetzen. Prinzipiell kann CFTR als Plasmid-DNA (pDNA), als mRNA oder als Protein gegeben werden. Allerdings war die Proteinersatztherapie mit humanem *CFTR* (hCFTR) in Form von pDNA in klinischen Studien bisher nicht erfolgreich. Die Therapie mittels h*CFTR* mRNA stellt daher eine weitere vielversprechende Alternative dar. Die größten Hindernisse, die dem therapeutischen Einsatz von mRNA im Wege stehen, sind ihre Immunogenität und Instabilität *in vivo*. Ein möglicher Ansatz diesen Problemen beizukommen, ist die sogenannte „Sequenzoptimierung“, beispielsweise durch Reduktion des Uridin-Gehalts von mRNA. Die Uridin-Depletion (UD) ermöglicht es, Immunreaktionen, die durch mRNA ausgelöst werden, zu reduzieren und gleichzeitig ihre Translation *in vivo* zu steigern.

Vor diesem Hintergrund untersuche ich im Rahmen meiner Dissertation die hCFTR Expression nach Gabe von UD h*CFTR* mRNA *in vitro* und *in vivo*.

In den *in vitro* Experimenten konnte gezeigt werden, dass UD h*CFTR* mRNA in CFBE41o$^{-}$-Zellen sowohl hCFTR Gen- als auch hCFTR Protein-Expression induziert und dabei der nicht-modifizierten h*CFTR* mRNA überlegen ist. Außerdem zeigte sich in einem MTT-Assay, dass durch die Uridin-Depletion die Zytotoxizität von h*CFTR* mRNA im Vergleich zur nicht-modifizierten mRNA gesenkt werden kann. Allerdings konnten wir nach der Behandlung von Cftr$^{-/-}$ Mäusen mit UD h*CFTR* mRNA nur eine geringfügige Verbesserung der Lungenfunktion feststellen. Außerdem zeigte die Untersuchung des murinen

Speichels keine reduzierte Chlorid-Konzentration, welche zu erwarten gewesen wäre. Auch die RT-qPCR und der hCFTR ELISA, die ich mit murinem Lungengewebe durchführte, zeigten keine deutliche hCFTR Expression nach Behandlung der Mäuse mit UD h*CFTR* mRNA. Abschließend wurden die Zytokinlevel in murinen Seren nach Gabe von h*CFTR* mRNA bestimmt. Hierbei konnte beobachtet werden, dass die UD h*CFTR* mRNA weiterhin eine Immunantwort *in vivo* auslöst. Diese Immunreaktionen konnten durch das Einfügen zusätzlicher chemischer Modifikationen in die UD h*CFTR* mRNA deutlich gesenkt werden. Die Kombination von Uridin-Depletion und Basen-Modifikation der h*CFTR* mRNA scheint daher ein möglicher Weg hin zur Proteinersatztherapie mittels mRNA zu sein.

Zusammenfassend komme ich zu dem Schluss, dass die Gabe von UD h*CFTR* mRNA *in vitro* erfolgreich hCFTR Expression induzieren kann und dabei ihrem nicht-modifizierten Gegenstück überlegen ist. Die Uridin-Depletion allein scheint aber nicht auszureichen, um die Immunantwort *in vivo*, die durch die Behandlung mit h*CFTR* mRNA ausgelöst wird, erfolgreich zu senken. Allerdings konnte durch das zusätzliche Einfügen chemischer Modifikationen, eine deutliche Minimierung der Immunantwort *in vivo* erreicht werden, eine wichtige Voraussetzung für erfolgreiche Translation und Expression von hCFTR. Für die zukünftige Forschung wird die tiefergehende Untersuchung sequenzoptimierter und chemisch modifizierter h*CFTR* mRNA und ihrer Anwendbarkeit *in vivo* ein wichtiges Ziel sein. Auf dieser Grundlage könnte die Proteinersatztherapie mittels h*CFTR* mRNA in Zukunft eine effiziente, mutationsunabhängige und kausale Therapie für die Lungenerkrankung bei Zystischer Fibrose darstellen.

# 7 Bibliography


1. Alton E, Armstrong DK, Ashby D, Bayfield KJ, Bilton D, Bloomfield EV, et al. Efficacy and Mechanism Evaluation. A randomised, double-blind, placebo-controlled trial of repeated nebulisation of non-viral cystic fibrosis transmembrane conductance regulator (CFTR) gene therapy in patients with cystic fibrosis. Southampton (UK): NIHR Journals Library

Copyright (c) Queen's Printer and Controller of HMSO 2016. This work was produced by Alton et al. under the terms of a commissioning contract issued by the Secretary of State for Health. This issue may be freely reproduced for the purposes of private research and study and extracts (or indeed, the full report) may be included in professional journals provided that suitable acknowledgement is made and the reproduction is not associated with any form of advertising. Applications for commercial reproduction should be addressed to: NIHR Journals Library, National Institute for Health Research, Evaluation, Trials and Studies Coordinating Centre, Alpha House, University of Southampton Science Park, Southampton SO16 7NS, UK.; 2016.

2. Robinson E, MacDonald KD, Slaughter K, McKinney M, Patel S, Sun C, et al. Lipid Nanoparticle-Delivered Chemically Modified mRNA Restores Chloride Secretion in Cystic Fibrosis. Mol Ther. 2018;26(8):2034-46.
3. Schwarz C. Zystische Fibrose: Mukoviszidose ist längst keine Kinderkrankheit mehr. Dtsch Arztebl International. 2017;114(9):[14].
4. Hwang T-C, Kirk KL. The CFTR ion channel: gating, regulation, and anion permeation. Cold Spring Harbor perspectives in medicine. 2013;3(1):a009498-a.
5. van Meegen MA, Terheggen SW, Koymans KJ, Vijftigschild LA, Dekkers JF, van der Ent CK, et al. CFTR-mutation specific applications of CFTR-directed monoclonal antibodies. J Cyst Fibros. 2013;12(5):487-96.
6. Linsdell P. Cystic fibrosis transmembrane conductance regulator chloride channel blockers: Pharmacological, biophysical and physiological relevance. World J Biol Chem. 2014;5(1):26-39.
7. Pezzulo AA, Tang XX, Hoegger MJ, Abou Alaiwa MH, Ramachandran S, Moninger TO, et al. Reduced airway surface pH impairs bacterial killing in the porcine cystic fibrosis lung. Nature. 2012;487(7405):109-13.
8. Montoro DT, Haber AL, Biton M, Vinarsky V, Lin B, Birket SE, et al. A revised airway epithelial hierarchy includes CFTR-expressing ionocytes. Nature. 2018;560(7718):319-24.
9. Plasschaert LW, Žilionis R, Choo-Wing R, Savova V, Knehr J, Roma G, et al. A single-cell atlas of the airway epithelium reveals the CFTR-rich pulmonary ionocyte. Nature. 2018;560(7718):377-81.
10. Matsui H, Grubb BR, Tarran R, Randell SH, Gatzy JT, Davis CW, et al. Evidence for Periciliary Liquid Layer Depletion, Not Abnormal Ion Composition, in the Pathogenesis of Cystic Fibrosis Airways Disease. Cell. 1998;95(7):1005-15.
11. Griesenbach U, Pytel KM, Alton EW. Cystic Fibrosis Gene Therapy in the UK and Elsewhere. Hum Gene Ther. 2015;26(5):266-75.
12. Sahu I, Haque A, Weidensee B, Weinmann P, Kormann MSD. Recent Developments in mRNA-Based Protein Supplementation Therapy to Target Lung Diseases. Mol Ther. 2019;27(4):803-23.

13. Kreda SM, Davis CW, Rose MC. CFTR, mucins, and mucus obstruction in cystic fibrosis. Cold Spring Harb Perspect Med. 2012;2(9):a009589.
14. Masood A, Yi M, Belcastro R, Li J, Lopez L, Kantores C, et al. Neutrophil elastase-induced elastin degradation mediates macrophage influx and lung injury in 60% O2-exposed neonatal rats. Am J Physiol Lung Cell Mol Physiol. 2015;309(1):L53-62.
15. Herold G, editor. Innere Medizin 2020 : eine vorlesungsorientierte Darstellung : unter Berücksichtigung des Gegenstandskataloges für die Ärztliche Prüfung : mit ICD 10-Schlüssel im Text und Stichwortverzeichnis. Köln: Gerd Herold; 2020.
16. Davies JC, Alton EWFW, Bush A. Cystic fibrosis. BMJ. 2007;335(7632):1255-9.
17. Amaral MD. CFTR and chaperones: processing and degradation. J Mol Neurosci. 2004;23(1-2):41-8.
18. Farinha CM, Canato S. From the endoplasmic reticulum to the plasma membrane: mechanisms of CFTR folding and trafficking. Cell Mol Life Sci. 2017;74(1):39-55.
19. Colledge WH, Abella BS, Southern KW, Ratcliff R, Jiang C, Cheng SH, et al. Generation and characterization of a delta F508 cystic fibrosis mouse model. Nat Genet. 1995;10(4):445-52.
20. Herold G, editor. Innere Medizin 2018 : eine vorlesungsorientierte Darstellung : unter Berücksichtigung des Gegenstandskataloges für die Ärztliche Prüfung : mit ICD 10-Schlüssel im Text und Stichwortverzeichnis. Köln: Gerd Herold; 2018.
21. Van Goor F, Hadida S, Grootenhuis PDJ, Burton B, Stack JH, Straley KS, et al. Correction of the F508del-CFTR protein processing defect in vitro by the investigational drug VX-809. Proc Natl Acad Sci U S A. 2011;108(46):18843-8.
22. Ramsey BW, Davies J, McElvaney NG, Tullis E, Bell SC, Dřevínek P, et al. A CFTR potentiator in patients with cystic fibrosis and the G551D mutation. The New England journal of medicine. 2011;365(18):1663-72.
23. Davies JC, Wainwright CE, Canny GJ, Chilvers MA, Howenstine MS, Munck A, et al. Efficacy and safety of ivacaftor in patients aged 6 to 11 years with cystic fibrosis with a G551D mutation. American journal of respiratory and critical care medicine. 2013;187(11):1219-25.
24. Hoy SM. Elexacaftor/Ivacaftor/Tezacaftor: First Approval. Drugs. 2019;79(18):2001-7.
25. Gentzsch M, Mall MA. Ion Channel Modulators in Cystic Fibrosis. Chest. 2018;154(2):383-93.
26. Clancy JP, Rowe SM, Accurso FJ, Aitken ML, Amin RS, Ashlock MA, et al. Results of a phase IIa study of VX-809, an investigational CFTR corrector compound, in subjects with cystic fibrosis homozygous for the F508del-CFTR mutation. Thorax. 2012;67(1):12-8.
27. Wainwright CE, Elborn JS, Ramsey BW, Marigowda G, Huang X, Cipolli M, et al. Lumacaftor-Ivacaftor in Patients with Cystic Fibrosis Homozygous for Phe508del CFTR. N Engl J Med. 2015;373(3):220-31.
28. FDA approves new breakthrough therapy for cystic fibrosis [press release]. Food and Drug Administration, October 10, 2019.
29. European Commission Approves KAFTRIO® (ivacaftor/tezacaftor/elexacaftor) in Combination With Ivacaftor to Treat Cystic Fibrosis in People Ages 12 Years and Older [press release]. Vertex Pharmaceuticals Incorporated August 21, 2020.

30. Heijerman HGM, McKone EF, Downey DG, Van Braeckel E, Rowe SM, Tullis E, et al. Efficacy and safety of the elexacaftor plus tezacaftor plus ivacaftor combination regimen in people with cystic fibrosis homozygous for the F508del mutation: a double-blind, randomised, phase 3 trial. Lancet. 2019;394(10212):1940-8.
31. Middleton PG, Mall MA, Drevinek P, Lands LC, McKone EF, Polineni D, et al. Elexacaftor-Tezacaftor-Ivacaftor for Cystic Fibrosis with a Single Phe508del Allele. N Engl J Med. 2019;381(19):1809-19.
32. Elborn JS, Ramsey BW, Boyle MP, Konstan MW, Huang X, Marigowda G, et al. Efficacy and safety of lumacaftor/ivacaftor combination therapy in patients with cystic fibrosis homozygous for Phe508del CFTR by pulmonary function subgroup: a pooled analysis. The Lancet Respiratory medicine. 2016;4(8):617-26.
33. Taylor-Cousar JL, Munck A, McKone EF, van der Ent CK, Moeller A, Simard C, et al. Tezacaftor-Ivacaftor in Patients with Cystic Fibrosis Homozygous for Phe508del. N Engl J Med. 2017;377(21):2013-23.
34. Jennings MT, Dezube R, Paranjape S, West NE, Hong G, Braun A, et al. An Observational Study of Outcomes and Tolerances in Patients with Cystic Fibrosis Initiated on Lumacaftor/Ivacaftor. Ann Am Thorac Soc. 2017;14(11):1662-6.
35. Labaste A, Ohlmann C, Mainguy C, Jubin V, Perceval M, Coutier L, et al. Real-life acute lung function changes after lumacaftor/ivacaftor first administration in pediatric patients with cystic fibrosis. J Cyst Fibros. 2017;16(6):709-12.
36. Ridley K, Condren M. Elexacaftor-Tezacaftor-Ivacaftor: The First Triple-Combination Cystic Fibrosis Transmembrane Conductance Regulator Modulating Therapy. J Pediatr Pharmacol Ther. 2020;25(3):192-7.
37. Therapy ASoGaC. Gene Therapy Basics 2021 [Available from: https://patienteducation.asgct.org/gene-therapy-101.
38. Marangi M, Pistritto G. Innovative Therapeutic Strategies for Cystic Fibrosis: Moving Forward to CRISPR Technique. Front Pharmacol. 2018;9:396-.
39. Yan Z, McCray PB, Jr., Engelhardt JF. Advances in gene therapy for cystic fibrosis lung disease. Hum Mol Genet. 2019;28(R1):R88-r94.
40. Russell S, Bennett J, Wellman JA, Chung DC, Yu ZF, Tillman A, et al. Efficacy and safety of voretigene neparvovec (AAV2-hRPE65v2) in patients with RPE65-mediated inherited retinal dystrophy: a randomised, controlled, open-label, phase 3 trial. Lancet. 2017;390(10097):849-60.
41. Shirley JL, de Jong YP, Terhorst C, Herzog RW. Immune Responses to Viral Gene Therapy Vectors. Mol Ther. 2020;28(3):709-22.
42. Ramjeesingh, Huan, Wilschanski, Durie, Li, Gyomorey, et al. Assessment of the Efficacy of In Vivo CFTR Protein Replacement Therapy in CF Mice. Human Gene Therapy. 1998;9(4):521-8.
43. Griesenbach U, Alton EWFW. Moving forward: cystic fibrosis gene therapy. Human molecular genetics. 2013;22(R1):R52-R8.
44. Rosenfeld MA, Yoshimura K, Trapnell BC, Yoneyama K, Rosenthal ER, Dalemans W, et al. In vivo transfer of the human cystic fibrosis transmembrane conductance regulator gene to the airway epithelium. Cell. 1992;68(1):143-55.
45. Zabner J, Couture LA, Gregory RJ, Graham SM, Smith AE, Welsh MJ. Adenovirus-mediated gene transfer transiently corrects the chloride transport defect in nasal epithelia of patients with cystic fibrosis. Cell. 1993;75(2):207-16.

46. Zabner J, Ramsey BW, Meeker DP, Aitken ML, Balfour RP, Gibson RL, et al. Repeat administration of an adenovirus vector encoding cystic fibrosis transmembrane conductance regulator to the nasal epithelium of patients with cystic fibrosis. J Clin Invest. 1996;97(6):1504-11.
47. Crystal RG, McElvaney NG, Rosenfeld MA, Chu CS, Mastrangeli A, Hay JG, et al. Administration of an adenovirus containing the human CFTR cDNA to the respiratory tract of individuals with cystic fibrosis. Nat Genet. 1994;8(1):42-51.
48. Knowles MR, Hohneker KW, Zhou Z, Olsen JC, Noah TL, Hu PC, et al. A controlled study of adenoviral-vector-mediated gene transfer in the nasal epithelium of patients with cystic fibrosis. The New England journal of medicine. 1995;333(13):823-31.
49. Moss RB, Milla C, Colombo J, Accurso F, Zeitlin PL, Clancy JP, et al. Repeated Aerosolized AAV-CFTR for Treatment of Cystic Fibrosis: A Randomized Placebo-Controlled Phase 2B Trial. Human Gene Therapy. 2007;18(8):726-32.
50. Harvey BG, Hackett NR, Ely S, Crystal RG. Host responses and persistence of vector genome following intrabronchial administration of an E1(-)E3(-) adenovirus gene transfer vector to normal individuals. Molecular therapy : the journal of the American Society of Gene Therapy. 2001;3(2):206-15.
51. Kushwah R, Cao H, Hu J. Characterization of pulmonary T cell response to helper-dependent adenoviral vectors following intranasal delivery. Journal of immunology (Baltimore, Md : 1950). 2008;180(6):4098-108.
52. Duan D, Yue Y, Yan Z, Yang J, Engelhardt JF. Endosomal processing limits gene transfer to polarized airway epithelia by adeno-associated virus. The Journal of clinical investigation. 2000;105(11):1573-87.
53. Zabner J, Freimuth P, Puga A, Fabrega A, Welsh MJ. Lack of high affinity fiber receptor activity explains the resistance of ciliated airway epithelia to adenovirus infection. J Clin Invest. 1997;100(5):1144-9.
54. Schneider-Futschik EK. Beyond cystic fibrosis transmembrane conductance regulator therapy: a perspective on gene therapy and small molecule treatment for cystic fibrosis. Gene Ther. 2019;26(9):354-62.
55. Mitomo K, Griesenbach U, Inoue M, Somerton L, Meng C, Akiba E, et al. Toward gene therapy for cystic fibrosis using a lentivirus pseudotyped with Sendai virus envelopes. Mol Ther. 2010;18(6):1173-82.
56. Griesenbach U, Inoue M, Meng C, Farley R, Chan M, Newman NK, et al. Assessment of F/HN-pseudotyped lentivirus as a clinically relevant vector for lung gene therapy. Am J Respir Crit Care Med. 2012;186(9):846-56.
57. Alton EW, Beekman JM, Boyd AC, Brand J, Carlon MS, Connolly MM, et al. Preparation for a first-in-man lentivirus trial in patients with cystic fibrosis. Thorax. 2017;72(2):137-47.
58. Booth C, Romano R, Roncarolo MG, Thrasher AJ. Gene therapy for primary immunodeficiency. Hum Mol Genet. 2019;28(R1):R15-r23.
59. Griesenbach U, Davies JC, Alton E. Cystic fibrosis gene therapy: a mutation-independent treatment. Curr Opin Pulm Med. 2016;22(6):602-9.
60. Hyde SC, Gill DR, Higgins CF, Trezise AE, MacVinish LJ, Cuthbert AW, et al. Correction of the ion transport defect in cystic fibrosis transgenic mice by gene therapy. Nature. 1993;362(6417):250-5.

61. Hyde SC, Southern KW, Gileadi U, Fitzjohn EM, Mofford KA, Waddell BE, et al. Repeat administration of DNA/liposomes to the nasal epithelium of patients with cystic fibrosis. Gene Ther. 2000;7(13):1156-65.
62. Caplen NJ, Alton EW, Middleton PG, Dorin JR, Stevenson BJ, Gao X, et al. Liposome-mediated CFTR gene transfer to the nasal epithelium of patients with cystic fibrosis. Nat Med. 1995;1(1):39-46.
63. Alton EW, Stern M, Farley R, Jaffe A, Chadwick SL, Phillips J, et al. Cationic lipid-mediated CFTR gene transfer to the lungs and nose of patients with cystic fibrosis: a double-blind placebo-controlled trial. Lancet. 1999;353(9157):947-54.
64. Alton E, Armstrong DK, Ashby D, Bayfield KJ, Bilton D, Bloomfield EV, et al. Repeated nebulisation of non-viral CFTR gene therapy in patients with cystic fibrosis: a randomised, double-blind, placebo-controlled, phase 2b trial. Lancet Respir Med. 2015;3(9):684-91.
65. Alberts B, Johnson A, Lewis J, Morgan D, Raff M, Roberts K, et al. Molekularbiologie der Zelle. Weinheim, GERMANY: John Wiley & Sons, Incorporated; 2017.
66. Decroly E, Ferron F, Lescar J, Canard B. Conventional and unconventional mechanisms for capping viral mRNA. Nat Rev Microbiol. 2011;10(1):51-65.
67. Hyde JL, Diamond MS. Innate immune restriction and antagonism of viral RNA lacking 2-O methylation. Virology. 2015;479-480:66-74.
68. Yamamoto A, Kormann M, Rosenecker J, Rudolph C. Current prospects for mRNA gene delivery. Eur J Pharm Biopharm. 2009;71(3):484-9.
69. Mignone F, Gissi C, Liuni S, Pesole G. Untranslated regions of mRNAs. Genome Biol. 2002;3(3):REVIEWS0004-REVIEWS.
70. Wolff JA, Malone RW, Williams P, Chong W, Acsadi G, Jani A, et al. Direct gene transfer into mouse muscle in vivo. Science. 1990;247(4949 Pt 1):1465-8.
71. Jirikowski GF, Sanna PP, Maciejewski-Lenoir D, Bloom FE. Reversal of diabetes insipidus in Brattleboro rats: intrahypothalamic injection of vasopressin mRNA. Science. 1992;255(5047):996-8.
72. Martinon F, Krishnan S, Lenzen G, Magne R, Gomard E, Guillet JG, et al. Induction of virus-specific cytotoxic T lymphocytes in vivo by liposome-entrapped mRNA. Eur J Immunol. 1993;23(7):1719-22.
73. Boczkowski D, Nair SK, Snyder D, Gilboa E. Dendritic cells pulsed with RNA are potent antigen-presenting cells in vitro and in vivo. J Exp Med. 1996;184(2):465-72.
74. Nair SK. Immunotherapy of cancer with dendritic cell-based vaccines. Gene Ther. 1998;5(11):1445-6.
75. Vaidyanathan S, Azizian KT, Haque A, Henderson JM, Hendel A, Shore S, et al. Uridine Depletion and Chemical Modification Increase Cas9 mRNA Activity and Reduce Immunogenicity without HPLC Purification. Mol Ther Nucleic Acids. 2018;12:530-42.
76. Alexopoulou L, Holt AC, Medzhitov R, Flavell RA. Recognition of double-stranded RNA and activation of NF-kappaB by Toll-like receptor 3. Nature. 2001;413(6857):732-8.
77. Diebold SS, Kaisho T, Hemmi H, Akira S, Reis e Sousa C. Innate antiviral responses by means of TLR7-mediated recognition of single-stranded RNA. Science. 2004;303(5663):1529-31.

78. Heil F, Hemmi H, Hochrein H, Ampenberger F, Kirschning C, Akira S, et al. Species-specific recognition of single-stranded RNA via toll-like receptor 7 and 8. Science. 2004;303(5663):1526-9.
79. Diebold SS, Massacrier C, Akira S, Paturel C, Morel Y, Reis e Sousa C. Nucleic acid agonists for Toll-like receptor 7 are defined by the presence of uridine ribonucleotides. Eur J Immunol. 2006;36(12):3256-67.
80. Uzri D, Gehrke L. Nucleotide sequences and modifications that determine RIG-I/RNA binding and signaling activities. J Virol. 2009;83(9):4174-84.
81. Anderson BR, Muramatsu H, Jha BK, Silverman RH, Weissman D, Kariko K. Nucleoside modifications in RNA limit activation of 2'-5'-oligoadenylate synthetase and increase resistance to cleavage by RNase L. Nucleic Acids Res. 2011;39(21):9329-38.
82. Anderson BR, Muramatsu H, Nallagatla SR, Bevilacqua PC, Sansing LH, Weissman D, et al. Incorporation of pseudouridine into mRNA enhances translation by diminishing PKR activation. Nucleic Acids Res. 2010;38(17):5884-92.
83. Chiang C, Beljanski V, Yin K, Olagnier D, Ben Yebdri F, Steel C, et al. Sequence-Specific Modifications Enhance the Broad-Spectrum Antiviral Response Activated by RIG-I Agonists. J Virol. 2015;89(15):8011-25.
84. Kariko K, Buckstein M, Ni H, Weissman D. Suppression of RNA recognition by Toll-like receptors: the impact of nucleoside modification and the evolutionary origin of RNA. Immunity. 2005;23(2):165-75.
85. Kariko K, Muramatsu H, Welsh FA, Ludwig J, Kato H, Akira S, et al. Incorporation of pseudouridine into mRNA yields superior nonimmunogenic vector with increased translational capacity and biological stability. Mol Ther. 2008;16(11):1833-40.
86. Andries O, Mc Cafferty S, De Smedt SC, Weiss R, Sanders NN, Kitada T. N1-methylpseudouridine-incorporated mRNA outperforms pseudouridine-incorporated mRNA by providing enhanced protein expression and reduced immunogenicity in mammalian cell lines and mice. Journal of Controlled Release. 2015;217:337-44.
87. Warren L, Manos PD, Ahfeldt T, Loh YH, Li H, Lau F, et al. Highly efficient reprogramming to pluripotency and directed differentiation of human cells with synthetic modified mRNA. Cell Stem Cell. 2010;7(5):618-30.
88. Karikó K, Muramatsu H, Keller JM, Weissman D. Increased erythropoiesis in mice injected with submicrogram quantities of pseudouridine-containing mRNA encoding erythropoietin. Molecular therapy : the journal of the American Society of Gene Therapy. 2012;20(5):948-53.
89. Zangi L, Lui KO, von Gise A, Ma Q, Ebina W, Ptaszek LM, et al. Modified mRNA directs the fate of heart progenitor cells and induces vascular regeneration after myocardial infarction. Nat Biotechnol. 2013;31(10):898-907.
90. Kormann MS, Hasenpusch G, Aneja MK, Nica G, Flemmer AW, Herber-Jonat S, et al. Expression of therapeutic proteins after delivery of chemically modified mRNA in mice. Nat Biotechnol. 2011;29(2):154-7.
91. Kariko K, Muramatsu H, Ludwig J, Weissman D. Generating the optimal mRNA for therapy: HPLC purification eliminates immune activation and improves translation of nucleoside-modified, protein-encoding mRNA. Nucleic Acids Res. 2011;39(21):e142.

92. Kim CH, Oh Y, Lee TH. Codon optimization for high-level expression of human erythropoietin (EPO) in mammalian cells. Gene. 1997;199(1-2):293-301.
93. Kudla G, Lipinski L, Caffin F, Helwak A, Zylicz M. High guanine and cytosine content increases mRNA levels in mammalian cells. PLoS Biol. 2006;4(6):e180.
94. Ngumbela KC, Ryan KP, Sivamurthy R, Brockman MA, Gandhi RT, Bhardwaj N, et al. Quantitative effect of suboptimal codon usage on translational efficiency of mRNA encoding HIV-1 gag in intact T cells. PLoS One. 2008;3(6):e2356.
95. Zhong F, Cao W, Chan E, Tay PN, Cahya FF, Zhang H, et al. Deviation from major codons in the Toll-like receptor genes is associated with low Toll-like receptor expression. Immunology. 2005;114(1):83-93.
96. Gustafsson C, Govindarajan S, Minshull J. Codon bias and heterologous protein expression. Trends Biotechnol. 2004;22(7):346-53.
97. Presnyak V, Alhusaini N, Chen YH, Martin S, Morris N, Kline N, et al. Codon optimality is a major determinant of mRNA stability. Cell. 2015;160(6):1111-24.
98. Brule CE, Grayhack EJ. Synonymous Codons: Choose Wisely for Expression. Trends Genet. 2017;33(4):283-97.
99. Pechmann S, Chartron JW, Frydman J. Local slowdown of translation by nonoptimal codons promotes nascent-chain recognition by SRP in vivo. Nat Struct Mol Biol. 2014;21(12):1100-5.
100. Thess A, Grund S, Mui BL, Hope MJ, Baumhof P, Fotin-Mleczek M, et al. Sequence-engineered mRNA Without Chemical Nucleoside Modifications Enables an Effective Protein Therapy in Large Animals. Molecular therapy : the journal of the American Society of Gene Therapy. 2015;23(9):1456-64.
101. Kauffman KJ, Mir FF, Jhunjhunwala S, Kaczmarek JC, Hurtado JE, Yang JH, et al. Efficacy and immunogenicity of unmodified and pseudouridine-modified mRNA delivered systemically with lipid nanoparticles in vivo. Biomaterials. 2016;109:78-87.
102. Sanders N, Rudolph C, Braeckmans K, De Smedt SC, Demeester J. Extracellular barriers in respiratory gene therapy. Adv Drug Deliv Rev. 2009;61(2):115-27.
103. Widdicombe JG. Airway liquid: a barrier to drug diffusion? Eur Respir J. 1997;10(10):2194-7.
104. Button B, Cai LH, Ehre C, Kesimer M, Hill DB, Sheehan JK, et al. A periciliary brush promotes the lung health by separating the mucus layer from airway epithelia. Science. 2012;337(6097):937-41.
105. Sanders NN, De Smedt SC, Cheng SH, Demeester J. Pegylated GL67 lipoplexes retain their gene transfection activity after exposure to components of CF mucus. Gene Ther. 2002;9(6):363-71.
106. Yin H, Kanasty RL, Eltoukhy AA, Vegas AJ, Dorkin JR, Anderson DG. Non-viral vectors for gene-based therapy. Nat Rev Genet. 2014;15(8):541-55.
107. Kaczmarek JC, Patel AK, Kauffman KJ, Fenton OS, Webber MJ, Heartlein MW, et al. Polymer–Lipid Nanoparticles for Systemic Delivery of mRNA to the Lungs. Angewandte Chemie International Edition. 2016;55(44):13808-12.
108. Pardi N, Tuyishime S, Muramatsu H, Kariko K, Mui BL, Tam YK, et al. Expression kinetics of nucleoside-modified mRNA delivered in lipid nanoparticles to mice by various routes. J Control Release. 2015;217:345-51.
109. Li W, Szoka FC, Jr. Lipid-based nanoparticles for nucleic acid delivery. Pharm Res. 2007;24(3):438-49.

110. Scheule RK, St George JA, Bagley RG, Marshall J, Kaplan JM, Akita GY, et al. Basis of pulmonary toxicity associated with cationic lipid-mediated gene transfer to the mammalian lung. Hum Gene Ther. 1997;8(6):689-707.
111. Lee ER, Marshall J, Siegel CS, Jiang C, Yew NS, Nichols MR, et al. Detailed analysis of structures and formulations of cationic lipids for efficient gene transfer to the lung. Hum Gene Ther. 1996;7(14):1701-17.
112. Akinc A, Thomas M, Klibanov AM, Langer R. Exploring polyethylenimine-mediated DNA transfection and the proton sponge hypothesis. J Gene Med. 2005;7(5):657-63.
113. Schuster BS, Suk JS, Woodworth GF, Hanes J. Nanoparticle diffusion in respiratory mucus from humans without lung disease. Biomaterials. 2013;34(13):3439-46.
114. Schneider CS, Xu Q, Boylan NJ, Chisholm J, Tang BC, Schuster BS, et al. Nanoparticles that do not adhere to mucus provide uniform and long-lasting drug delivery to airways following inhalation. Sci Adv. 2017;3(4):e1601556.
115. Haque A, Dewerth A, Antony JS, Riethmuller J, Schweizer GR, Weinmann P, et al. Chemically modified hCFTR mRNAs recuperate lung function in a mouse model of cystic fibrosis. Sci Rep. 2018;8(1):16776.
116. Sanders NN, De Smedt SC, Van Rompaey E, Simoens P, De Baets F, Demeester J. Cystic fibrosis sputum: a barrier to the transport of nanospheres. Am J Respir Crit Care Med. 2000;162(5):1905-11.
117. Dawson M, Wirtz D, Hanes J. Enhanced viscoelasticity of human cystic fibrotic sputum correlates with increasing microheterogeneity in particle transport. J Biol Chem. 2003;278(50):50393-401.
118. Broughton-Head VJ, Smith JR, Shur J, Shute JK. Actin limits enhancement of nanoparticle diffusion through cystic fibrosis sputum by mucolytics. Pulm Pharmacol Ther. 2007;20(6):708-17.
119. Ferrari S, Kitson C, Farley R, Steel R, Marriott C, Parkins DA, et al. Mucus altering agents as adjuncts for nonviral gene transfer to airway epithelium. Gene Ther. 2001;8(18):1380-6.
120. Islam N, Dmour I, Taha MO. Degradability of chitosan micro/nanoparticles for pulmonary drug delivery. Heliyon. 2019;5(5):e01684.
121. Lv H, Zhang S, Wang B, Cui S, Yan J. Toxicity of cationic lipids and cationic polymers in gene delivery. J Control Release. 2006;114(1):100-9.
122. Kreuter J. Evaluation of nanoparticles as drug-delivery systems. III: materials, stability, toxicity, possibilities of targeting, and use. Pharm Acta Helv. 1983;58(9-10):242-50.
123. Sahin U, Kariko K, Tureci O. mRNA-based therapeutics--developing a new class of drugs. Nat Rev Drug Discov. 2014;13(10):759-80.
124. Grenha A, Seijo B, Remunan-Lopez C. Microencapsulated chitosan nanoparticles for lung protein delivery. Eur J Pharm Sci. 2005;25(4-5):427-37.
125. Mays LE, Ammon-Treiber S, Mothes B, Alkhaled M, Rottenberger J, Muller-Hermelink ES, et al. Modified Foxp3 mRNA protects against asthma through an IL-10-dependent mechanism. J Clin Invest. 2013;123(3):1216-28.
126. Zeyer F, Mothes B, Will C, Carevic M, Rottenberger J, Nurnberg B, et al. mRNA-Mediated Gene Supplementation of Toll-Like Receptors as Treatment Strategy for Asthma In Vivo. PLoS One. 2016;11(4):e0154001.

127. Connolly B, Isaacs C, Cheng L, Asrani KH, Subramanian RR. SERPINA1 mRNA as a Treatment for Alpha-1 Antitrypsin Deficiency. J Nucleic Acids. 2018;2018:8247935.
128. Gan LM, Lagerstrom-Fermer M, Carlsson LG, Arfvidsson C, Egnell AC, Rudvik A, et al. Intradermal delivery of modified mRNA encoding VEGF-A in patients with type 2 diabetes. Nat Commun. 2019;10(1):871.
129. Mahiny AJ, Dewerth A, Mays LE, Alkhaled M, Mothes B, Malaeksefat E, et al. In vivo genome editing using nuclease-encoding mRNA corrects SP-B deficiency. Nature Biotechnology. 2015;33(6):584-6.
130. Antony JS, Latifi N, Haque A, Lamsfus-Calle A, Daniel-Moreno A, Graeter S, et al. Gene correction of HBB mutations in CD34(+) hematopoietic stem cells using Cas9 mRNA and ssODN donors. Mol Cell Pediatr. 2018;5(1):9.
131. Bangel-Ruland N, Tomczak K, Fernandez Fernandez E, Leier G, Leciejewski B, Rudolph C, et al. Cystic fibrosis transmembrane conductance regulator-mRNA delivery: a novel alternative for cystic fibrosis gene therapy. J Gene Med. 2013;15(11-12):414-26.
132. Study to Evaluate the Safety & Tolerability of MRT5005 Administered by Nebulization in Adults With Cystic Fibrosis (RESTORE-CF) [Internet]. ClinicalTrials.gov. 2017 [cited March 31, 2020]. Available from: https://clinicaltrials.gov/ct2/show/NCT03375047.
133. Translate Bio Announces Interim Results from Phase 1/2 Clinical Trial of MRT5005 in Patients with Cystic Fibrosis [press release]. Translate Bio, July 31, 2019.
134. Antony JS, Dewerth A, Haque A, Handgretinger R, Kormann MSD. Modified mRNA as a new therapeutic option for pediatric respiratory diseases and hemoglobinopathies. Molecular and Cellular Pediatrics. 2015;2(1):11.
135. Chu CS, Trapnell BC, Curristin SM, Cutting GR, Crystal RG. Extensive posttranscriptional deletion of the coding sequences for part of nucleotide-binding fold 1 in respiratory epithelial mRNA transcripts of the cystic fibrosis transmembrane conductance regulator gene is not associated with the clinical manifestations of cystic fibrosis. The Journal of clinical investigation. 1992;90(3):785-90.
136. Al-Nemrawi NK, Alshraiedeh NH, Zayed AL, Altaani BM. Low Molecular Weight Chitosan-Coated PLGA Nanoparticles for Pulmonary Delivery of Tobramycin for Cystic Fibrosis. Pharmaceuticals (Basel). 2018;11(1).
137. Ramos KJ, Smith PJ, McKone EF, Pilewski JM, Lucy A, Hempstead SE, et al. Lung transplant referral for individuals with cystic fibrosis: Cystic Fibrosis Foundation consensus guidelines. J Cyst Fibros. 2019;18(3):321-33.
138. Kerem E, Reisman J, Corey M, Canny GJ, Levison H. Prediction of mortality in patients with cystic fibrosis. N Engl J Med. 1992;326(18):1187-91.

# 8 Declaration

This thesis was conducted and written in the Klinik für Kinder- und Jugendmedizin, Tübingen and supervised by Prof. Dr. rer. nat. Michael S.D. Kormann.

All experiments, except those listed below, were conducted by myself.
Animal experiments were performed under supervision of Dr. AKM Ashiqul Haque.

$FEV_{0.1}$ measurements of $Cftr^{+/+}$ mice and ELISA measurement of immune responses *in vivo* (Method 2.2.15) were conducted by Dr. AKM Ashiqul Haque.

Statistical analyses were performed autonomously.

I affirm, that I have written the dissertation myself and that I have not used any sources other than those indicated.

Tübingen, den 30.04.2021

# 9 Acknowledgements

Genesis and development of this thesis would not have been possible without the close supervision, guidance, and support of a whole team!

I want to thank Prof. Dr. Julia Skokowa for undertaking responsibility for my project and enabling me to finish my thesis.

I want to thank Prof. Dr. Michael Kormann for giving me the chance to be part of this promising and inspiring research on gene therapy to cure Cystic Fibrosis.

Also, I want to particularly thank Dr. Itishri Sahu for being my close and patient supervisor throughout the performance of my experiments. Working with and learning from her every day was an amazing experience and will always be an important part of my medical studies.

Moreover, I want to thank Dr. AKM Ashiqul Haque, Brian Weidensee and Petra Weinmann, who supported and instructed me every day during my laboratory work. I want to especially thank Brian Weidensee, who supported me not only during my time in the laboratory but also throughout the whole writing process.

Finally, I want to thank my family and my partner for their calmness, humor, love, and support throughout the whole process of experimenting, analyzing, and writing this thesis!